

PURDUE UNIVERSITY
GRADUATE SCHOOL
Thesis/Dissertation Acceptance

This is to certify that the thesis/dissertation prepared

By Angela Kay Deem

Entitled
Genome-destabilizing and Mutagenic Effects of Break-induced Replication in *Saccharomyces cerevisiae*

For the degree of Doctor of Philosophy



Is approved by the final examining committee:

Cynthia V. Stauffacher

Chair

John Turchi

Martin Bard

Anna Malkova

Stephen K. Randall

To the best of my knowledge and as understood by the student in the *Research Integrity and Copyright Disclaimer (Graduate School Form 20)*, this thesis/dissertation adheres to the provisions of Purdue University's "Policy on Integrity in Research" and the use of copyrighted material.

Approved by Major Professor(s): Cynthia V. Stauffacher

Approved by: Simon J. Atkinson

Head of the Graduate Program

02/10/2011

Date

**PURDUE UNIVERSITY
GRADUATE SCHOOL**

Research Integrity and Copyright Disclaimer

Title of Thesis/Dissertation:

Genome-destabilizing and Mutagenic Effects of Break-induced Replication in *Saccharomyces cerevisiae*

For the degree of Doctor of Philosophy



I certify that in the preparation of this thesis, I have observed the provisions of *Purdue University Executive Memorandum No. C-22*, September 6, 1991, *Policy on Integrity in Research*.*

Further, I certify that this work is free of plagiarism and all materials appearing in this thesis/dissertation have been properly quoted and attributed.

I certify that all copyrighted material incorporated into this thesis/dissertation is in compliance with the United States' copyright law and that I have received written permission from the copyright owners for my use of their work, which is beyond the scope of the law. I agree to indemnify and save harmless Purdue University from any and all claims that may be asserted or that may arise from any copyright violation.

Angela Kay Deem

Printed Name and Signature of Candidate

02/10/2011

Date (month/day/year)

*Located at http://www.purdue.edu/policies/pages/teach_res_outreach/c_22.html

GENOME-DESTABILIZING AND MUTAGENIC EFFECTS OF BREAK-
INDUCED REPLICATION IN *SACCHAROMYCES CEREVISIAE*

A Dissertation

Submitted to the Faculty

of

Purdue University

by

Angela Kay Deem

In Partial Fulfillment of the

Requirements for the Degree

of

Doctor of Philosophy

May 2011

Purdue University

Indianapolis, Indiana

This is dedicated to my parents, who taught me to work hard, never to fear failure, and never to quit before I am satisfied.

ACKNOWLEDGMENTS

The author would like to thank the team of amazing women who assisted with this work. In alphabetical order, Tiffany Blackgrove, Barbara Coffey, Claire Fisher, Ruchi Mathur, Kelly Van Hulle, and Alexandra Vayl were the most dedicated, supportive, and committed team of scientists anyone could ever ask to work with. Simply put, the work presented in this dissertation would not have been possible without their constant willingness to learn, work, and succeed. I could go on for many pages about the strength and character of each of these women, but I hope that my words and actions in person have let them know how much I value each of them long before typing these letters. The amount and quality of work accomplished by this group in such a short period of time speaks volumes about the talent of each of them. I wish for them all to find the opportunities and happiness in their careers that I know they have worked so hard for.

TABLE OF CONTENTS

	Page
LIST OF TABLES	vi
LIST OF FIGURES	vii
LIST OF ABBREVIATIONS	viii
ABSTRACT	x
CHAPTER 1. INTRODUCTION	1
1.1. Objectives.....	1
1.2. Organization	2
CHAPTER 2. LITERATURE REVIEW	3
2.1. Types of DNA Damage.....	3
2.2. DSB Repair Pathways in <i>S. cerevisiae</i>	4
2.2.1. Gene Conversion.....	7
2.2.2. Break-induced Replication.....	8
2.2.3. Single-strand Annealing	12
2.2.4. Non-homologous End Joining	12
2.3. Yeast Recombination Proteins	13
2.3.1. BIR and Rad51p.....	19
2.4. The DNA Damage Checkpoint	19
CHAPTER 3. MATERIALS AND METHODS.....	22
3.1. Media and Strains.....	22
3.1.1. Strain Construction	22
3.1.2. Media and Growth Conditions	40
3.2. Yeast Recombinant DNA Techniques	41
3.2.1. PCR.....	41
3.2.2. Restriction Digests.....	42
3.3. DNA Extractions	43
3.3.1. Glass Bead Genomic DNA Extraction from Yeast.....	43
3.3.2. High-molecular Weight DNA Extractions	44
3.4. Plasmids	45
3.4.1. Bacterial Transformations.....	45
3.4.2. Plasmid Purification	45
3.5. Pulsed-field Gel Electrophoresis.....	46
3.5.1. Southern Hybridization of CHEF	47
3.6. Analysis of DNA Repair Outcomes in AM1003-9 and Its Mutant Derivatives	48

	Page
3.6.1. Analysis of HCO molecules	48
3.6.2. Statistical Analysis of BIR Repair Outcomes	49
3.7. Mutagenesis associated with DSB repair	49
3.7.1. Determining Mutation Frequencies	49
3.7.2. Calculations of BIR efficiency	52
3.7.3. Analysis of Mutation Spectra	52
CHAPTER 4. GENOME-DESTABILIZING EFFECTS OF BREAK-INDUCED REPLICATION	55
4.1. Background	55
4.2. Experimental System	57
4.2.1. Characterization of the <i>pol32Δ</i> defect	61
4.3. Checkpoint-deficient mutants and BIR	73
4.3.1. BIR efficiency is reduced in <i>rad9Δ</i> and <i>rad24Δ</i> mutants	75
4.3.2. Sectoring of colonies in <i>rad9Δ</i> and <i>rad24Δ</i> mutants	79
4.3.3. HCOs in <i>rad9Δ</i> and <i>rad24Δ</i> mutants	83
4.4. The Effect of Replication-inhibiting Drugs on BIR	84
4.5. Discussion	87
4.5.1. <i>pol32Δ</i> , <i>rad9Δ</i> , and <i>rad24Δ</i> are defective in BIR repair	88
4.5.2. Interrupted BIR leads to HCOs	90
4.5.3. Summary	93
CHAPTER 5. FRAMESHIFT MUTAGENESIS ASSOCIATED WITH BREAK- INDUCED REPLICATION	95
5.1. Introduction	95
5.2. Characterization of BIR Frameshift Mutagenesis	98
5.2.1. Experimental System	98
5.2.2. Rate of Frameshift Mutagenesis during BIR	106
5.2.3. Sequencing Analysis of BIR Mutations	117
5.3. Genetic Control of BIR Frameshift Mutagenesis	121
5.3.1. The Role of Translesion DNA Synthesis	121
5.3.2. The Role of MMR	125
5.3.3. The Role of Polymerase Proofreading	131
5.3.4. The Role of Pif1p Helicase	142
5.3.5. The Role of dNTP Levels	145
5.4. Discussion	149
5.4.1. Conclusions	154
REFERENCES	156
VITA	178
PUBLICATIONS	182

LIST OF TABLES

Table	Page
Table 3.1. List of strains used in this study.	24
Table 3.2. Primers used in strain construction and characterization.	31
Table 4.1. Repair of HO-induced DSBs in strain AM1003-9 and its <i>pol32Δ</i> and <i>rad51Δ</i> derivatives.	62
Table 4.2. BIR efficiency in strain AM1003-9 and its <i>rad9Δ</i> , <i>rad24Δ</i> , and <i>rad9Δrad50Δ</i> derivatives.	76
Table 4.3. Analysis of retention of <i>NAT</i> marker among BIR repair outcomes.	80
Table 4.4. Effect of checkpoint deficiency on formation of sectorized events.	82
Table 4.5. HCOs in strain AM1003-9 and its <i>rad9Δ</i> and <i>rad24Δ</i> derivatives.	84
Table 4.6. Replication-inhibiting drugs used in BIR studies.	86
Table 4.7. Effect of MMS on HCO formation in cells undergoing BIR repair.	87
Table 5.1. BIR efficiency in wild type and mutant strains. ^a	105
Table 5.2. The rate of spontaneous and DSB-associated Lys ⁺ mutations.	109
Table 5.3. Spectrum of BIR-associated and spontaneous Lys ⁺ mutations in MMR ⁺ and <i>msh2Δ</i> strains.	118
Table 5.4. Efficiency of MMR during BIR repair.	130
Table 5.5. The rate of spontaneous and DSB-associated Lys ⁺ mutations in <i>pif1-m2</i>	144

LIST OF FIGURES

Figure	Page
Figure 2.1. Mechanisms of DSB repair in <i>S. cerevisiae</i>	6
Figure 2.2. Two pathways of GC	9
Figure 4.1. Disomic experimental system to study BIR.....	59
Figure 4.2. Analysis of DSB repair in AM1003-9 and its <i>pol32Δ</i> derivative	64
Figure 4.3. Structural analysis of Ade ⁺ Leu ⁻ repair outcomes.....	67
Figure 4.4. Structural analysis of HCO outcomes.....	71
Figure 4.5. Structural analysis of Ade ⁺ Leu ⁻ repair outcomes in <i>rad9Δ</i> and <i>rad24Δ</i>	81
Figure 4.6. Hypothetical mechanism of HCO formation	91
Figure 5.1. Experimental system to study BIR-associated mutagenesis	101
Figure 5.2. Arrest of wild type cells during mutagenesis experiments	104
Figure 5.3. BIR-associated mutagenesis determined by frameshift reporters at three chromosomal positions.....	108
Figure 5.4. Spectrum of BIR-associated and spontaneous Lys ⁺ mutations in MMR ⁺ and <i>msh2Δ</i> strains	120
Figure 5.5. The role of translesion polymerases in BIR-associated mutagenesis	122
Figure 5.6. Effect of UV damage on frameshift mutagenesis	124
Figure 5.7. The role of MMR in BIR-associated mutagenesis	128
Figure 5.8. The role of Pol ε proofreading in BIR-associated mutagenesis.	135
Figure 5.9. The role of Pol δ proofreading in BIR-associated mutagenesis	139
Figure 5.10. Growth characteristics of wild type and its <i>pol3-5DVmsh3Δ</i> derivatives	141
Figure 5.11. The role Pif1p helicase in BIR-associated mutagenesis.....	143
Figure 5.12. Role of DNA damage checkpoint response on dNTP levels.	146
Figure 5.13. Effect of mutations affecting dNTP levels on BIR-associated mutagenesis	148

LIST OF ABBREVIATIONS

ALT	Alternative telomere lengthening
BIR	Break-induced replication
Cisplatin	Cis-diamine-dichloro-platinum(II)
DNA	Deoxyribonucleic acid
DSB	Double-strand break
DSBR	Double-strand break repair
GC	Gene conversion
GCR	Gross chromosomal rearrangement
HR	Homologous recombination
HU	Hydroxyurea
IR	Ionizing radiation
MHEJ	Microhomology-mediated end joining
MMS	Methylmethane sulfonate
NHEJ	Non-homologous end joining
NRT	Non-reciprocal translocation
PCR	Polymerase chain reaction
PFGE	Pulsed-field gel electrophoresis
Pol	Polymerase

PIKK	phosphoinositol-3-kinase-related kinase
RDR	Recombination-dependent replication
RNR	Ribonucleotide reductase
SDSA	Synthesis-dependent strand annealing
SSA	Single-strand annealing
ssDNA	Single-stranded DNA

ABSTRACT

Deem, Angela Kay Ph.D., Purdue University, May 2011. Genome-destabilizing and Mutagenic Effects of Break-induced Replication in *Saccharomyces cerevisiae*. Major Professor: Cynthia V. Stauffacher.

DNA suffers constant damage, leading to a variety of lesions that require repair. One of the most devastating lesions is a double-strand break (DSB), which results in physical dissociation of two pieces of a chromosome. Necessarily, cells have evolved a number of DSB repair mechanisms. One mechanism of DSB repair is break-induced replication (BIR), which involves invasion of one side of the broken chromosome into a homologous template, followed by copying of the donor molecule through telomeric sequences. BIR is an important cellular process implicated in the restart of collapsed replication forks, as well as in various chromosomal instabilities. Furthermore, BIR uniquely combines processive replication involving a replication fork with DSB repair. This work employs a system in *Saccharomyces cerevisiae* to investigate genetic control, physical outcomes, and frameshift mutagenesis associated with BIR initiated by a controlled HO-endonuclease break in a chromosome. Mutations in *POL32*, which encodes a third, non-essential subunit of polymerase δ (Pol δ), as well as *RAD9* and *RAD24*, which participate in the DNA damage checkpoint response, resulted in a BIR defect characterized by decreased BIR repair and increased

loss of the broken chromosome. Also, increased incidence of chromosomal fusions determined to be half-crossover (HCO) molecules was confirmed in *pol32Δ* and *rad24Δ*, as well as a *rad9Δrad50S* double mutant. HCO formation was also stimulated by addition of a replication-inhibiting drug, methyl-methane sulfonate (MMS), to cells undergoing BIR repair. Based on these data, it is proposed that interruption of BIR after it has initiated is one mechanism of HCO formation. Addition of a frameshift mutation reporter to this system allowed mutagenesis associated with BIR DNA synthesis to be measured. It is demonstrated that BIR DNA synthesis is intrinsically inaccurate over the entire path of the replication fork, as the rate of frameshift mutagenesis during BIR is up to 2800-fold higher than normal replication. Importantly, this high rate of mutagenesis was observed not only close to the DSB where BIR is less stable, but also far from the DSB where the BIR replication fork is fast and stabilized. Pol δ proofreading and mismatch repair (MMR) are confirmed to correct BIR errors. Based on these data, it is proposed that a high level of DNA polymerase errors that is not fully compensated by error-correction mechanisms is largely responsible for mutagenesis during BIR. Pif1p, a helicase that is non-essential for DNA replication, and elevated dNTP levels during BIR also contributed to BIR mutagenesis. Taken together, this work characterizes BIR as an essential repair process that also poses risks to a cell, including genome destabilization and hypermutagenesis.

CHAPTER 1. INTRODUCTION

1.1. Objectives

The overall goal of this research was to elucidate the deleterious effects of break-induced replication (BIR), a homologous recombination (HR) pathway of chromosome double-strand break (DSB) repair. Broadly, this research describes two potential consequences of BIR: 1) genome destabilization resulting from faulty BIR repair, and 2) frameshift mutagenesis associated with new DNA synthesis during BIR. The specific objectives were to:

1. Characterize the BIR defect in a *po/32Δ* mutant;
2. Analyze specific genome rearrangements, half-crossovers (HCOs), observed in the *po/32Δ* background;
3. Test the effects of faulty DNA-damage checkpoint response on BIR repair;
4. Test the effects of replication-inhibiting drugs on BIR repair;
5. Determine the fidelity of new DNA synthesis associated with BIR; and
6. Examine the roles of various DNA replication and repair components in BIR mutagenesis.

1.2. Organization

This dissertation provides a literature review (Chapter 2) to orient the reader to the field of DNA repair, with special emphasis on HR repair mechanisms, including BIR. Materials and methods used in this research are described in Chapter 3. Data obtained during this research are presented in two chapters, each of which contains an independent introduction and discussion. Chapter 4 summarizes findings relevant to the genome-destabilizing effects of BIR (objectives 1 through 4), and Chapter 5 summarizes findings relevant to BIR mutagenesis (objectives 5 and 6).

CHAPTER 2. LITERATURE REVIEW

2.1. Types of DNA Damage

DNA is subjected to constant assaults by both endogenous and exogenous sources. Inside the cell, molecules such as reactive oxygen species can attack DNA and cause a myriad of alterations, including nucleotide modifications, abasic sites, and breaks in the DNA backbone (reviewed in (Jackson and Loeb, 2001)). Cells may also be exposed to a variety of exogenous damaging agents, including environmental toxins, ultraviolet light, and gamma irradiation. Primarily, all of these sources of damage affect one of the two strands of the DNA double helix, although gamma irradiation can sometimes create double-strand breaks (DSBs) in the DNA molecule. Even single-strand damage, however, can result in DSBs when it interferes with DNA metabolism. For example, when a progressing replication fork encounters an unrepaired lesion or a single-strand break, the replication fork may collapse, resulting in a DSB (Aguilera A., 2007; Kuzminov, 1995). Though not as common as single-strand breaks, DSBs are more dangerous to cells, as failure of the break to be properly repaired can result in chromosome aberrations ((Natarajan et al., 1980); reviewed in (Haber, 2006)). Fortunately, cells have evolved multiple paythways to repair DSBs. The following discussion will focus on DSB repair in yeast, *Saccharomyces cerevisiae*, which

was the model organism used in the dissertation research. *S. cerevisiae* is a valuable model organism to study DSB repair because its genome is both relatively small and easy to manipulate, allowing advantageous placement of genetic and physical markers. Also, yeast divide quickly and can exist as either haploids or diploids, the former of which is especially convenient for genetic screens. Because repair proteins and pathways are widely conserved among eukaryotes, investigations into DSB repair in yeast are highly relevant to the human condition, including the phenomena of aging and disease genesis.

2.2. DSB Repair Pathways in *S. cerevisiae*

It is estimated that approximately 10% of *S. cerevisiae* cells undergoing replication will incur one or more DSBs (Aguilera A., 2007). The strategies employed by a cell to repair these and other DSBs can be broadly divided into two categories: 1) mechanisms that exploit homology within the genome, and 2) mechanisms for which extensive homology is not a pre-requisite (Figure 2.1). The former category encompasses a number of mechanisms collectively termed homologous recombination (HR), while the latter category describes re-ligation of the broken molecule through non-homologous end joining (NHEJ). The preferred donor sequence for HR repair is the sister chromatid (Kadyk and Hartwell, 1992); thus, HR repair is often coupled with replication and is highly active during S phase and G2 ((Aylon et al., 2004; Ira et al., 2004); reviewed in (Aguilera A., 2007)). DSBs incurred during G0 or G1 primarily repair through NHEJ (Aylon et al., 2004; Ira et al., 2004).

In addition to spontaneous DSBs, mating type switching in yeast begins with the creation of a DSB in the *MAT* locus in Chromosome III that is repaired through HR with one of two silenced HM donor cassettes near either end of the chromosome (Strathern et al., 1982). This DSB is created by a meganuclease, HO endonuclease, that makes a 4-bp staggered cut at a 24-bp recognition site (Colleaux et al., 1988; Nickoloff et al., 1986). The specificity of HO endonuclease made it an obvious experimental asset for yeast genetics, and it was cloned under the control of a galactose promoter (Jensen and Herskowitz, 1984) to allow studies designed to induce a timed, controlled cut in a population of cells that could be monitored by diverse methods for repair outcomes. Varied placement of the HO recognition site provides for building powerful systems with DSBs induced in different contexts within the genome, thereby altering the preferred pathway of repair.

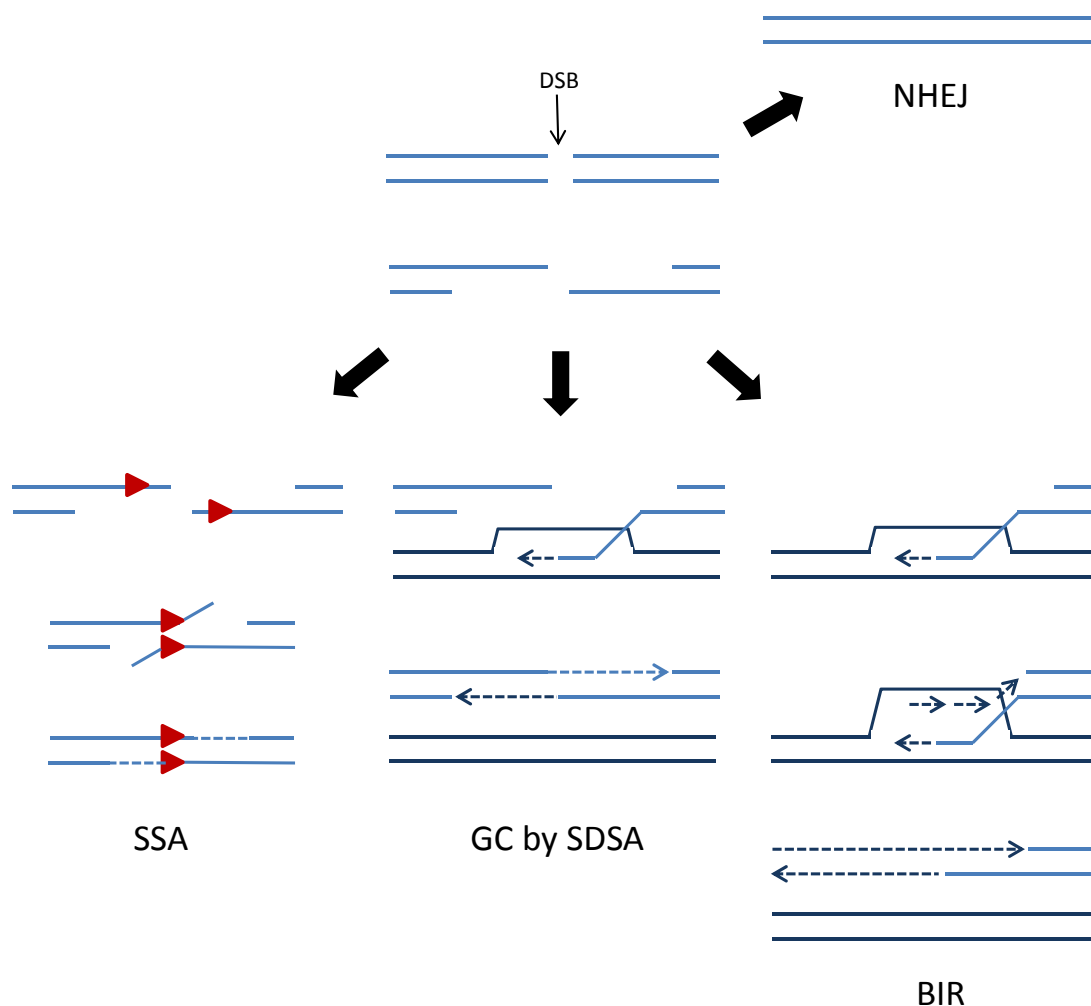


Figure 2.1. Mechanisms of DSB repair in *S. cerevisiae*. DSBs can be repaired through one of three HR repair pathways (SSA, GC, or BIR), or through NHEJ. Selection of repair pathway is dependent on the context of the lesion, as well as the cell cycle. For GC, two possible pathways are possible, and the pathway used helps determine strand inheritance. For mitotic GC repair, evidence suggests the SDSA model shown in this figure is preferred. The other GC pathway, DSBR, which is more common during meiosis, is depicted in Figure 2.2. See text for further details.

2.2.1. Gene Conversion

The favored pathway for HR repair of mitotic DSBs in yeast is gene conversion (GC), a process in which a relatively small patch of DNA is copied from a homologous donor sequence to replace the missing information in the broken molecule. GC is also the primary repair pathway of DSBs induced during meiosis. A striking difference between meiotic GC outcomes versus mitotic GC outcomes is that, in meiosis, GC is frequently associated with “crossing over” of adjacent DNA sequences, while this phenomenon is rare in mitosis. It is now widely held that the suppression of reciprocal exchange observed in mitotic DSB repair is the result of differing repair processes. Meiotic GC, which is commonly referred to as double-strand break repair (DSBR), proceeds through two-ended invasion into the donor molecule and formation of two Holliday junctions that must be resolved (resolution of which is believed to be random and result in an approximately 1:1 ratio of non-crossover:crossover events; (Orr-Weaver and Szostak, 1983; Orr-Weaver et al., 1981; Szostak et al., 1983)). In contrast, mitotic GC most likely completes through synthesis-dependent strand annealing (SDSA; (Ira et al., 2003; Paques and Haber, 1999; Strathern et al., 1982); reviewed in (Andersen and Sekelsky, 2010)), which does not require enzymatic resolution of joint molecules (i.e., does not involve formation of Holliday junctions; Figure 2.2). Rather, mitotic GC of a DSB proceeds through: 1) 5'-to-3' resection of both sides of the break, 2) invasion by at least one of the ssDNA ends into the donor sequence, 3) new DNA synthesis using the donor molecule template, 4) dissociation of the heteroduplex molecule, 5) re-annealing of the broken

molecule via newly synthesized sequences, and 6) sealing of single-strand gaps (Figures 2.1, 2.2).

2.2.2. Break-induced Replication

In contrast to GC, break-induced replication (BIR) repairs DSBs in which only one side of the DSB is able to participate in HR (Figure 2.1). This phenomenon was first proposed to explain the mechanism of host infection by a linear chromosome employed by bacteriophage T4 (Luder and Mosig, 1982). Subsequent studies confirmed that the ends of the infecting chromosome indeed initiated replication in an HR-dependent manner ((George and Kreuzer, 1996; Kreuzer et al., 1995; Mosig, 1998; Mueller et al., 1996); reviewed in (Kreuzer, 2000)). This mechanism, termed recombination-dependent DNA replication (RDR) was also confirmed in *Escherichia coli*, where it is involved in DSB repair ((Asai et al., 1994); reviewed in (Kogoma, 1997; Kuzminov, 1999)) and restart of collapsed replication forks (Kogoma, 1997; Kuzminov, 1995; Marians, 2000; Motamedi et al., 1999); reviewed in (Michel et al., 2001)). In yeast, several

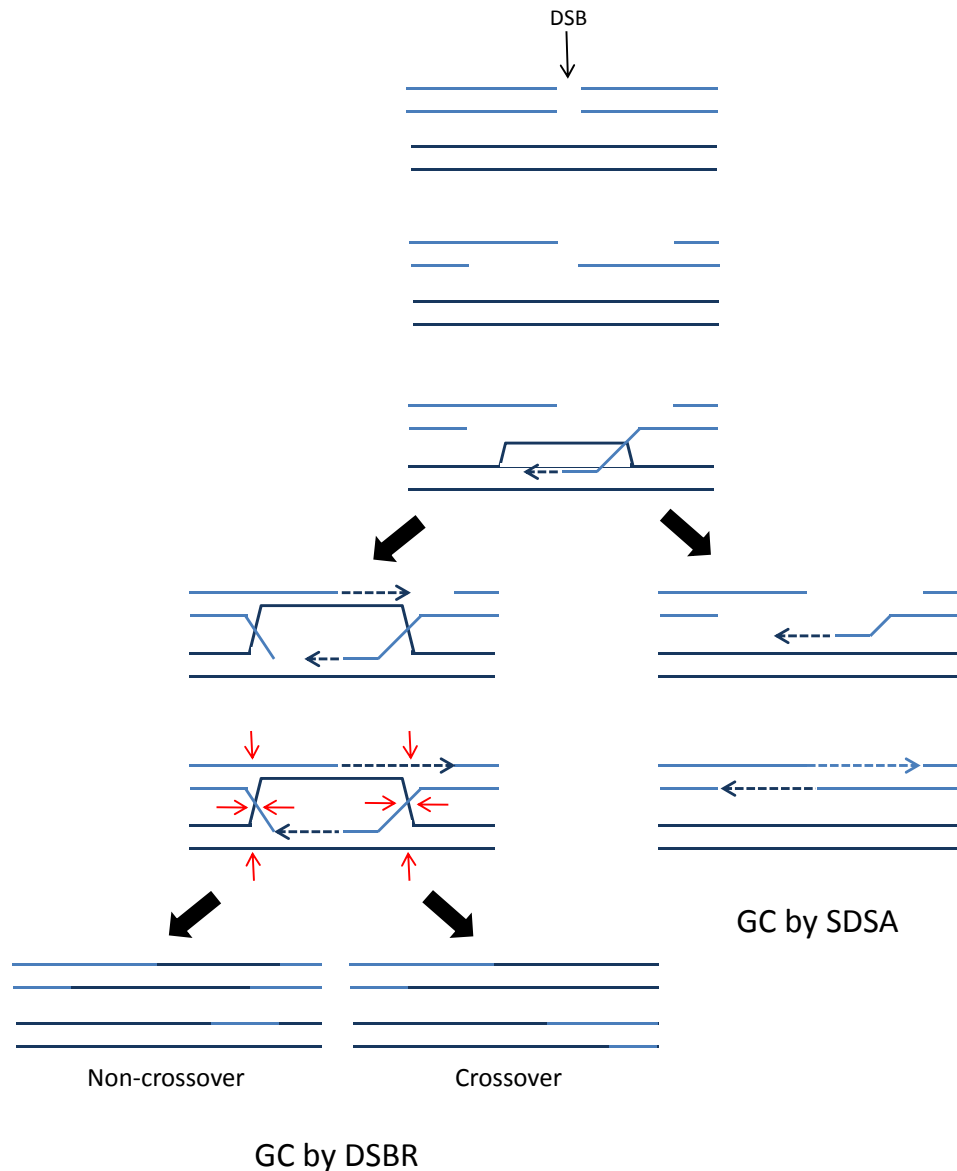


Figure 2.2. Two pathways of GC. Repair of a DSB by GC can proceed through two mechanisms. During meiosis, invasion of both sides of the DSB into the donor template requires resolution of Holliday junctions and results in an approximately equal distribution of crossover versus non-crossover molecules (GC by DSBR). Strong evidence suggests that mitotic GC does not require Holliday junction resolution. Rather, after invasion of one side of the DSB and new DNA synthesis, the duplex molecule dissociates and re-anneals to the other side of the lesion, making crossover outcomes rare (GC by SDSA).

genetic investigations confirmed an analogous mechanism of a single 3'-ended ssDNA invasion into a homologous sequence and extensive synthesis to the end of the donor chromosome (Bosco and Haber, 1998; Davis and Symington, 2004; Malkova et al., 1996b; Morrow et al., 1997; Paques and Haber, 1999; Voelkel-Meiman and Roeder, 1990). BIR plays an important role in maintenance of the yeast genome, and is implicated in telomere maintenance in the absence of telomerase (Dunn et al., 1984; Lundblad and Blackburn, 1993; Lydeard et al., 2007), known as alternative telomere maintenance (ALT). Also, a variety of indirect evidence suggests that an HR mechanism – likely BIR based on the physical structure of a collapsed replication fork – is a pathway to rescue collapsed replication forks. In yeast, this evidence includes the association between HR and phases of the cell cycle in which a sister chromatid is present (Aylon et al., 2004; Ira et al., 2004), the role of S-phase checkpoint proteins to prevent chromosome aberrations (Enserink et al., 2006; Kolodner et al., 2002; Myung et al., 2001b), and the observation of spontaneous foci of the required HR protein Rad52p during S phase that are largely absent during other phases of the cell cycle (Lisby et al., 2001).

GC and BIR initiate in a similar manner (Figure 2.1). In both pathways, the DSB is followed by 5'-to-3' resection and followed by invasion of a 3' ssDNA nucleoprotein filament (ssDNA coated with Rad51p; see Section 2.3 for details) into a homologous donor sequence. However, the ability of only one side of the DSB to participate in repair makes reannealing and ligation impossible. Instead,

the current model of BIR describes that the one-ended invasion intermediate becomes a substrate for assembly of a repair-related replication fork that synthesizes new DNA along the length of the donor template. Though the exact composition of the fork remains unknown, the idea that a processive fork is assembled during BIR is supported by its requirement for all replication initiation factors (aside from those involved exclusively in sensing of a replication origin; (Lydeard et al. 2010)), combined with a rate of replication that mimics that observed in S-phase (Malkova et al., 2005). While BIR replication is fast, the early steps of BIR are slow, and it takes approximately 6 hours for a BIR product to be observed by physical analysis, compared with less than two hours for a comparable GC event (Malkova et al., 2005). It is not entirely clear why such a long delay exists between the initial invasion and processive replication, though some recent findings shed light on this issue. First, the one-ended invasion that occurs during BIR initiation is unstable, and multiple rounds of invasion and short DNA synthesis can occur in different templates before processive replication of a donor molecule begins (Smith et al., 2007). Also, Jain et al. (2009) described an event termed the “recombination execution checkpoint” in which cells undergoing DSB repair do not initiate DNA synthesis until after the structure of the break has been defined. That is, commitment to the BIR repair pathway occurs only after the cell has “confirmed” the absence of a second end to participate in repair, and both the distance between and orientation of the DSB ends affect whether the cell senses the break as 1- or 2-sided.

2.2.3. Single-strand Annealing

Single-strand annealing (SSA) is an efficient repair pathway that repairs a DSB by annealing of complementary sequences on either side of the lesion (Figure 2.1; (Fishman-Lobell and Haber, 1992); reviewed in (Aguilera A., 2007; Paques and Haber, 1999)). Annealing of the repeated sequences requires that they first become single-stranded and, thus, the kinetics of this process depends upon the position of the sequences used for repair and corresponds with the rate of post-DSB resection (Fishman-Lobell and Haber, 1992; Jain et al., 2009). After annealing of complementary sequences, the nonhomologous “flaps” are clipped off (Fishman-Lobell and Haber, 1992; Ivanov and Haber, 1995) and the resultant gap filled via repair synthesis. The repair product is a chromosome with deletion of one of the direct repeats involved in annealing, as well as all intervening sequences. Such deletions could pose a great risk to a cell's viability, making SSA a seemingly undesirable repair pathway compared to GC. However, it has been shown that SSA efficiently competes with the GC pathway, representing approximately 30% of DSB repair outcomes even when a homologous sequence for GC is available (Wu et al., 1997).

2.2.4. Non-homologous End Joining

Non-homologous end joining (NHEJ) repairs DSBs through re-ligation of the two chromosomal fragments (Figure 2.1). This process can either be high-fidelity, or it can be accompanied by insertions or deletions (reviewed in (Daley et al., 2005)). Unlike HR, in which the DSB is repaired through copying of another

chromosome with a homologous template, inter-chromosomal interactions during NHEJ repair are greatly suppressed (Lee et al., 2008). The role of NHEJ in yeast is still being investigated. Recently, it was shown that DSBs induced through different mechanisms during G1, either through an endonuclease cut or by ionizing radiation (IR), are processed differently. While endonuclease-induced lesions in G1 are not resected and repair primarily through NHEJ (Aylon et al., 2004; Barlow et al., 2008; Ira et al., 2004), IR-induced lesions are resected during G1, and many of these lesions actually persist into S phase, where they are repaired through HR (Barlow et al., 2008). Also, religation of chromosome fragments in the absence of the required NHEJ proteins in yeast led to the discovery of a related mechanism, microhomology-mediated end joining (MMEJ), in which resection creates ssDNA that is annealed based on only minimal complementarity and the molecule fragments are religated (Ma et al., 2003). Though the genetic control of NHEJ and MMEJ are different, they both involve ligation of a broken molecule in the absence of a homologous donor, and they are both critical to DSB repair in their respective contexts (Lee and Lee, 2007; Ma et al., 2003). Notably, NHEJ is more prevalent in mammalian cells compared to yeast, and is critical in antibody development (reviewed in (Sonoda et al., 2006; Stavnezer et al., 2008)).

2.3. Yeast Recombination Proteins

A number of genetic screens for mutants sensitive to DNA damaging agents or with altered recombination phenotypes has identified many of the central players

in HR in *S. cerevisiae*. Many of the primary players belong to the *RAD52* epistasis group of genes, which include *RAD50*, *MRE11*, *XRS2*, *RAD51*, *RAD55*, *RAD57*, *RAD54*, *RDH54/TID1*, and *RAD59*. Other proteins are essential for resection, ligation, chromatin remodeling, etc. Though DSB repair is a multi-faceted process, this brief review will focus on the main participants involved in post-DSB resection, nucleoprotein filament formation, synapsis, and DNA synthesis associated with GC (SDSA), BIR, and SSA.

DSBs that occur in vegetative cells of *S. cerevisiae* are rapidly recognized by a multi-protein complex that consists of three members of the Rad52p epistasis group: Mre11p, Rad50p, and Xrs2p. Currently, this complex is recognized to perform two essential functions. First, the crystal structure of Rad50p indicates that it forms dimers capable of tethering together the two sides of the DSB (Hopfner et al., 2002; Kaye et al., 2004; Lobachev et al., 2004), as well as playing a role in sister chromatid association during HR (Kaye et al., 2004; Williams and Tainer, 2007), making the MRX complex an important player in the physical positioning of DSB repair substrates. Second, Mre11p contains an endonucleatic activity that is now recognized to clip the ends of the DSB (Mimitou and Symington, 2008) prior to more effective and extensive 5'-to-3' resection by a number of other enzymes. Xrs2p is the least characterized of the three components of the MRX complex, but it plays a role in targeting of the MRX complex to the break site (Trujillo et al., 2003).

Only recently have the players involved in extensive post-DSB resection in yeast been identified. This is partly because resection has two distinct phases: end processing by the MRX complex, followed by extensive resection accomplished by a combination of helicase and nuclease activities (reviewed in (Mimitou and Symington, 2009)). The endonuclease Sae2p associates transiently with the MRX complex at the DSB site with kinetics that suggest it is involved in the transition between MRX-mediated end processing and efficient 5'-to-3' end resection (Lisby et al., 2004). Subsequently, the helicase Sgs1p works in concert with the endonucleatic activity of Dna2p to unwind and clip off the 5' end of free DNA strands, and/or the exonuclease Exo1p (Mimitou and Symington, 2008; Zhu et al., 2008). Redundancy appears to exist between these two alternative resection pathways (Zhu et al., 2008).

The obvious consequence of extensive 5'-to-3' resection is exposure of 3' ssDNA. Exposed ssDNA is quickly coated by RPA, the homolog of *E. coli* SSB, which protects the ssDNA and removes secondary structures. For repair by SSA, Rad52p facilitates annealing between exposed, complementary sequences on ssDNA, and repair is completed by repair synthesis and ligation ((Sugiyama et al., 1998); reviewed in (Krogh and Symington, 2004)). For GC and BIR, additional processing of the ssDNA is needed. Specifically, the 3' ssDNA tails must be coated with the DNA strand exchange protein, Rad51p, to form a nucleoprotein filament (Sung, 1994). The displacement of RPA by Rad51p requires facilitator proteins, as it has been shown in vitro that RPA outcompetes

Rad51p for ssDNA binding sites (Sung, 1997). Among these facilitator proteins is Rad52p which, in addition to helping load Rad51p onto RPA-coated ssDNA (New et al., 1998; Shinohara and Ogawa, 1998), facilitates strand exchange by pairing complementary sequences between the nucleoprotein filament and the donor chromosome (Mortensen et al., 1996). Additionally, Rad55p and Rad57p form a heterodimer that mediates formation of the Rad51p nucleoprotein filament (Sung, 1997). Finally, Rad54p is believed to play a less critical role in nucleation of the Rad51p nucleoprotein filament (Wolner et al., 2003), but Rad54p also has other, more unique roles in HR. For example, although the Rad51p nucleoprotein filament is capable of strand exchange on its own, the strand exchange process is greatly enhanced by Rad54p (Petukhova et al., 1998). This is believed to be related to the translocase (Amitani et al., 2006; Jaskelioff et al., 2003; Van Komen et al., 2000) and branch migration (Bugreev et al., 2006; Solinger and Heyer, 2001) activities of Rad54p. There is also evidence that Rad54p is important for chromatin remodeling during HR (Alexeev et al., 2003; Jaskelioff et al., 2003), although the importance of this activity for the success of HR remains unclear. *RDH54/TID1* shares significant sequence homology with *RAD54* and appears to play similar (and often redundant) roles in HR, but its activities are more critical during meiotic recombination (Klein, 1997; Shinohara et al., 1997).

Regardless of the HR repair mechanism, synthesis of new DNA is necessary to fully repair a DSB. Both SSA and GC are known to proceed through repair

synthesis, which involves polymerization by processive polymerases δ (*POL3*; Pol δ) and ϵ (*POL2*; Pol ϵ) in the absence of a replication fork (Hicks et al., 2010; Holmes and Haber, 1999; Li et al., 2009; Wang et al., 2004). Also, non-processive translesion polymerase ζ (Rev3p/Rev7p; Pol ζ) is recruited to the DSB in a checkpoint-dependent fashion (Hirano and Sugimoto, 2006), and polymerase ζ as well as translesion polymerase η (Rad30p; Pol η) are involved in repair synthesis, though the exact nature of their role in this process remains somewhat undefined (Hicks et al., 2010; Holbeck and Strathern, 1997). Repair synthesis by SSA is necessarily constrained to the broken molecule, as no other chromosome is involved in repair. Interestingly, density-transfer assays showed that all DNA synthesis during GC repair is also inherited by the recipient (broken) molecule (Ira et al., 2006). In both cases, 3' nonhomologous tails are cleaved by the Rad1p/Rad10p endonuclease (Bardwell et al., 1994; Ivanov and Haber, 1995) before ligation presumably by either Dnl4p or Cdc9p. However, mating-type switching has been shown to complete even in the absence of both of these ligase enzymes, suggesting the presence of at least one additional ligase activity in *S. cerevisiae* (Wang et al., 2004). During SSA, the Msh2p/Msh3p complex also plays a role in stabilizing the branched molecule to allow Rad1p/Rad10p cutting of the flap, especially when the direct repeats being used for annealing are short (Sugawara et al., 1997).

DNA synthesis during BIR differs from that during SSA and GC in that it is believed to involve formation of a replication fork with both leading- and lagging-

strand synthesis. Support for formation of a processive replication fork during BIR is three-pronged. First, initiation of BIR replication requires all essential S-phase replication factors, with the exception of those involved in origin recognition (Lydeard et al., 2010). This includes Cdc45p, the GINS complex (containing Sld5p, Psf1p, Psf2p, and Psf3p subunits), and Mcm2p-7p, which together provide replicative helicase activity during replication (Gambus et al., 2006), as well as the Dpt11p-Sld2p-Sld3p complex, Cdt1p, and Mcm10p, which are involved in recruiting the previously named helicase proteins (Kamimura et al., 1998; Kamimura et al., 2001; Sawyer et al., 2004). Second, all three replicate polymerases involved in S-phase replication, polymerase α -primase (Pol α), Pol δ , and Pol ϵ , participate in BIR DNA synthesis (Lydeard et al., 2007) (note that Pol α is non-essential for other HR repair (Wang et al., 2004)). Third, after the cell commits to BIR repair, the kinetics of repair suggest that DNA is being synthesized by a processive replication fork (Jain et al., 2009; Malkova et al., 1996a). Taken together, these data strongly suggest formation of a processive replication fork during BIR; however, the exact composition of the BIR replication fork is not known. Currently it is known that the BIR replication fork differs from the S-phase replication fork in its requirement for Pol32p: while it is dispensable for normal replication, it is required for ectopic BIR (Lydeard et al., 2007), and makes allelic BIR less efficient (Deem et al., 2008). It is reasonable to believe that other differences between the two forks exist, and it is even possible that strand inheritance during BIR repair differs from the semi-conservative nature observed during S-phase replication.

2.3.1. BIR and Rad51p

BIR represents a special case where the dispensability of Rad51p is not fully understood. While a *RAD51*-independent pathway of BIR has been characterized (Fasullo et al., 2001; Malkova et al., 1996a; Malkova et al., 2001), it is possible that such *RAD51*-independent BIR events result from another mechanism that can produce similar physical outcomes. *RAD51*-independent BIR remains *RAD52*-dependent, which mimics the genetic requirements of SSA (Malkova et al., 1996a). Thus, it is possible that repetitive sequences within the genome play a role in so-called *RAD51*-independent BIR events such that Rad52p facilitates annealing of complementary sequences, resulting in fragment stabilization (Downing et al., 2008; Kang and Symington, 2000).

2.4. The DNA Damage Checkpoint

In *S. cerevisiae*, two primary checkpoints exist. In S-phase, the cell cycle may be altered due to replication stress (Santocanale and Diffley, 1998) or DNA damage (Paulovich et al., 1997; Putnam et al., 2009). The second checkpoint, the G2/M checkpoint, is a cellular response to DNA damage that aims to prevent separation of sister chromatids prior to damage repair (reviewed in (Harrison and Haber, 2006)). Induction of DNA damage by both irradiation (Weinert and Hartwell, 1988) and meganucleases (Lee et al., 1998) can initiate the G2/M checkpoint (commonly referred to as the DNA damage checkpoint).

The cellular machinery that first recognizes the DSB is the MRX complex, which both stabilizes the lesion and initiates resection (see Section 2.3). Afterwards, the DNA damage checkpoint is mediated through two phosphoinositol-3-kinase-related kinase (PIKK) proteins, Mec1p and Tel1p, which are homologs of human ATR and ATM, respectively, mutations of which are associated with human disease states. The MRX complex, specifically Xrs2p, directly recruits Tel1p (Nakada et al., 2003) to the damage site, where it phosphorylates histone protein H2AX (producing gamma-H2AX), which recruits various chromatin-remodelling proteins (Downs et al., 2004; Morrison et al., 2004; van Attikum et al., 2004). Tel1p is recruited quickly to the DSB during the DNA damage checkpoint; however, its primary role in the cell appears to be during G1 arrest, as Tel1p foci form spontaneously throughout the cell cycle and disappear prior to recruitment of HR proteins during the DNA damage checkpoint (Lisby et al., 2004). Like Tel1p, Mec1p also phosphorylates histone proteins and is the more important PIKK during the DNA damage checkpoint, which is likely related to cell cycle-related regulation of post-DSB resection by Cdk1p (Ira et al., 2004). Mec1p is recruited to the damage site through its interaction with Ddc2p (Paciotti et al., 2000), which binds to RPA-coated ssDNA (thus, Mec1p arrives at the damage site after 5'-to-3' resection; (Lisby et al., 2004; Zou and Elledge, 2003)).

Concurrent with, but independent of, Mec1p localization to the site of damage, the checkpoint clamp, or 9-1-1 clamp, is loaded onto dsDNA by the so-called checkpoint clamp loader (Melo et al., 2001; Thelen et al., 1999). The clamp

loader, which consists of Rad24p along with Rfc2p-5p (Green et al., 2000), is recruited to RPA-coated ssDNA and loads the 9-1-1 clamp (Rad17p/Mec3p/Ddc3p) at 5'-ssDNA/dsDNA junctions (Lisby et al., 2004; Zou et al., 2003). Loading of the 9-1-1 clamp to the damage site activates Mec1p kinase activity (Bonilla et al., 2008), and may play a role in recruitment of other Mec1p substrates (Harrison and Haber, 2006). After activation, Mec1p initiates a phosphor-signal cascade that begins with Rad9p, which localizes to Tel1p- and Mec1p-phosphorylated H2AX (Hammet et al., 2007). Phosphorylated Rad9p interacts with the damage checkpoint effector kinase, Rad53p, bringing it into proximity of Mec1p for phosphorylation (Sun et al., 1998). Likewise, phosphorylation of the effector kinase Chk1p by Mec1p is mediated through interactions with Rad9p (Blankley and Lydall, 2004).

The effector kinases Rad53p and Chk1p have two important functions. First, both kinases play a role in cell cycle arrest through their interactions with securin (Pds1p), which inhibits anaphase by binding the separase enzyme, Esp1p (Cohen-Fix and Koshland, 1997; Yamamoto et al., 1996). Pds1p is activated by Chk1p phosphorylation (Cohen-Fix and Koshland, 1997), while both Chk1p and Rad53p prevent Pds1p degradation to maintain cell cycle arrest (Agarwal et al., 2003). Second, the DNA damage response results in transcriptional activation of damage-related genes. This includes activation of ribonucleotide reductase by Rad53p substrate, Dun1p (Chen et al., 2007; Elledge, 2003).

CHAPTER 3. MATERIALS AND METHODS

3.1. Media and Strains

3.1.1. Strain Construction

The genotypes of all strains used in this work are shown in Table 3.1.

Construction of the primary system, disomic strain AM1003-9, which contains a haploid chromosome set as well as a second, truncated copy of chromosome III, is described in (Deem et al., 2008). AM1003-9 is a chromosome III disome with the following genotype: *hmlΔ::ADE1/hmlΔ::ADE3 MATa-LEU2-tel/MATα-inc hmrΔ::HYG FS2Δ::NAT/FS2 leu2/leu2-3,112 thr4 ura3-52 ade3::GAL::HO ade1 met13*. In this strain, the HO endonuclease-induced DSBs introduced at *MATa* are predominantly repaired by BIR because the portion of the chromosome centromere-distal to *MATa* is truncated to leave only 46 bp of homology with the donor sequence. Primers used to alter AM1003-9 are described in text (below) and/or in Table 3.2.

All single-gene deletion mutants described in Chapter 4 are isogenic to AM1003-9 and were constructed using a PCR-derived *KAN-MX* module flanked by short terminal sequences homologous to the sequences flanking the open reading frame of each gene (Wach et al., 1994). The *rad9Δrad50Δ* double

mutant was created by transformation of the *rad9Δ* strain with pNKY83 digested by BglIII/EcoRI to completely delete *RAD50* replaced with *hisG-URA3-hisG*, which was selectable as URA⁺ (Alani et al., 1989).

All strains used for measuring mutagenesis (Chapter 5) also originated as AM1003-9 and were constructed using PCR-based gene disruption and direct genome modification by oligonucleotides as described (Storici et al., 2001; Storici and Resnick, 2006). First, AM1229 was constructed by deleting the *LYS2* gene in AM1003-9 from its native position on chromosome II by the *delitto perfetto* protocol (Storici et al., 2001; Storici and Resnick, 2006) which involved two steps. Initially, AM1257 was constructed by transformation of AM1003-9 with a DNA fragment generated by PCR amplification of pCORE (Storici and Resnick, 2006) using primers OL681 and OL682 (Tables 3.1, 3.2). Subsequently, AM1229 was constructed by transformation of AM1257 with a mixture of two oligonucleotides containing complementary sequences that corresponded to positions upstream and downstream of *LYS2* (OL683, OL684; Tables 3.1, 3.2). Second, AM1248 was constructed by transformation of AM1229 with a DNA fragment generated by PCR amplification of *THR4* with OL874 and OL877 to create a Thr⁺ strain

Table 3.1. List of strains used in this study.

Strain	Genotype	Source
AM1003-9	<i>MATa-LEU2-tel/MATα-inc ade1 met13 ura3-52 leu2-3,112/leu2-3,112 thr4 hmlΔ::ADE1/hmlΔ::ADE3 hmrΔ::HYG ade3::GAL-HO FS2Δ::NAT</i>	Carolyn Brennan
AM1014	AM1003-9, but <i>pol32Δ::KAN</i>	This study
AM1079	AM1003-9, but <i>rad51Δ::KAN</i>	This study
AM1152	AM1014, but <i>pho87Δ::URA3</i>	This study
AM1017	AM1003-9, but <i>rad24Δ::KAN</i>	This study
AM1228	AM1003-9, but <i>rad9Δ::KAN</i>	This study
AM1039	AM1228, but <i>rad50Δ</i>	This study
AM1887	AM1003-9, but <i>lys2::Ins(A₄)</i>	This study
AM1892	AM1003-9, but <i>lys2::Ins(A₇)</i>	This study
AM1895	AM1003-9, but <i>lys2::Ins(A₁₄)</i>	This study
AM1257	AM1003-9, but <i>lys2::pCORE</i>	This study
AM1229	AM1003-9, but <i>lys2Δ</i>	This study
AM1248	AM1229, but <i>THR4</i>	This study
AM1247	AM1248, but <i>LYS2</i> on Chr III at the “16-kb” position and <i>thr4</i>	This study
AM1291	AM1247, but <i>lys2::Ins(A₄)</i>	This study
AM1449	AM1291, but <i>MATα-inc-LEU2-tel/MATα-inc</i>	This study
AM1462-1	AM1291, but <i>msh2Δ::KAN</i>	This study
AM1555	AM1462-1, but <i>MATα-inc-LEU2-tel/MATα-inc</i>	This study
AM1599	AM1291, but <i>pol2-4</i>	This study
AM1684	AM1599, but <i>MATα-inc-LEU2-tel/MATα-inc</i>	This study
AM1601	AM1291, but <i>pol3-5DV</i>	This study
AM1685	AM1601, but <i>MATα-inc-LEU2-tel/MATα-inc</i>	This study
AM1371	AM1291, but <i>rev3Δ::KAN</i>	This study
AM1672	AM1371, but <i>MATα-inc-LEU2-tel/MATα-inc</i>	This study
AM1766	AM1291, but <i>rad30Δ::KAN</i>	This study
AM1858	AM1766, but <i>MATα-inc-LEU2-tel/MATα-inc</i>	This study
AM1575	AM1291, but <i>dun1Δ::KAN</i>	This study
AM1786	AM1575, but <i>MATα-inc-LEU2-tel/MATα-inc</i>	This study

Strain	Genotype	Source
AM1657	AM1291, but <i>sml1</i> Δ::KAN	This study
AM1788	AM1657, but <i>MATα-inc-LEU2-tel/MATα-inc</i>	This study
AM1909	AM1291, but <i>msh3</i> Δ::KAN	This study
AM1959	AM1909, but <i>MATα-inc-LEU2-tel/MATα-inc</i>	This study
AM1917	AM1599, but <i>msh3</i> Δ::KAN	This study
AM1973	AM1917, but <i>MATα-inc-LEU2-tel/MATα-inc</i>	This study
AM1915	AM1601, but <i>msh3</i> Δ::KAN	This study
AM1977	AM1915, but <i>MATα-inc-LEU2-tel/MATα-inc</i>	This study
AM1292	AM1247, but <i>lys2</i> :: <i>Ins(A₇)</i>	This study
AM1450	AM 1292, but <i>MATα-inc-LEU2-tel/MATα-inc</i>	This study
AM1466-1	AM1292, but <i>msh2</i> Δ::KAN	This study
AM1533	AM1466-1, but <i>MATα-inc-LEU2-tel/MATα-inc</i>	This study
AM1515	AM1292, but <i>pol2-4</i>	This study
AM1683	AM1515, but <i>MATα-inc-LEU2-tel/MATα-inc</i>	This study
AM1497	AM1292, but <i>pol3-5DV</i>	This study
AM1682	AM1497, but <i>MATα-inc-LEU2-tel/MATα-inc</i>	This study
AM1528	AM1292, but <i>rev3</i> Δ::KAN	This study
AM1695	AM1528, but <i>MATα-inc-LEU2-tel/MATα-inc</i>	This study
AM1708	AM1292 but <i>rad30</i> Δ::KAN	This study
AM1854	AM1708, but <i>MATα-inc-LEU2-tel/MATα-inc</i>	This study
AM1921	AM1292, but <i>msh3</i> Δ::KAN	This study
AM1983	AM1921, but <i>MATα-inc-LEU2-tel/MATα-inc</i>	This study
AM1923	AM1515, but <i>msh3</i> Δ::KAN	This study
AM1981	AM1923, but <i>MATα-inc-LEU2-tel/MATα-inc</i>	This study
AM1925	AM1497, but <i>msh3</i> Δ::KAN	This study
AM1971	AM1925, but <i>MATα-inc-LEU2-tel/MATα-inc</i>	This study
AM1293	AM1247, but <i>lys2</i> :: <i>Ins(A₁₄)</i>	This study
AM1451	AM1293, but <i>MATα-inc-LEU2-tel/MATα-inc</i>	This study
AM1355	AM1248, but <i>MATα-LEU2-tel/MATα-inc::LYS2</i>	This study

Strain	Genotype	Source
AM1411	AM1355, but <i>MATa</i> - <i>LEU2</i> -tel/ <i>MATα-inc::lys2::Ins(A₄)</i>	This study
AM1473	AM1411, but <i>MATα-inc::lys2::Ins(A₄)</i> - <i>LEU2</i> -tel/ <i>MATα-inc::lys2::Ins(A₄)</i>	This study
AM1461-1	AM1411, but <i>msh2Δ::KAN</i>	This study
AM1546	AM1461-1, but <i>MATα-inc::lys2::Ins(A₄)</i> - <i>LEU2</i> -tel/ <i>MATα-inc::lys2::Ins(A₄)</i>	This study
AM1604	AM1411, but <i>pol2-4</i>	This study
AM1686	AM1604, but <i>MATα-inc::lys2::Ins(A₄)</i> - <i>LEU2</i> -tel/ <i>MATα-inc::lys2::Ins(A₄)</i>	This study
AM1676	AM1411, but <i>pol3-5DV</i>	This study
AM1850	AM1676, but <i>MATα-inc::lys2::Ins(A₄)</i> - <i>LEU2</i> -tel/ <i>MATα-inc::lys2::Ins(A₄)</i>	This study
AM1523	AM1411, but <i>rev3Δ::KAN</i>	This study
AM1723	AM1523, but <i>MATα-inc::lys2::Ins(A₄)</i> - <i>LEU2</i> -tel/ <i>MATα-inc::lys2::Ins(A₄)</i>	This study
AM1710	AM1411, but <i>rad30Δ::KAN</i>	This study
AM1778	AM1710, but <i>MATα-inc::lys2::Ins(A₄)</i> - <i>LEU2</i> -tel/ <i>MATα-inc::lys2::Ins(A₄)</i>	This study
AM1569	AM1411, but <i>dun1Δ::KAN</i>	This study
AM1903	AM1569, but <i>MATα-inc::lys2::Ins(A₄)</i> - <i>LEU2</i> -tel/ <i>MATα-inc::lys2::Ins(A₄)</i>	This study
AM1785	AM1411, but <i>sml1Δ::KAN</i>	This study
AM1790	AM1785, but <i>MATα-inc::lys2::Ins(A₄)</i> - <i>LEU2</i> -tel/ <i>MATα-inc::lys2::Ins(A₄)</i>	This study
AM1968	AM1411, but <i>msh3Δ::KAN</i>	This study
AM2029	AM1968, but <i>MATα-inc::lys2::Ins(A₄)</i> - <i>LEU2</i> -tel/ <i>MATα-inc::lys2::Ins(A₄)</i>	This study
AM1912	AM1604, but <i>msh3Δ::KAN</i>	This study
AM1961	AM1912, but <i>MATα-inc::lys2::Ins(A₄)</i> - <i>LEU2</i> -tel/ <i>MATα-inc::lys2::Ins(A₄)</i>	This study
AM1965	AM1676, but <i>msh3Δ::KAN</i>	This study
AM2028	AM1965, but <i>MATα-inc::lys2::Ins(A₄)</i> - <i>LEU2</i> -tel/ <i>MATα-inc::lys2::Ins(A₄)</i>	This study
AM1827	AM1411, but <i>mlh1Δ::KAN</i>	This study
AM1998	AM1827, but <i>MATα-inc::lys2::Ins(A₄)</i> - <i>LEU2</i> -tel/ <i>MATα-inc::lys2::Ins(A₄)</i>	This study
AM1407	AM1355, but <i>MATa</i> - <i>LEU2</i> -tel/ <i>MATα-inc::lys2::Ins(A₇)</i>	This study
AM1472	AM1407, but <i>MATα-inc::lys2::Ins(A₇)</i> - <i>LEU2</i> -tel/ <i>MATα-inc::lys2::Ins(A₇)</i>	This study
AM1464	AM1407, but <i>msh2Δ::KAN</i>	This study
AM1550	AM1464, but <i>MATα-inc::lys2::Ins(A₇)</i> - <i>LEU2</i> -tel/ <i>MATα-inc::lys2::Ins(A₇)</i>	This study
AM1612	AM1407, but <i>pol2-4</i>	This study

Strain	Genotype	Source
AM1687	AM1612, but <i>MATα-inc::lys2::Ins(A₇)-LEU2-tel/MATα-inc::lys2::Ins(A₇)</i>	This study
AM1613	AM1407, but <i>pol3-5DV</i>	This study
AM1688	AM1613, but <i>MATα-inc::lys2::Ins(A₇)-LEU2-tel/MATα-inc::lys2::Ins(A₇)</i>	This study
AM1518	AM1407, but <i>rev3Δ::KAN</i>	This study
AM1674	AM1518, but <i>MATα-inc::lys2::Ins(A₇)-LEU2-tel/MATα-inc::lys2::Ins(A₇)</i>	This study
AM1709	AM1407, but <i>rad30Δ::KAN</i>	This study
AM1856	AM1709, but <i>MATα-inc::lys2::Ins(A₇)-LEU2-tel/MATα-inc::lys2::Ins(A₇)</i>	This study
AM1798	AM1407, but <i>msh3Δ::KAN</i>	This study
AM1902	AM1798, but <i>MATα-inc::lys2::Ins(A₇)-LEU2-tel/MATα-inc::lys2::Ins(A₇)</i>	This study
AM1820	AM1612, but <i>msh3Δ::KAN</i>	This study
AM1996	AM1820, but <i>MATα-inc::lys2::Ins(A₇)-LEU2-tel/MATα-inc::lys2::Ins(A₇)</i>	This study
AM1962	AM1613, but <i>msh3Δ::KAN</i>	This study
AM2000	AM1962, but <i>MATα-inc::lys2::Ins(A₇)-LEU2-tel/MATα-inc::lys2::Ins(A₇)</i>	This study
AM1378	AM1355, but <i>MATa-LEU2-tel/MATα-inc::lys2::Ins(A₁₄)</i>	This study
AM1474	AM1407, but <i>MATα-inc::lys2::Ins(A₁₄)-LEU2-tel/MATα-inc::lys2::Ins(A₁₄)</i>	This study
AM1284	AM1248, but <i>LYS2</i> on Chr III at the “36-kb” position	This study
AM1482	AM1284, but <i>lys2::Ins(A₄)</i>	This study
AM1649	AM1482, but <i>MATα-inc-LEU2-tel/MATα-inc</i>	This study
AM1721	AM1482, but <i>msh2Δ::KAN</i>	This study
AM2027	AM1721, but <i>MATα-inc-LEU2-tel/MATα-inc</i>	This study
AM1630	AM1482, but <i>pol2-4</i>	This study
AM1675	AM1630, but <i>MATα-inc-LEU2-tel/MATα-inc</i>	This study
AM1628	AM1482, but <i>pol3-5DV</i>	This study
AM1690	AM1628, but <i>MATα-inc-LEU2-tel/MATα-inc</i>	This study
AM1634	AM1482, but <i>rev3Δ::KAN</i>	This study
AM1692	AM1634, but <i>MATα-inc-LEU2-tel/MATα-inc</i>	This study
AM1699	AM1482, but <i>rad30Δ::KAN</i>	This study
AM1779	AM1699, but <i>MATα-inc-LEU2-tel/MATα-inc</i>	This study
AM1594	AM1482, but <i>dun1Δ::KAN</i>	This study

Strain	Genotype	Source
AM1787	AM1594, but <i>MATα-inc-LEU2-tel/MATα-inc</i>	This study
AM1733	AM1482, but <i>smI1Δ::KAN</i>	This study
AM1789	AM1733, but <i>MATα-inc-LEU2-tel/MATα-inc</i>	This study
AM1919	AM1482, but <i>msh3Δ::KAN</i>	This study
AM1979	AM1919, but <i>MATα-inc-LEU2-tel/MATα-inc</i>	This study
AM1806	AM1630, but <i>msh3Δ::KAN</i>	This study
AM1900	AM1806, but <i>MATα-inc-LEU2-tel/MATα-inc</i>	This study
AM1814	AM1628, but <i>msh3Δ::KAN</i>	This study
AM2026	AM1814, but <i>MATα-inc-LEU2-tel/MATα-inc</i>	This study
AM1833	AM1482, but <i>mlh1Δ::KAN</i>	This study
AM1863	AM1833, but <i>MATα-inc-LEU2-tel/MATα-inc</i>	This study
AM1313	AM1284, but <i>lys2::Ins(A₇)</i>	This study
AM1468	AM1313, but <i>MATα-inc-LEU2-tel/MATα-inc</i>	This study
AM1465-1	AM1313, but <i>msh2Δ::KAN</i>	This study
AM1542	AM1465-1, but <i>MATα-inc-LEU2-tel/MATα-inc</i>	This study
AM1607	AM1313, but <i>pol2-4</i>	This study
AM1742	AM1607, but <i>MATα-inc-LEU2-tel/MATα-inc</i>	This study
AM1615	AM1313, but <i>pol3-5DV</i>	This study
AM1689	AM1615, but <i>MATα-inc-LEU2-tel/MATα-inc</i>	This study
AM1521	AM1313, but <i>rev3Δ::KAN</i>	This study
AM1670	AM1521, but <i>MATα-inc-LEU2-tel/MATα-inc</i>	This study
AM1740	AM1313, but <i>rad30Δ::KAN</i>	This study
AM1781	AM1740, but <i>MATα-inc-LEU2-tel/MATα-inc</i>	This study
AM1802	AM1313, but <i>msh3Δ::KAN</i>	This study
AM1975	AM1802, but <i>MATα-inc-LEU2-tel/MATα-inc</i>	This study
AM1809	AM1607, but <i>msh3Δ::KAN</i>	This study
AM1905	AM1809, but <i>MATα-inc-LEU2-tel/MATα-inc</i>	This study
AM1811	AM1615, but <i>msh3Δ::KAN</i>	This study
AM1899	AM1811, but <i>MATα-inc-LEU2-tel/MATα-inc</i>	This study

Strain	Genotype	Source
AM1312	AM1284, but <i>lys2::Ins(A₁₄)</i>	This study
AM1469	AM1313, but <i>MATα-inc-LEU2-tel/MATα-inc</i>	This study

(Tables 3.1, 3.2). Third, three derivatives of AM1248 with the *LYS2* ORF inserted at three different positions of the *MAT α -inc* containing chromosome were created. The primers used to create the three strains were: 1) To create AM1355 with *LYS2* in the *MAT α -inc* gene (“*MAT*” position), OL1333 and OL1334; 2) To create AM1247 with *LYS2* at the 16-kb position inserted between *RSC6* and *THR4*, OL994 and OL997; and 3) To create AM1284 with *LYS2* at the 36-kb position between *SED4* and *ATG15*, OL1021 and OL1022 (Tables 3.1, 3.2). Finally, the *lys2(A₄)*, *lys2(A₇)*, or *lys2(A₁₄)* frameshift reporters were inserted into each of these constructs by one-step transformation of *HpaI*-digested plasmid and Ura⁺ selection (Tran et al., 1997). Insertion of the fragment was confirmed by sequencing with primers OL1106 and OL1199. All single-gene deletion mutants in any of the parent strains were constructed by transformation with a PCR-derived *KAN-MX* module flanked by terminal sequences homologous to the sequences flanking the open reading frame of each gene (Wach et al., 1994). All constructs were confirmed by PCR (Table 3.2) and by phenotype. Proofreading-deficient mutant *pol3-5DV* was constructed as described (Jin et al., 2005) and confirmed by PCR followed by restriction analysis with *HaeIII*. Control no-DSB strains were obtained from each experimental strain by plating on YEP-Gal media, followed by selection of Ade⁺Leu⁺ colonies resulting from GC repair of the DSB at *MAT α* .

Table 3.2. Primers used in strain construction and characterization.

Malkova Lab Database Name	5' to 3' Sequence	Description
OL17	GAGTTAGCCTTAGTGGAAGCCTTC	P1 used to examine HCO molecules (see Figure 4.1A)
OL8	GATATGTCGGTATCTAGAATGTAG	P2 used to examine HCO molecules (see Figure 4.1A)
OL5	CTACATTCTAGATACCGACATATC	P3 used to examine HCO molecules (see Figure 4.1A)
OL26	CCTCGACATCATCTGCCC	Used to confirm insertion of <i>KAN-MX</i> (Wach et al.) to delete gene function. Within TEF terminator, 174 bp from the MX18 primer pointing towards the MX18 primer.
OL27	CAGCGAGGAGCCGTAATTTT	Used to confirm insertion of <i>KAN-MX</i> (Wach et al.) to delete gene function. Within the TEF promote, 269 bp from the MX19 primer pointing towards the MX19 primer.
OL366	CTTACCTAGTAGCATGGCAACACT	P1 to amplify <i>pol32::KAN</i> fragment
OL367	TTCCGACGGAAGTAGTAAACGCG	P2 to amplify <i>pol32::KAN</i> fragment
OL368	GGATGAAGATTCAGTGGCGACAGT	P1 to confirm integration of <i>pol32::KAN</i> fragment
OL369	TCATTCTAACACAGCTCAGTGTGC	P2 to confirm integration of <i>pol32::KAN</i> fragment
OL764	GACCCGCAACTTCAACACCACCACGC	P1 to confirm elimination of wt <i>POL32</i>
OL765	TAATTTCTTGGCCATGGATGGGCC	P2 to confirm elimination of wt <i>POL32</i>
OL370	CGAAGGCTCACGGTAAATCTTCCA	P1 to amplify <i>rad24::KAN</i> fragment
OL371	CAAGGAATCTATAGAAGAAGATCC	P2 to amplify <i>rad24::KAN</i> fragment
OL372	GCACAGGCCCTGTCCCATATCCTT	P1 to confirm integration of <i>rad24::KAN</i> fragment
OL373	GGTGAAGCTAGTACAAGCTGCACC	P2 to confirm integration of <i>rad24::KAN</i> fragment
OL785	TATGGCCACTTGCTCCAAACAATT	P1 to confirm elimination of wt <i>RAD24</i>
OL786	AGGGACAGAAGGCTTCGCATGTTG	P2 to confirm elimination of wt <i>RAD24</i>
OL741	CAAGATGCAAGCCTAAAATATATGC	P1 to amplify <i>rad9::KAN</i> fragment

Malkova Lab Database Name	5' to 3' Sequence	Description
OL742	CGGCTTTGAATTTTCAGAGTGCAG	P2 to amplify <i>rad9::KAN</i> fragment (antisense)
OL743	TGCGGGAGAACACCGATCTTATCT	P1 to confirm integration of <i>rad9::KAN</i> fragment
OL744	GCTCCCCATCAAAATAAGGTCTAA	P2 to confirm integration of <i>rad9::KAN</i> fragment
OL809	GCGCAGGTAGAATGCTTACAATTG	P1 to confirm elimination of wt <i>RAD9</i> (antisense)
OL810	CATCATGTCTTGGACTCTCGTCAAG	P2 to confirm elimination of wt <i>RAD9</i>
OL662	GGACGGTAAATGTTGGAAATGCACCA	P1 to amplify <i>rad51::KAN</i> fragment
OL663	CGTCGAAACGAAGACAAGGA	P2 to amplify <i>rad51::KAN</i> fragment
OL664	ACCGGCAGTGCCATCCGGTCACAT	P1 to confirm integration of <i>rad51::KAN</i> fragment
OL665	GTCAACCGTACTTCTCTTGCTGTT	P2 to confirm integration of <i>rad51::KAN</i> fragment
OL815	CTCCTGCAATCCGCCACCATCGCC	P1 to confirm elimination of wt <i>RAD51</i>
OL816	GGCACATTCTTCCACCACGCGATT	P2 to confirm elimination of wt <i>RAD51</i>
OL681	CCACGAGCACCAGCACCTGAAGCAACT AGACTTATTTGCGCTTGAGTTAGgagctcggttcgacactgg	P1 to amplify <i>lys2::pCORE</i> fragment. Caps: genomic sequence; LC: pCORE sequence
OL682	GGTCTGGATAGAGAAGTTGGATAATCCA ACTCTTTCAGTGTTACCACATGtccttaccattagttgatc	P2 to amplify <i>lys2::pCORE</i> fragment. Caps: genomic sequence; LC: pCORE sequence
OL683	CATATTTAATTATTGTACATGGACATAT CATACGTAATGCTCAACCTgcaagtgaattccgctggcaaactattgaagagttttcctcgc	IRO 1 to remove <i>lys2::pCORE</i> ; complementary to OL684
OL684	gcgaggaaaactcttcaatagttttgccagcggaattccacttgcA GGTTGAGCATTACGTATGATATGTCCAT GTACAATAATTAAATATG	IRO 2 to remove <i>lys2::pCORE</i> ; complementary to OL683
OL685	AATGCGAGGTTTTCTTGGTCA	P1 to confirm recombination by OL683, OL684

Malkova Lab Database Name	5' to 3' Sequence	Description
OL686	ATGGTCACTTGCTGCCTGAAA	P2 to confirm recombination by OL683, OL684 (antisense)
OL874	TGCTACCACCTTGGATGTAGATGT	P1 to amplify wt <i>THR4</i> fragment
OL877	GTGTCATCGATGATAATGATCCGT	P2 to amplify wt <i>THR4</i> fragment
OL954	GCCTTCACCTCGTTTGTCTTCATCT	P1 to confirm integration of pNKY83 (<i>rad50S</i> mutation)
OL969	CTAAGCAACAGAAGCGTTATCAC	P2 to confirm integration of pNKY83 (<i>rad50S</i> mutation)
OL958	CGCCACCTCTTATCCTCACCTGCT	P1 to confirm presence of HISG (<i>rad50S</i> mutation)
OL959	AGCAGGTGAGGATAAGAGGTGGCG	P2 to confirm presence of HISG (<i>rad50S</i> mutation)
OL956	TCATATTGAGTCCATTGGCACTCG	P1 to confirm elimination of wt <i>RAD50</i>
OL957	GTGGCGTAATTGCACTAGACGAACCT	P2 to confirm elimination of wt <i>RAD50</i>
OL994	GAGTAGTGACCGTGCGAACAAAAGAGT CATTACAACGAGGAAATAGAAGaattacat aaaaaattccggcg	P1 to insert <i>LYS2</i> into intergenic region 3' of <i>THR4</i> on Chr III. Caps: target sequence; LC: <i>LYS2</i> sequence
OL997	ATATAAGATACACAATATAGATAGTATT AAAAAAACGTGTATACGTTATTttaagctgct gcggagcttcc	P2 to insert <i>LYS2</i> into intergenic region 3' of <i>THR4</i> on Chr III. Caps: target sequence; LC: <i>LYS2</i> sequence
OL1004	CTTCCACTGCCAAGTATAGAACTA	P1 inside <i>LYS2</i> to determine presence of <i>LYS2</i> on Chr III
OL1005	AACTATCATGAGGCACATCGAGC	P2 inside <i>LYS2</i> to determine presence of <i>LYS2</i> on Chr III
OL1006	GACAGGTCACCTAATGGGCAATATCT	P1 to confirm integration of <i>LYS2</i> into intergenic region 3' of <i>THR4</i> on Chr III
OL1007	AAGACCACCGTCAGTGGCCAGACC	P2 to confirm integration of <i>LYS2</i> into intergenic region 3' of <i>THR4</i> on Chr III
OL1021	AAATCGTAAATACATAGGCTGGGCCATA TACACTAACATGTGTCGTGACCAttaagctgc tgcgagcttcc	P1 to insert <i>LYS2</i> between <i>SED4</i> and <i>ATG15</i> on Chr III. Caps: target sequence; LC: <i>LYS2</i> sequence

Malkova Lab Database Name	5' to 3' Sequence	Description
OL1022	TTATTTTCTTTCCGATGTTATGCTTATTA TATCTGTGATTGATAAGAGAAaattacataaaa aattccggcgg	P2 to insert <i>LYS2</i> between <i>SED4</i> and <i>ATG15</i> on Chr III. Caps: target sequence; LC: <i>LYS2</i> sequence
OL1065	AGCACCATATATCGGATATCCGACGTC	P1 to check integration of <i>LYS2</i> between <i>SED4</i> and <i>ATG15</i> . Caps: target sequence; LC: <i>LYS2</i> sequence
OL1066	TGCATCCTAGATGCAAAGGAGAAGC	P2 to check integration of <i>LYS2</i> between <i>SED4</i> and <i>ATG15</i> . Caps: target sequence; LC: <i>LYS2</i> sequence
AM1104	AAATGTCACTGCAAATTATGCGGAAGAC	P1 to make 400-bp sequencing fragment to characterize <i>LYS2::Ins</i> frameshift mutations
OL1181	CCATCCACTTCTCATCTGAAAGACC	P2 to make 400-bp sequencing fragment to characterize <i>LYS2::Ins</i> frameshift mutations
AM1106	GTTCGTACCCCTCTCGAGAATA	P1 to sequence 400-bp <i>LYS2::Ins</i> fragment made with OL1104 and OL1181
OL1199	ATTTGAGGCAAATTTTTCGTTCCAA	P2 to sequence 400-bp <i>LYS2::Ins</i> fragment made with OL1104 and OL1181
OL1133	TTTATCATATCTTGAGTTACCACATTA TACCAACCCATCCGCCGATTTaattacataaaa aattccggcgg	P1 to insert <i>LYS2</i> into <i>MATα-inc</i> . Caps: target sequence; LC: <i>LYS2</i> sequence
OL1134	TTCAGCGAGCAGAGAAGACAAGACATT TTGTTTTACACCGGAGCCAAACTGaagetg tcgagacttc	P2 to insert <i>LYS2</i> between <i>SED4</i> and <i>ATG15</i> on Chr III. Caps: target sequence; LC: <i>LYS2</i> sequence
OL1138	TGCGGGTTAAGGTTAAAAAAGAGC	P1 to make <i>dun1::KAN</i> fragment
OL1140	GAAGATAAGGAATAGAAGCCCCTG	P2 to make <i>dun1::KAN</i> fragment
OL1137	TCCGTTGAGGAAAGGTGAAGGCCC	P1 to confirm integration of <i>dun1::KAN</i> fragment
OL1139	CACAACTGTAAGAGATGTCAGGCA	P2 to confirm integration of <i>dun1::KAN</i> fragment
OL1141	ACAGCAACAAAGCTCGGTCTCATT	P1 to confirm elimination of wt <i>DUN1</i>

Malkova Lab Database Name	5' to 3' Sequence	Description
OL1142	TTCACCAGATGGCCCAGACAAGTG	P2 to confirm elimination of wt <i>DUN1</i>
OL1222	TAATAGCGGCGTTTATCTGCTCAG	P1 to make <i>sml1::KAN</i> fragment
OL1223	GCCGTCGAACGTCGCGGCGGTCTT	P2 to make <i>sml1::KAN</i> fragment
OL1225	CCCAAGGATCACGTTCCCTTCTGCC	P1 to confirm integration of <i>sml1::KAN</i> fragment
OL1224	TTCTGTGGCCGTGGAATTAGCAGC	P2 to confirm integration of <i>sml1::KAN</i> fragment
OL1147	GGTACGCAATGTGGAAGGGGCTTG	P1 to confirm elimination of wt <i>SML1</i>
OL1148	GGATTTGGAGGAGAGACTCAACTC	P2 to confirm elimination of wt <i>SML2</i>
OL1154	ATGTCCTCCACTAGGCCAGAGCTAAAAT TCTCTGATGTATCAGAGGAGAGAACTT CTAAAGAAGTATATcagctgaagcttcgtacgc	P1 to make <i>msh2::KAN</i> fragment. Caps: target sequence; LC: MX2 plasmid sequence
OL1155	TTATAACAACAAGGCTTTTATATATTTT AGGTAATTATCGTTTTCTTTCTGGTTC ATTGCTATAGCAgcatagccactagtggatctg	P2 to make <i>msh2::KAN</i> fragment. Caps: target sequence; LC: MX2 plasmid sequence
OL1158	TCCAATCAGAACTCCAGCACTCCG	P1 to confirm integration of <i>msh2::KAN</i> fragment from OL1154, OL1155. Also used with OL1159 to make <i>msh2::KAN</i> fragment with long targeting tails from genomic DNA
OL1159	TCCAGTGGTCTAGAGACCCCTG	P2 to confirm integration of <i>msh2::KAN</i> fragment from OL1154, OL1155. Also used with OL1158 to make <i>msh2::KAN</i> fragment with long targeting tails from genomic DNA
OL1210	CGAACCATGTGTCTTCTTCTGACGA	P1 to check <i>msh2::KAN</i> integration of fragment made with OL1158 and OL1159
OL1211	CAGAAGACTTTGCGGAGGAAGCACC	P2 to check integration of <i>msh2::KAN</i> fragment made with OL1158 and OL1159
OL1216	CGCGTAGTTCTGAAGACTCTAGT	FP to check integration of <i>msh2::KAN</i> fragment made by OL1210 and OL1211

Malkova Lab Database Name	5' to 3' Sequence	Description
OL1217	GAGGTTATGTATCAGTTCTCTACTG	RP to check integration of <i>msh2::KAN</i> fragment made by OL1210 and OL1211
OL1156	TCGACAATATCAAGCATTCACC	P1 to confirm elimination of wt <i>MSH2</i>
OL1157	GTTGAGCCTGGTATTTTCAGATCAG	P2 to confirm elimination of wt <i>MSH2</i>
OL1183	ATGTCAAAATTTACTTGGAAGGAGTTGA TTCAGCTTGGTTCCCCCAGTAAAGCATA CGAGcagctgaagcttcgtacgc	P1 to make <i>rad30::KAN</i> fragment. Caps: target sequence; LC: MX2 plasmid sequence
OL1184	AGATGTAACCTGTTTCTTCTGAGGTGTG GCAGTATGTTGTGAGTTTGGTCTTTTCCG TGAgcataggccactagtgatctg	P2 to make <i>rad30::KAN</i> fragment. Caps: target sequence; LC: MX2 plasmid sequence
OL1242	GAACCCTCATGACATCATTGAAGG	P1 to make <i>rad30::KAN</i> fragment
OL1243	CAAACCAATTCCTGCTTTAAACGC	P2 to make <i>rad30::KAN</i> fragment
OL1244	GTCAAGCATAGCGGTAACATCCAAT	P1 to confirm integration of <i>rad30::KAN</i> fragment
OL1245	AATATTACTTGCAATTATTATTCTTCAG	P2 to confirm integration of <i>rad30::KAN</i> fragment
OL1193	ACCGGATCTTCTTTGCTTAAGCC	P1 to confirm elimination of wt <i>RAD30</i>
OL1194	GGCTCTTCAAGAGCACGCAGACTA	P2 to confirm elimination of wt <i>RAD30</i>
OL1185	GAGGATACGAAGATTCCTCAAAAG	P1 to make <i>rev3::KAN</i> fragment
OL1186	CTTTGATATATACAACCTGTGTTTGTAC	P2 to make <i>rev3::KAN</i> fragment
OL1198	GATATGACCCTGTCAAACAACCTTTGA	P1 to confirm integration of <i>rev3::KAN</i> fragment
OL1196	GTTCCATTCCACTCAAATTTGGG	P2 to confirm integration of <i>rev3::KAN</i> fragment
OL1197	CGTGTGCAGGACGTGCAGTTATCGT	P1 to confirm elimination of wt <i>REV3</i>
OL1203	GCAGGCTTTCACCGTGCGATGGG	P2 to confirm elimination of wt <i>REV3</i>

Malkova Lab Database Name	5' to 3' Sequence	Description
OL1226	ATTCCAATCAGTTATTCGAGGCCAG	P1 to amplify fragment to verify integration of <i>pol2-4</i> mutation by sequencing
OL1227	CACCATTGAAGGTGGATATAACAGT	P2 to amplify fragment to verify integration of <i>pol2-4</i> mutation by sequencing
OL1228	GTAGAAGCGCCACTTCATCG	P1 to sequence fragment made with OL1226 and OL1227 to verify integration of <i>pol2-4</i> mutation
OL1229	GGTGAATGATTTCCATA	P1 to amplify fragment to verify integratin of <i>pol3-5DV</i> by restriction digest
OL1230	GGTACATCGTAATAACCACG	P2 to amplify fragment to verify integratin of <i>pol3-5DV</i> by restriction digest
OL1298	GATCACAATATCTTAACCTACTCTG	P1 to amplify <i>msh3::KAN</i> fragment
OL1299	AGATGCTGTGTTCAAATCACGG	P2 to amplify <i>msh3::KAN</i> fragment
OL1300	GTGGTCGTTCTTAAGAAACCAAGA	P1 to confirm integration of <i>msh3::KAN</i>
OL1301	ATCTACGGACGACCTGTCTAA	P2 to confirm integration of <i>msh3::KAN</i>
OL1302	GCTATCATTAGTTACTGTTGTGCT	P1 to confirm elimination of wt <i>MSH3</i>
OL1303	ATCATATGGATTACGTGGAAGAAC	P2 to confirm elimination of wt <i>MSH3</i>
OL1318	GTCATGAGGCGTATGTATTATCGG	P1 to amplify <i>mlh1::KAN</i> fragment
OL1319	GGA CTCGGTCTTTGGTACCGTTG	P2 to amplify <i>mlh1::KAN</i> fragment
OL1320	CTTAAGTCCTCATCTGAATCGCCTC	P1 to confirm integration of <i>mlh1::KAN</i>
OL1321	GGGACAAGGTACAGCTTCTAGATT	P2 to confirm integration of <i>mlh1::KAN</i>
OL1322	CGCATCGATGGAATTCTCCATCA	P1 to confirm elimination of wt <i>MLH1</i>
OL1323	GACACATTCTCAAGGATGTCGTGG	P2 to confirm elimination of wt <i>MLH1</i>

Abbreviations: HCO = half-crossover.

3.1.1.1. One-step Transformation

Most simple deletion strains (either using the *KAN-MX* library (Wach et al., 1994) or insertion of a linearized plasmid) were constructed by one-step transformation (Chen et al., 1992). 1 mL of saturated liquid culture grown overnight at 30° C with agitation in YPD (approximately 2×10^8 cells/mL) was centrifuged at 3,000 x g to harvest cells. Cells were resuspended in 100 µL one-step buffer, consisting of 100 mM dithiothreitol and 0.2 M lithium acetate in 40% poly-ethylene glycol (3350) (5.5). To this mixture, 30 µg single-stranded salmon sperm DNA (heated to 100° C and placed directly on ice) and between 50 ng and 1 µg of precipitated pcr fragment or plasmid DNA was added. Mixture was incubated at 45° C for 30 min, then either plated directly onto selective medium, or outgrown for 4 to 5 hours at 30° C with agitation before plating on antibiotic medium. Plates were incubated at 30° C for 3 to 5 days. In cases where *URA3* was used for positive selection, the marker may have been retrieved by allowing cells to grow for 2 days on YPD plate medium, followed by growth on 5-fluoro-orotic acid plate medium to select for recombinants that lost the *URA3* marker (Alani et al., 1987). Transformants were confirmed genetically and/or by pcr analysis.

3.1.1.2. Delitto Perfetto

Parent strains used in mutagenesis studies required removal and/or movement of genetic markers by the *delitto perfetto* protocol (Storici et al., 2001; Storici and Resnick, 2006). To insert the selectable *KAN-MX* and *URA3* cassettes, a 5-mL

inoculum was grown to saturation (approximately 2×10^8 cells/mL) overnight at 30° C with agitation in YPD. 1.5 mL of cells was diluted into 50 mL fresh YPD liquid and grown at 30° C while shaking at 250 rpm for approximately 3 hours, or until cells were in logarithmic phase (OD_{600} of ~0.3 to 0.6). The entire culture was centrifuged at 3,000 x g for 3 min to harvest cells, washed with 50 mL ddH₂O, centrifuged as previously, washed in 0.1 M lithium acetate 1x TE (7.5) solution, centrifuged as previously, and re-suspended in 250 µL of 0.1 M lithium acetate 1x TE (7.5) solution. Transformation reactions consisted of 50 µL of 0.1 M lithium acetate 1x TE (7.5) cell suspension, 300 µL 0.1 M lithium acetate 1x TE (7.5) in 50% PEG (4000), approximately 50 µg denatured salmon sperm DNA, and 10 µL of concentrated pcr fragment (from approximately 100 µL of PCR reactions) obtained by amplifying a 3.2-kb piece of the pCORE plasmid (Storici and Resnick, 2006) that includes the *KAN-MX* and *URA3* markers. The reaction is incubated at 30° C with agitation for 30 min, then heat shocked for 15 min at 42° C. 1 mL liquid YPD was added to reactions, and reactions were outgrown for 4 to 5 hours at 30° C with agitation before plating on G418 antibiotic medium and Ura drop-out medium. Plates were grown for 3 to 5 days at 30° C.

Complete elimination of a section of the genome was accomplished by transformation with oligonucleotides designed to eliminate the *KAN-MX* and *URA3* cassettes and flanking regions. This transformation protocol is the same as above, but replaces the pCORE pcr fragment with 0.5 nmol of each of two

complementary oligonucleotides (approximately 100 bp each) that have been mixed, denatured at 100° C for ≥5 min and placed directly on ice. After incubation and heat shock (see above), cells are plated on non-selective medium and grown overnight at 30° C. Replica plating onto 5-fluoro-orotic acid plate medium allows selection of recombinants lacking the *URA3* cassette. Recombinants are confirmed genetically and/or by PCR analysis.

3.1.2. Media and Growth Conditions

3.1.2.1. Media

Non-selective growth of all yeast strains was accomplished in YPD medium, which contained 1% yeast extract, 2% Bacto peptone, 2% dextrose, and 8 mL 0.5% adenine in 0.05N HCl. YEP-galactose was made using the same recipe, but with dextrose substituted by galactose. A 20% w/v galactose solution was dissolved in dH₂O, filter sterilized, and added to autoclaved media to a concentration of 2% w/v. For induction of the GAL::HO DSB, which requires glucose-free medium, YEP-Lactate was made with 1% yeast extract and 2% Bacto peptone media supplemented with 3.7% lactic acid. All media was adjusted to pH 5.5.

For selection of yeast auxotrophic markers, yeast were grown in synthetic drop-out media missing the nutrient required by the auxotroph. Drop-out medium contained 1% yeast extract, 2% Bacto peptone, 2% dextrose, and amino acids as required for selection (Guthrie and Fink, 1991). For pop-in/pop-out constructs,

loss of *URA3* was screened for on minimal medium containing 1 g/L fluoro-ototic acid. The pH of all yeast media (except medium containing fluoro-ototic acid, which was not pH-adjusted due to its need to stay below a pH of 5.0) was adjusted to 5.5. Plate media contained between 20 g and 25 g granulated agar.

Selection for drug resistance was accomplished using YPD media with addition of the drug of interest. Drugs used included G418 (either 0.3 g/L or 0.5 g/L) and nourseothricin sulfate (0.1 g/L). Drugs were dissolved in 5 to 10 mL ddH₂O and filter sterilized prior to addition to media cooled to approximately 55° C.

3.1.2.2. Measurement of growth

Growth of strains in YEPD was measured by OD₆₀₀ (SpectraMax M2, Molecular Devices) after 2 mL of saturated inoculum was diluted into 50 mL of YEPD medium. Cells were allowed to adjust to new media for 2 hours prior to measuring the 0h timepoint. Growth of strains in YEP-Lac was measured as described for YEPD immediately after 2 mL of saturated inoculum was diluted into 50 mL of YEP-Lac medium and followed for 18 hours.

3.2. Yeast Recombinant DNA Techniques

3.2.1. PCR

DNA fragments were amplified by PCR in 25- or 50-μL reactions in thin-walled polypropylene tubes that contained the following: 1x Buffer E (a proprietary blend of buffer and dNTPs; Genaxxon), 50 μM each of two oligonucleotide

primers specific for relevant sequences in each strand, between 10 and 50 ng template DNA, and 1 unit *Taq* polymerase (Promega). For amplifications of long or difficult fragments, 50- μ L reactions contained: 1x Ex-Taq buffer, 0.2 mM dNTPs, 2.0 mM MgCl₂, 50 μ M each of two oligonucleotide primers specific for relevant sequences in each strand, between 10 and 50 ng template DNA, and 1U *Ex-Taq* polymerase (all from Takara). In some cases, PCR screening of transformants was performed directly from cells. In these cases, no template DNA was added.

Reactions were run on a Biorad MyCycler pcr machine. A typical PCR program was: denaturation at 94° C for 1 min, followed by 40 cycles of denaturation at 94° C for 30 s, annealing at 58° C for 1 min, and extension at 72° C for 1.5 min. A final extension for 10 min at 72° C was also included. For amplification of the pCORE cassette, *Ex-Taq* pcr reactions were performed under the following conditions: denaturation for 2 min at 94° C, 32 cycles of denaturation 94° C for 30 s, annealing at 57° C for 30 s, and extension at 72° C for 4 min. A final extension at 72° C for 10 min was also included.

3.2.2. Restriction Digests

Restriction enzymes from New England Biolabs were used according to manufacturer's recommendations. Generally, between 5 and 10 U of enzyme was allowed to digest approximately 1 μ g of plasmid DNA for approximately

2 hrs. For genomic DNA digests, an additional 5 to 10 U of enzyme was added after approximately 2 hours and allowed to incubate overnight at the recommended temperature. Digests were visualized using agarose gel electrophoresis.

3.3. DNA Extractions

3.3.1. Glass Bead Genomic DNA Extraction from Yeast

5-mL yeast cultures grown overnight at 30° C were harvested by centrifugation at 3000 x g for 3 min, and the supernatant discarded. Cell pellets were resuspended in a lysis buffer consisting of 1% sodium dodecyl sulfate, 10 mM Tris (8.0), 1 mM EDTA (8.0). 600 µL of the cell suspension was added to approximately 300 µL of sterile glass beads, followed by addition of 400 µL of Tris-buffered 50% phenol, 48% chloroform, 2% isoamyl alcohol. Samples were vortexed at high speed for 1 min, placed on ice for ≥1 min, and vortexed for an additional 1 min. Samples were centrifuged at 15,000 rpm for 15 min at 4° C, and the aqueous phase was transferred to a clean microfuge tube. 400 µL of Tris-buffered 50% phenol, 48% chloroform, 2% isoamyl alcohol was added to the samples and the tubes were inverted several times to mix. Samples were centrifuged as previously. The resultant aqueous phase was transferred to a new microfuge tube, mixed with 50 µL 3 M ammonium acetate (5.5) and 600 µL isopropyl alcohol, and centrifuged as previously. The supernatant was discarded and the pellet was resuspended in 300 µL 1x TE buffer with 3 µL of 10 mg/mL

RNase, then incubated at 37° C for 30 min. After incubation, the samples were mixed with 30 μ L of 3 M ammonium acetate (5.5) and 300 isopropyl alcohol, then centrifuged as previously. Supernatants were discarded, and pellets were washed with 300 μ L 70% ethanol.

3.3.2. High-molecular Weight DNA Extractions

Samples were grown in YEP-Lactate media during timecourse experiments (between 50 and 100 mL per sample) or overnight in YEPD (50-mL cultures), and cells harvested by centrifugation at 3000 x g for 3 min. Pellets were washed in 50 mM EDTA (8.0), centrifuged as previously, and the supernatant removed. Pellets were gently resuspended in 400 μ L of a solution of SCE (1 M sorbitol, 0.1 M sodium citrate (5.8), 10 mM filter-sterilized EDTA) containing 25 μ L 2-mercaptoethanol and 1 mg zymolyase (100T) and incubated briefly at 45° C. 500 μ L of cell suspension was mixed with 1.2% molten low-melting point agarose in SCE cooled to 45° C and pipetted into plug molds. Plugs were allowed to solidify at 4° C for approximately 20 min, then expelled into 50-mL polypropylene tubes. Plugs were covered in 5 to 10 mL of a solution of 0.5 M EDTA, 10 mM Tris (8.0), 7% 2-mercaptoethanol, 1 μ L/mL of 10 mg/mL RNase and incubated at 37° C for at least 1 hr. After incubation, the solution was removed and replaced with 5 to 10 mL of a solution of 1% N-lauroyl sarcosine in 0.5 M EDTA (9.0) with 1 mg/mL proteinase K and incubated at 50° C over night. After incubation, the solution is removed and replaced with 5 to 10 mL of 1x TE buffer for short-term

(approximately 1 wk) storage at 4° C, or with 50 mL of 50% glycerol for longer-term storage at -20° C.

3.4. Plasmids

3.4.1. Bacterial Transformations

Plasmids were transformed in chemically competent XL1-Blue chemically competent *E. coli* cells (Stratagene) per the manufacturer's instructions. Briefly, 100 µL of cells were thawed on ice and gently mixed with 1.7 µL β-mercaptoethanol and incubated on ice with intermittent, gentle mixing for 10 min. After incubation, between 0.1 and 50 ng of plasmid DNA was added to the cells, gently mixed, and placed on ice for 30 min. Samples were heat-pulsed for 45 sec at 42° C, then placed on ice for 2 min. Then, 0.9 mL of pre-warmed (42° C) Luria broth was added to the samples, and they were grown with agitation (300 rpm) for 1 hr at 37° C. Cells were plated on Luria broth plates containing 100 µg/mL ampicillin and grown overnight at 37° C.

3.4.2. Plasmid Purification

Plasmids were isolated from *E. coli* using the Quiagen Maxiprep Kit (Quiagen). Briefly, a 5-mL inoculum of the desired strain was grown approximately 12 hrs at 37° C with agitation (300 rpm) in LB containing 100 µg/mL ampicillin. The inoculum was diluted at 1:500 into fresh LB containing 50 µg/mL ampicillin into a volume of at least 250 mL and grown for approximately 16 hrs under the same conditions. To harvest cells, samples were centrifuged at 6000 x g for 15 min at

4° C. The cell pellet was resuspended in 20 mL of Buffer P1 (50 mM Tris-HCl, 10 mM EDTA (8.0), 100 µg RNaseA). Next, 20 mL of Buffer P2 (200 mM NaOH, 1% (w/v) SDS) was added, and samples were gently inverted several times. Following a 5-min incubation at room temperature, 20 mL of chilled Buffer P3 (3 M potassium acetate (5.5)) was added and samples were gently inverted several times to mix. Debris was removed by centrifugation at 20,000 x g for 30 min at 4° C. The supernatant containing plasmid DNA was applied to a Quiagen-tip 500 column that was equilibrated with 10 mL of QBT buffer (750 mM NaCl₂, 50 mM MOPS, 15% ethanol (7.0)). Next, the column was washed 2x with 30 mL Buffer QC (1 M NaCl₂, 50 mM MOPS, 15% ethanol, (8.5)), then the plasmid DNA was eluted in 15 mL of Buffer QF (1.25 M NaCl₂, 50 mM Tris-HCl, 15% ethanol (8.5)). Plasmid DNA was precipitated with 0.7 volumes isopropanol and centrifugation at 15,000 x g for 30 min at 4° C. The pellet was washed with 70% ethanol and centrifuged as previously. DNA was resuspended in 200 to 400 µL TE buffer and stored at -20° C.

3.5. Pulsed-field Gel Electrophoresis

DNA plugs were run in 1.5% low-endoosmosis agarose (Biorad) gels in 0.5x TBE buffer (for 1x buffer: 10.3 g Tris, 5.5 g boric acid, 0.93 g disodium EDTA per L) in constantly-circulating 0.5x TBE at 10° C. Resolution to visualize repair products from Chromosome III was accomplished with the following settings entered into a CHEF-DR II system (Biorad): 6V/cm, 10-35 sec pulse time, 40 hrs run time.

Bands were visualized in UV light after 15 min incubation in 1x TBE with ethidium bromide.

3.5.1. Southern Hybridization of CHEF

To fully characterize the repair products separated on the CHEF gel, Southern hybridization with specific probes was needed. After UV visualization, the agarose gel was exposed to 600 microjoules UV treatment in a Stratalinker UV crosslinker. The gel was then incubated in buffer containing 0.5M NaOH 1.5 M NaCl (7.0) with gentle shaking for 40 min, then transferred to a buffer containing 1 M Tris-HCl, 1.5 M NaCl (7.0) with gentle shaking for 40 min. DNA is transferred to a nylon membrane (Hybond N⁺, Amersham) using upward capillary transfer in 10x sodium chloride, sodium citrate buffer. Membranes were probed using a *Sa*I fragment from pJH879, which hybridizes to *ADE1*, or with other probes described in Figure 4.1 generated by PCR amplification (Deem et al., 2008). The locations of the probes depicted in Figure 4.1 on chromosome III were as follows: 1) *THR4*-specific: 216965 - 217264 (probe 1); 2) *FEN2*-specific: 172065 - 172372 (probe 2); 3) *FS1*-proximal: 148247 - 148547 (probe 3); 4) *MRPL32*-specific: 118654 - 119073 (probe 4). The location of the *ADE3*-specific probe on chromosome VII was 907979 - 908735. For all probes mentioned above, the starting and ending coordinates on the corresponding chromosomes are derived from SGD. Probes were labeled using the Stratagene Prime-It random primer labeling kit.

3.6. Analysis of DNA Repair Outcomes in AM1003-9 and Its Mutant Derivatives

In order to monitor the repair of HO-induced DSBs, 5 mL inoculums were grown in YPD over night at 30° C with agitation, then diluted at approximately 1:20 in YEP-Lactate media for between 24 and 48 hours (depending on growth characteristics of the strain). Appropriate dilutions were plated on YEP-Gal and allowed to grow for 3 to 5 days at 30° C. The resulting colonies were then replica plated onto drop-out media to examine the *ADE1*, *ADE3*, *NAT*, and/or *LEU2*, markers of these strains. Cell viability following HO induction was derived by dividing the number of colony-forming units (CFUs) on YEP-Galactose by the number of CFUs on YPD. Unless otherwise indicated, a minimum of 3 plating experiments was used to calculate the averages and standard deviations for viability.

3.6.1. Analysis of HCO molecules

The site of molecular fusion of HCOs was analyzed by PCR amplification using primers 1 and 2 and primers 1 and 3 in combination, as depicted in Figure 4.1A. The sequences for these primers are provided in Table 3.2, and correspond to OL17 (primer 1), OL8 (primer 2), and OL5 (primer 3) in the Malkova Lab Database.

3.6.2. Statistical Analysis of BIR Repair Outcomes

All mutants were analyzed for their effect on BIR repair in at least three independent plating experiments, unless otherwise noted. Results from these independent experiments were pooled if it was determined that the distributions of all events were statistically similar to each other using a chi-square test ([HTTP://WWW.PSYCH.KU.EDU/PREACHER/CHISQ/CHISQ.HTM](http://www.psych.ku.edu/preacher/chisq/chisq.htm)). The effects of individual mutations on DSB repair were determined by comparing the resulting pooled distributions of repair outcomes obtained for mutants to the distribution obtained for the wild type strain (AM1003-9) by chi-square tests. Specifically, to determine the effect of various mutations on the efficiency of BIR, all repair outcomes were divided into two groups: BIR (Ade⁺Leu⁻ outcomes) and others (combining all other groups). Comparison of the distributions between these two classes in specific mutants versus wild type was used to determine whether those mutations affected the efficiency of BIR. The effect of mutations on other DSB repair outcomes was determined similarly. For checkpoint mutants, several unique variables were analyzed by chi-square comparison between mutant and wild type strains, with specifics of each comparison described within the tables.

3.7. Mutagenesis associated with DSB repair

3.7.1. Determining Mutation Frequencies

To determine mutation frequency, yeast strains were grown from individual colonies with agitation in liquid synthetic media lacking leucine for approximately

20 hours, diluted 20-fold with fresh YEP-Lac, and grown to logarithmic phase for approximately 16 hours. Next, 20% galactose was added to the culture to a final concentration of 2%, and cells were incubated with agitation for 7 hours. No-DSB control strains were subjected to the same incubation and plating processes.

Samples from each culture were plated at appropriate concentrations on YEPD and lysine drop-out media before (0h) and seven hours after the addition of galactose (7h) to measure the frequency of Lys⁺ cells. (For YPD, cells were plated to obtain single colonies, while concentrations on Lys drop-out plates were based on the expected frequency of Lys⁺ events (based on pilot experiments), but were not plated at concentrations above approximately 1×10^8 cells/plate.) Cells were grown at 30° C for a minimum of 5 days. Due to variable expression of lysine, in some cases plates were grown for an additional 2 days. Generally, lower expression of lysine (i.e., slower growth on Lys drop-out media) was observed for strains that contained the A₇ reporter at either the *MAT* or 36-kb positions and experienced a frameshift mutation in the poly-A run. Thus, A₇ strains with a mutation that conferred MMR deficiency were especially prone to small, late-forming colonies, and were grown for 7 days.

3.7.1.1. Calculation of Mutation Rates

Because spontaneous mutation frequencies were calculated based on the number of mutations accumulated during many cell generations, mutation rates

were calculated for spontaneous and BIR mutagenesis using modifications of the Drake equation (Drake, 1991). Specifically, the rate of spontaneous mutagenesis in experimental strains was calculated using mutation frequencies at 0h in experimental and no-DSB control strains using the following formula: $\mu = 0.4343f/\log(N\mu)$, where μ = the rate of spontaneous mutagenesis, f = mutation frequency at time 0h, and N = the number of cells in yeast culture at 0h. Because most strains with a DSB site exhibited residual DSB formation even at 0h, the rate of spontaneous mutagenesis was more accurately determined from 0h Lys⁺ frequencies in no-DSB controls using the same formula. For the no-DSB controls with reporters at *MAT*, the median, calculated based on the equation shown above, was divided by two to correct for the presence of two *LYS2* reporters in these strains. The rate of mutations after galactose treatment (μ_7) was determined using a simplified version of the Drake equation: $\mu_7 = (f_7 - f_0)$, where f_7 and f_0 are the mutation frequencies at times 7h and 0h, respectively. This modification was necessary because experimental strains did not divide between 0h and 7h, while no-DSB controls underwent ≤ 1 division between 0h and 7h.

Rates are reported as the median value, and the 95% confidence limits for the median are calculated for the strains with a minimum of 6 individual experiments as described and reported in Table S1 (Dixon and Massey, 1969) (Tables 5.2, 5.5; Figures 5.3, 5.5, 5.7-5.9, 5.11). For strains with <6 individual experiments, the range of the median was calculated. Statistical comparisons between

median mutation rates were performed using the Mann-Whitney U test (Mann and Whitney, 1947).

3.7.2. Calculations of BIR efficiency

BIR efficiency was estimated in all strains with a DSB site, typically in a subset of 3 experiments per strain. Colonies plated on YPD seven hours after addition of galactose were replica plated onto omission media to examine the *ADE1*, *ADE3*, and *LEU2* markers. Colonies formed by BIR displayed an Ade⁺Leu⁻, Ade^{+/-}Leu⁻, or Ade⁺Leu^{+/-} phenotype (Deem et al., 2008). The efficiency of BIR in individual experiments was estimated as the sum of all Ade⁺Leu⁻ events plus one half of all BIR sectored (Ade^{+/-}Leu⁻ or Ade⁺Leu^{+/-}) events, divided by the total number of colonies analyzed. Typically, ≥50 colonies were analyzed for individual experiments. To compare wild type and mutant strains, BIR efficiency was determined by combining data from isogenic 16- and 36-kb A₄ strains (strains with the reporter at *MAT* were omitted due to the effect of mating type on BIR efficiency (Malkova et al., 2005)). Medians were compared using the Mann-Whitney U test (Mann and Whitney, 1947).

3.7.3. Analysis of Mutation Spectra

A portion of the *LYS2* gene was sequenced from independent Lys⁺ outcomes using one or both of the primers used to confirm insertion of the *LYS2* reporters (OL1104 and OL1181 were used to make the fragment, and sequencing was accomplished using OL1106 and/or OL1199; Table 3.2). Sequencing reactions

were performed at the IUPUI Sequencing Core Facility using an ABI 3100 genetic analyzer.

For experimental strains undergoing BIR repair, 7h Lys⁺ BIR events (confirmed as Ade⁺Leu⁻ on selective media) were sequenced. Because these strains did not divide between the 0h and 7h timepoints and the Lys⁺ frequency at 7h significantly exceeded that at 0h, all Lys⁺ events resulting from DSB repair were considered independent. In *msh2Δ* A₇ experimental strains, in which the 0h rate was extremely elevated, candidates for sequencing were chosen from experiments with a ≥10-fold difference in mutation frequencies between 0h and 7h. Because differential expression of lysine was observed, measures were taken to ensure that the mutation spectrum represented among BIR outcomes was not biased. These measures included taking all colonies from a randomly selected section of a Lys drop-out plate for sequencing, as well as determining the proportion of “large” versus “small” colonies for any particular strain and selecting colonies for sequencing that fairly represented this proportion. For no-DSB controls, independent Lys⁺ events were obtained by growing cultures from singles in YEPD overnight and choosing only one event from each culture. As described in Chapter 5 (Figure 5.1), BIR repair yielded a second copy of the *lys2::Ins* gene. Among Ade⁺Leu⁻ (BIR) Lys⁺ events, the site of the frameshift mutation during BIR repair was identified by analyzing .abi files for the first nucleotide where the amplified sequence became heterozygous (i.e., displayed two overlapping peaks of different nucleotides versus a single peak). In cases

where no heterozygosity was observed, these events were considered “templated” events in which the *lys2::Ins* mutation occurred prior to BIR repair and were not included in our analysis of BIR-related mutation spectra. Furthermore, sequencing runs in which peaks were not sufficiently clean to identify a clear switch to heterozygosity were not included in the analysis. For no-DSB controls with the *lys2::Ins* reporter at either the 16- or 36-kb position, where only a single copy of *lys2::Ins* was present after the mutation, only sequences from Ade⁺Leu⁺ (no-DSB) Lys⁺ events with clearly homozygous sequences were taken, and the site of the mutation was determined by comparing the sequence with the known sequence of the wild type parent strain. For no-DSB controls that with the *lys2::Ins* reporter at the *MAT* position, two copies of the reporter were present, and the site of the mutation was determined by heterozygosity, as it was for BIR events.

CHAPTER 4. GENOME-DESTABILIZING EFFECTS OF BREAK-INDUCED REPLICATION

4.1. Background

Double-strand DNA breaks (DSBs) often cause genetic instability due to the loss of important genetic information and, therefore, DSBs can threaten an organism's homeostasis. DSB-induced changes to the genome are implicated in a variety of human diseases, including birth defects and cancer. Thus, identification and characterization of the molecular mechanisms that repair DSBs are crucial for understanding how the integrity of living cells is maintained. Several different pathways to repair DSBs have been identified. In yeast, GC is the preferred pathway to repair DSBs generated by endonucleases, ionizing radiation, or mechanical rupture of chromosomes. However, other important pathways of DSB repair exist (see Chapter 2 for a more thorough discussion). One such DSB repair pathway is BIR which proceeds by invasion of one broken DNA end into the intact donor molecule followed by initiation of DNA synthesis that can continue as far as the end of the donor chromosome (Davis and Symington, 2004; McEachern and Haber, 2006). Although BIR effectively repairs DSBs, the repair product can be deleterious for the cell. For example, BIR is implicated in the generation of nonreciprocal translocations (Bosco and Haber, 1998; Malkova

et al., 2005), as well as formation of various types of GCRs (Le et al., 1999; Lydeard et al., 2007; Teng et al., 2000; Teng and Zakian, 1999).

The key to understanding the mechanism of BIR lies in the knowledge of specific proteins required for the process. So far, three categories of proteins that participate in BIR have been identified: recombination proteins, replication proteins, and proteins mediating recombination and replication (mediator proteins). Recombination proteins, including *RecA* in *E. coli*, *UvsX* in bacteriophage T4, and *RAD52*, *RAD51*, *RAD54*, *RAD55*, *RAD57* in *S. cerevisiae*, initiate BIR by promoting strand invasion and D-loop formation (Asai et al., 1993; Davis and Symington, 2004; Formosa and Alberts, 1986a, b; Lark et al., 1978; Malkova et al., 2005). The role of mediator proteins is to assemble a processive replication fork on the D-loop that is formed during the first step of BIR. In *E. coli*, this function is carried out by *PriA* with the help of several other proteins, including *PriB*, *PriC*, and *PriT*, while gp59 performs a similar function in bacteriophage T4 (Bleuit et al., 2001; George et al., 2001; Kogoma, 1976; Kogoma and Lark, 1975; Mariani, 2000). While it is not clear which protein(s) in eukaryotes directly recruits replication fork factors, it was recently established in *S. cerevisiae* that all S-phase replication factors, excepting those that function in replication origin recognition, are involved in BIR (Lydeard et al., 2010; See Section 2.3 for details). The last stage of BIR, DNA synthesis, is carried out by processive DNA polymerases working in conjunction with clamp and clamp-loader proteins, including the Pol III complex in *E. coli* (Kogoma and Lark, 1975),

the gp43/gp44/gp45/gp62 complex in T4 (reviewed in (Kreuzer, 2000)), and Pol α , Pol δ , and Pol ϵ complexes in yeast (Lydeard et al., 2007). However, many details related to DNA synthesis associated with BIR remain unknown.

While many of the proteins involved in BIR repair in yeast have been identified, little is known about the fate of cells that fail to complete BIR properly. This is because most yeast systems designed to study BIR select exclusively for events that successfully complete BIR while other cells die, or because the BIR system was a diploid that made construction of deletion strains cumbersome. This leaves open many questions regarding the actual efficiency of BIR, as well as the consequences of failed BIR repair. This chapter describes a novel yeast system that efficiently repairs DSBs by allelic BIR and my findings that a multitude of factors, including mutations in BIR genes, inappropriate DNA damage checkpoint control, and replication-inhibiting drugs, can alter expected BIR outcomes. In some cases, deficiencies in BIR manifest as half-crossover molecules, which closely approximate toxic NRTs reported in mammals that are implicated in the initiation of cascades of genomic instability characteristic of human cancer cells (Sabatier et al., 2005).

4.2. Experimental System

A diploid system in *S. cerevisiae* that efficiently repaired an HO-created DSB by allelic BIR was previously described (Malkova et al. 2005). In that system, HO was under the control of a galactose-inducible promoter, and the DSB was

created at the *MATa* locus of one copy of chromosome III, while a second copy contained an uncleavable *MAT α -inc* allele and served as the template for DSB repair. The preference for BIR repair, versus GC repair, resulted from truncation of the cut molecule via insertion of *LEU2* and telomeric sequences, leaving only 46 bp of homology on the centromere-distal side of the DSB. This system was used to characterize the kinetics of BIR, as well as the effects of various mutations on BIR efficiency. However, the systematic analysis of genetic control of BIR was difficult in this diploid strain due to the necessity of deleting or mutating both copies of the wild type gene of interest. To facilitate large-scale screening for genes that influence BIR, our lab created a modified version of this experimental system, AM1003-9 (Figure 4.1). AM1003-9 contains several important features relevant to the investigations described in this chapter: 1) This is a disomic strain that contains a haploid set of all chromosomes and a second copy of chromosome III; 2) As in the original diploid system, the *MATa*-containing copy of chromosome III is truncated distal to the *HO* DSB site to increase the efficiency of BIR repair using the uncleavable *MAT α -inc* allele and

Figure 4.1. Disomic experimental system to study BIR. (A) Arrangement of chromosome III markers of disomic strain AM1003-9 and its derivatives are indicated. A DSB is induced at *MATa* by a galactose-inducible *HO* gene. The *MATa*-containing copy of chromosome III is truncated by insertion of a *LEU2* gene fused to telomere sequences. The *MAT α* -containing copy is full-length and lacks the *HO* cut site. *HML* sequences are replaced by *ADE1* and *ADE3* genes in the truncated and full-length chromosomes, respectively, and *HMR* is replaced by *HYG*. On the truncated chromosome, *FS2* is replaced by *NAT*. Some isogenic derivatives of AM1003 contain *URA3* inserted 3 kb proximal to *MATa*. Primers 1, 2, and 3 (p1, p2, and p3, respectively) indicate positions of primers used for PCR analysis of half-crossover repair outcomes. The positions of probes used to analyze the structure of GCR repair outcomes are indicated by numbers (1, 2, 3, 4; see text for details). (B) GC outcome. (C) BIR repair outcome. (D) Chromosome loss when the *HO* cut is not repaired. (E) HCOs resulting from fusion of the left part of the truncated chromosome and the right part of the full-length chromosome. (F) GCRs resulting from repair of the broken chromatid with a non-homologous chromosome. For outcomes shown in B-F, the observed phenotypes are indicated.

distal sequences from the full-length copy of chromosome III as the donor; 3) *HML* on the truncated copy of chromosome III is replaced by *ADE1*; 4) *HML* and *HMR* on the full-length chromosome III are replaced by *ADE3* and *HPH* (*HYG*), respectively; 5) The native FS2 region located on the truncated copy of chromosome III (30 kb proximal to *MATa*), which consists of two copies of Ty1 transposons in inverted orientation (VanHulle et al., 2007), is replaced by *NAT*. The disomic system was determined to repair the DSB with kinetics similar to those reported for the diploid system (Malkova et al., 2005).

Our lab previously assayed the efficiency of BIR in the disomic strain AM1003-9 by plating on a galactose-containing medium to induce HO endonuclease, which leads to DSB formation. In wild type, approximately 78% of the colonies showed the expected BIR phenotype of Ade^+Leu^- , with only 7.5% of colonies displaying the Ade^+Leu^+ phenotype indicative of GC (Table 2.1; Figure 2.1). Another 1.5% of colonies were Ade^-Leu^- , indicating failed repair of the truncated copy of chromosome III. These failed repair events could be easily distinguished by accumulation of red pigment due to the absence of a functional *ADE1* gene (this phenotype is hereafter indicated by “ $\text{Ade}^{-\text{red}}$ ”). Approximately 7% were sectorial $\text{Ade}^{+/-\text{red}}$ colonies, which were likely to represent cases where one of two sister chromatids completed repair while the second chromatid was left unrepaired and lost in the next cell division. Alternatively, these sectorial $\text{Ade}^{+/-\text{red}}$ colonies may have resulted from cases in which the broken chromosome was replicated and inherited without repair for one or more divisions, after which some of the broken

chromosomes were lost and others were repaired. Approximately 3% of colonies presented a rare and unexpected phenotype: they were Ade⁻Leu⁻, but white (hereafter indicated by “A^{-white}”). In some of these cases, only a part of the colony was Ade^{-white}, while another part was Ade^{-red} or Ade⁺. The Ade^{-white} colonies or sectors were also confirmed as His⁻, indicating loss of the *ADE3* marker on the donor molecule, and were determined to represent HCO events that resulted from a fusion between the truncated and full-length copies of chromosome III (see Section 4.2.1.2).

4.2.1. Characterization of the *pol32Δ* defect

The disomic experimental system was used to test various mutations with respect to their effects on BIR. This mutant screen identified *pol32Δ* as a mutation that statistically significantly decreased BIR efficiency, increased chromosome loss, and increased HCO formation. The objective of my work was to further characterize the *pol32Δ* BIR defect, as well as to physically characterize the HCO outcomes.

Table 4.1. Repair of HO-induced DSBs in strain AM1003-9 and its *pol32Δ* and *rad51Δ* derivatives.

		Phenotype of colonies (%)									
Relevant Genotype	Strain	No. of colonies tested	Ade ⁺	Ade ⁺	Ade ⁺	Ade ^{+/-red}	Ade ^{-red}	Ade ^{-white}	Partial Ade ^{-white}	Viability on	
			Leu ⁺	Leu ^{+/-}	Leu ⁻	Leu ⁻	Leu ⁻	Leu ⁻	Leu ⁻	Leu ⁻	YEP-Gal
			(GC)	(GC/BIR)	(BIR) ^a	(BIR/loss) ^a	(loss)	(HCO)	(partial HCO) ^b		
wt	AM1003	684	7.5	2.1	78.1	7.4	1.5	0.3	3.1	94 ± 11	
<i>pol32Δ</i>	AM1014, AM1152 ^c	1549	0.5	0.0	18.9	19.0	38.0	7.0	16.6	90 ± 11	
<i>rad51Δ</i>	AM 1079	134	0.8	0.0	0.8 [*]	31.3	67.1	0.0	0.0	86 ± 18	

Abbreviations: Ade^{-red} = Ade⁻, His⁺ red colonies indicative of the *ade1 ADE3* genotype; Ade^{-white} = Ade⁻, His⁻ white colonies indicative of the *ADE1ade3* genotype; GC = gene conversion; BIR = break-induced replication; HCO = half-crossover; wt = wild type. Sectoring phenotypes are indicated by both phenotypes separated by a backslash. ^a At least some of these events could be HCOs (primarily in *pol32Δ*, see the text for details) or GCRs (primarily in *rad51Δ*, but also in other strains, see the text for details). ^b Partial HCOs in which part of the colony was Ade^{-white} while the other part represented chromosome loss, or BIR. ^c Data obtained for two isogenic *pol32Δ* strains, AM1152, which contains the *URA3* marker inserted 3 kb proximal to *MATa*, and AM1014, were indistinguishable from each other and therefore combined. * Indicates a statistically significant difference from the isogenic wild type strain (AM1003-9) (p<0.05).

The effect of *pol32Δ* on BIR was investigated further by following the kinetics of repair in a time-course experiment. The kinetics of DSB repair in wild type and *pol32Δ* was examined by PFGE followed by hybridization with an *ADE1*-specific probe to detect *hml::ADE1* located on the left arm of the truncated copy of chromosome III. We observed that, in *pol32Δ* cells, the repair product appeared with kinetics similar to the kinetics of BIR repair in wild type cells; i.e., approximately 4 hours after galactose induction of the DSB (Figure 4.2 A, B; pictures from Kelly VanHulle (Deem et al., 2008)). However, quantification of Southern blots indicated that the amount of BIR-sized product in *pol32Δ* mutants was less than wild type 6 hours after galactose induction of the DSB, and BIR product in *pol32Δ* was reduced to approximately 27% of the intensity of the unbroken chromosome, compared with approximately 70% in wild type at the 10-hour time point (Figure 4.2 D). Similar to wild type cells, induction of the DSB in *pol32Δ* cells led to nearly uniform arrest at the G2/M stage of the cell cycle, which was established approximately 4 hours after the DSB (Figure 4.2 C; data from Kelly VanHulle and Krista Hull (Deem et al., 2008)). However, recovery from arrest in *pol32Δ* was significantly delayed, with more than 50% of *pol32Δ* cells maintaining arrest 10 hours after DSB induction, compared with less than 20% of wild type cells remaining arrested at this time point. The delayed recovery from arrest is an additional indication that unrepaired DNA persists in *pol32Δ* cells, and also indicates that the defect of *pol32Δ* resides in its inability to carry out BIR rather than in a defective checkpoint response.

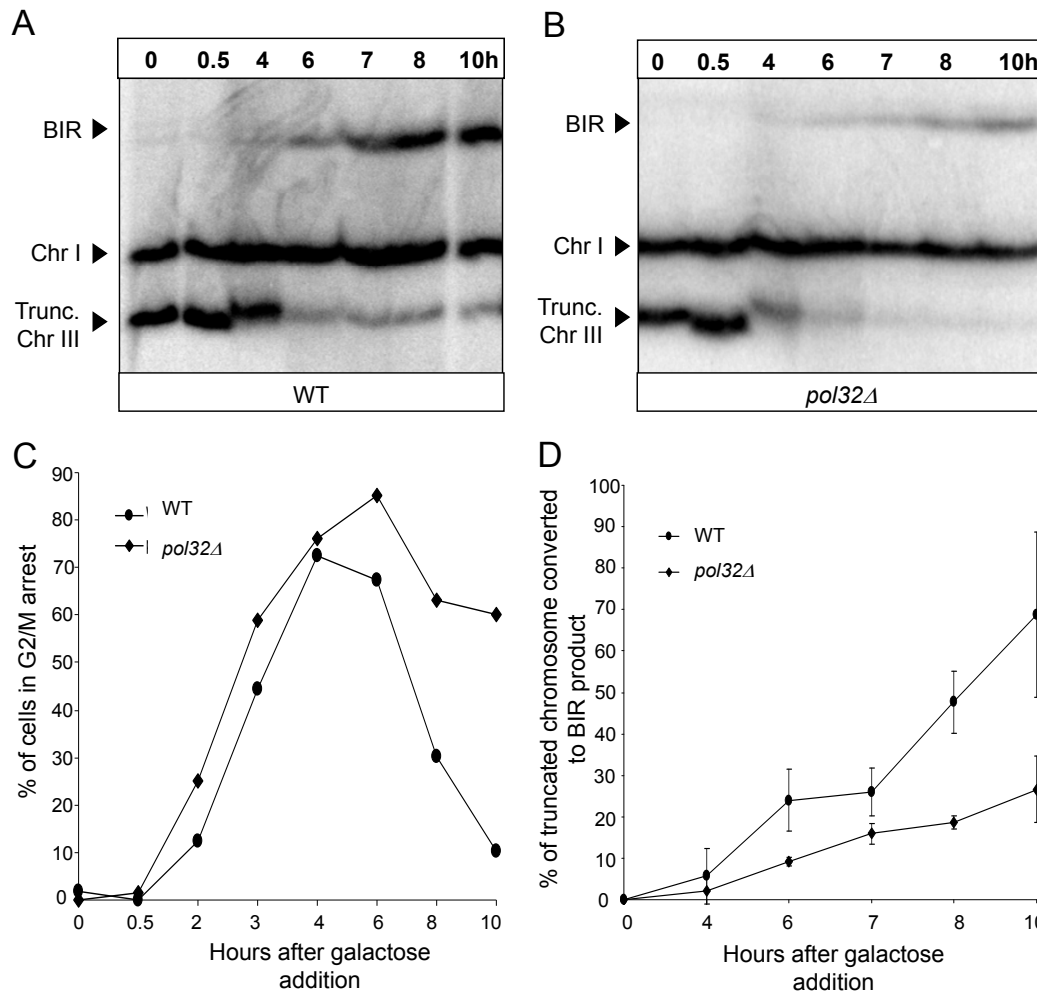


Figure 4.2. Analysis of DSB repair in AM1003-9 and its *pol32Δ* derivative. DNA was prepared for PFGE at intervals after induction of a DSB at *MATa*. Southern blots were probed with *ADE1*, which hybridizes to the truncated chromosome III (Trunc. Chr III, see Figure 4.1) and to its native position on chromosome I (Chr I), but not to the full length chromosome III (Chr III). Analysis of DSB repair in AM1003-9 (**A**) confirmed the kinetics of BIR in this strain to be similar to those previously characterized (Malkova et al., 2005). (**B**) The BIR-sized repair product was also observed in the *pol32Δ* derivative of AM1003-9 (AM1014). (**C**) G2/M arrest in cells undergoing BIR repair. Cells were removed at intervals during experiments described in A and B. These cells were fixed with ethanol, stained with DAPI, and analyzed by fluorescent microscopy. G2/M-arrested cells were defined as cells with dumb-bell morphology, where mother and daughter cells “shared” one nucleus. Approximately 200 cells were counted for each time point. (**D**) Quantification of the BIR repair product performed in AM1003-9 (WT) and AM1014 (*pol32Δ*) demonstrated that the kinetics of its accumulation in these two strains was similar, but the amount of BIR product was reduced in *pol32Δ* compared to WT.

4.2.1.1. POL32-independent BIR

Despite the fact that BIR was reduced in *pol32Δ* cells, a substantial number of cells succeeded in DSB repair and formed Ade⁺Leu⁻ or Ade^{+/-red}Leu⁻ colonies. This result contrasted with a previous report in which ectopic BIR was completely eliminated in a *pol32Δ* background (Lydeard et al., 2007), and merited further evaluation. We noted a difference in retention of the *NAT* marker located 30 kb centromere-proximal to the DSB site (Figure 4.1) between wild type and *pol32Δ* Ade⁺Leu⁻ or Ade^{+/-red}Leu⁻ outcomes, suggesting that the composition of the repair outcomes between these strains differed. Specifically, 99% (518/524) and 62% (31/50) of wild type Ade⁺ and Ade^{+/-red} repair outcomes, respectively, preserved the *NAT* marker and produced the Nat^r phenotype. In contrast, the *NAT* marker was preserved in 93% (271/293) of Ade⁺ outcomes and in 78% (230/293) of Ade^{+/-red} outcomes ($p < 0.0001$ for both wild type vs *pol32Δ* comparisons). We hypothesized that the NAT^s outcomes that had experienced extensive post-DSB resection may have repaired differently from the more common Nat^r outcomes, prompting us to compare these different events by means of physical analysis.

Individual Ade⁺Nat^rLeu⁻ repair outcomes from wild type and *pol32Δ* cells were analyzed by PFGE and Southern blots probed with an *ADE1*-specific probe. (Figure 4.3 A, B). In total, 35 Ade⁺Nat^rLeu⁻ repair outcomes obtained from *pol32Δ* were analyzed and compared with similar outcomes obtained from wild type cells. All wild type events analyzed (6/6) were confirmed to be allelic BIR

outcomes (Figure 4.3 A, B, lanes 1-3) that contained two copies of chromosome III: one copy was an unchanged 350 kb-long donor chromosome containing *ADE3*, while the second was the repaired chromosome that contained *ADE1* and was approximately 340 kb long (the difference in length was the result of replacement of the FS2 region by *NAT* in the truncated chromosome III). In addition, both copies of chromosome III hybridized to a *THR4*-specific probe (Figure 4.1 A, probe 1), confirming that the broken molecule had obtained DNA sequences located centromere-distal to the *MAT* break site, as predicted for BIR. Most of Ade⁺Nat^fLeu⁻ repair outcomes obtained from *po132Δ* (94%, 31 out of 33 analyzed) were similar to the wild type BIR events (Figure 4.3 A, B, lanes 5, 6). The two remaining events contained repair products approximately 250 kb long (not shown) that were not consistent with the expected BIR products and, thus, were indicative of GCRs, most likely translocations resulting from strand invasion into a non-homologous chromosome. Thus, we conclude that the chromosome structure of the vast majority (94%) of Ade⁺Nat^fLeu⁻ repair outcomes obtained from the progeny of *po132Δ* strains was consistent with allelic BIR.

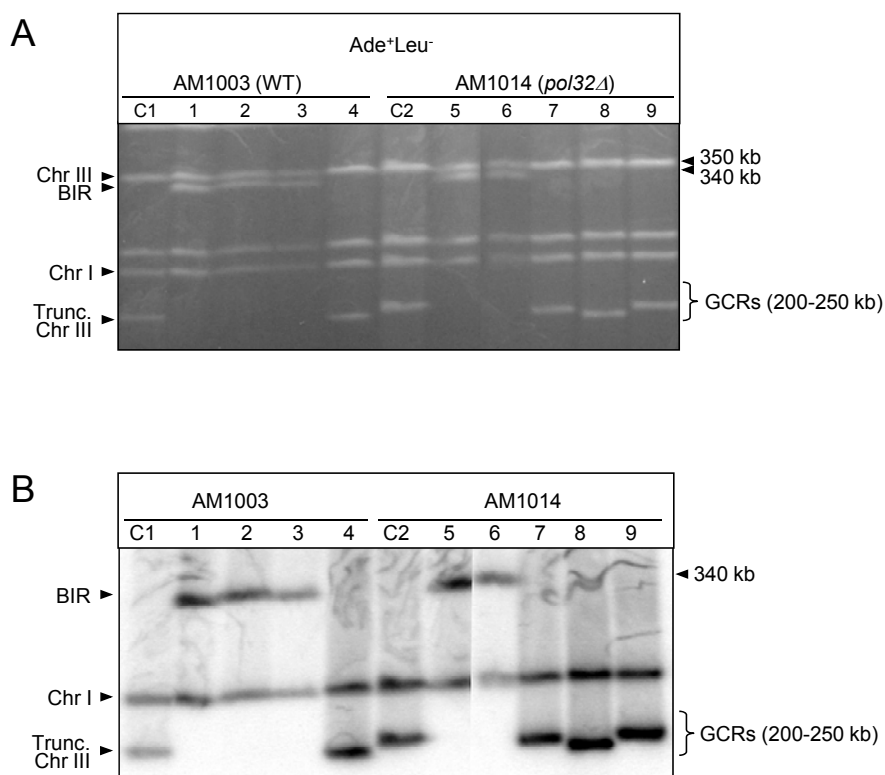


Figure 4.3. Structural analysis of Ade⁺Leu⁻ repair outcomes. (A) Ethidium bromide-stained PFGE gel of repair outcomes obtained from AM1003-9 (WT) and AM1014 (*pol32Δ*). **(B)** Southern blot analysis of the PFGE gel shown in (A) using an *ADE1*-specific probe, which hybridizes to truncated chromosome III (trunc. Chr III), and to chromosome I (Chr I). Lanes labeled C1 and C2 show DNA from AM1003-9 and AM1014 cells, respectively, in which the HO site was not cleaved. Other lanes contained DNA obtained from the following Ade⁺Leu⁻ repair outcomes: 1, 2, 3 – Nat^r outcomes from AM1003-9 (WT); 4 – Nat^s outcome from AM1003-9 (WT); 5, 6 – Nat^r outcomes from AM1014 (*pol32Δ*); 7, 8, 9 – Nat^s outcomes from AM1014 (*pol32Δ*). The majority of Nat^r outcomes contained a 340-kb repair product consistent with BIR, whereas many Nat^s events contained repair products that were different in size from the Chr III products expected from BIR or GC repair and, thus, were indicative of GCRs.

A second class of repair events analyzed consisted of cells that had lost the *NAT* marker located 30 kb centromere-proximal to the DSB site (*Ade*⁺*Nat*^s*Leu*⁻ colonies). These events were rare compared to *Nat*^r repair events in both *pol32Δ* and wild type cells. PFGE analysis of *Ade*⁺*Nat*^s*Leu*⁻ repair outcomes demonstrated that, in *pol32Δ* cells, over half of the repair outcomes (60%, 9/15 analyzed) had a chromosome III of altered size and, therefore, represented GCRs, while the other 40% (6/15) contained 350-kb repair bands consistent with allelic BIR that proceeded by strand invasion of the broken chromosome into the homolog at positions centromere-proximal to *NAT*. Analysis of five *Ade*⁺*Nat*^s*Leu*⁻ repair outcomes from wild type cells demonstrated that one of them was consistent with a GCR, while the other four were BIR outcomes.

Further analysis of six *pol32Δ* GCR outcomes demonstrated that each of them contained one repaired chromosome that hybridized to an *ADE1*-specific probe and were between 200 and 250 kb long (Figure 4.3 A, B, lanes 7-9). Hybridization with several other probes demonstrated that these 6 repair chromosomes did not hybridize to the *FEN2* probe (Figure 4.1 A, probe 2) located on chromosome III 30 kb proximal to *MAT*, or to the FS1-proximal probe (Figure 4.1 A, probe 3) located on chromosome III approximately 52 kb proximal to *MAT*. Because all 6 repaired chromosomes hybridized to the *MRPL32* probe (Figure 4.1 A, probe 4) located on chromosome III 80 kb proximal to *MAT*, we concluded that repair in these 6 GCR cases was initiated in the region between

positions 118654 (location of the *MRPL32* probe) and 148247 (location of the FS1-proximal probe), and then likely proceeded via invasion into some non-homologous chromosome resulting in translocations (Figure 4.1 A, F). These GCRs were similar to GCRs that our lab previously observed in *rad51Δ* diploids, where more than 80% of repair outcomes resulted from invasions into non-homologous chromosomes (VanHulle et al., 2007). We confirmed this result for the *rad51Δ* derivative of our disomic strain, where approximately 31% of repair outcomes were Ade^{+/-red}Nat^rLeu⁻ (Table 4.1). PFGE analysis of 6 of these events demonstrated that each of them contained a repaired chromosome III of altered size consistent with a GCR. The decreased frequency of GCRs in our disomic system (compared to the previously observed frequency in *rad51Δ* diploids) could be explained by the absence of FS2, which stimulated formation of GCRs in the *rad51Δ* derivative of our diploid system (VanHulle et al., 2007).

4.2.1.2. Half-crossover outcomes were increased in *pol32Δ* mutants

Among repair outcomes obtained in the progeny of *pol32Δ* mutants, we observed unexpected colonies that were fully or partially Ade^{-white}, as well as His⁻. This phenotype was rare in *POL32* cells (approximately 3% of all repair events) but increased to more than 23% of repair events in *pol32Δ* mutants when both full and partial events were combined (Table 4.1). An allelism test performed by crossing to *ade1* and *ade3* tester strains demonstrated the Ade^{-white}His⁻ cells to be *ADE1ade3* (mutations in the *ADE3* gene affect biosynthesis of both adenine

and histidine; thus, *ade3* mutants are Ade^{-white}His⁻, while *ade1* mutants are Ade^{-red}His⁺). PFGE analysis confirmed that Ade^{-white}His⁻ outcomes contained only a single, 340-kb copy of chromosome III (Figure. 4.4 A) that hybridized to an *ADE1*-specific probe (Figure 4.4 B), but not to an *ADE3*-specific probe (not shown). Thus, these events were determined to be the result of a fusion between the “left half” of the truncated chromosome III and the “right half” of the full-length chromosome III, while the remaining two halves were lost (see Figure 4.1 E). Such outcomes are similar to previously described HCO events in yeast (Haber and Hearn, 1985), and also strongly resemble NRT repair events in mammals that are a major pathway of exiting breakage-fusion-bridge cycles (Sabatier et al., 2005).

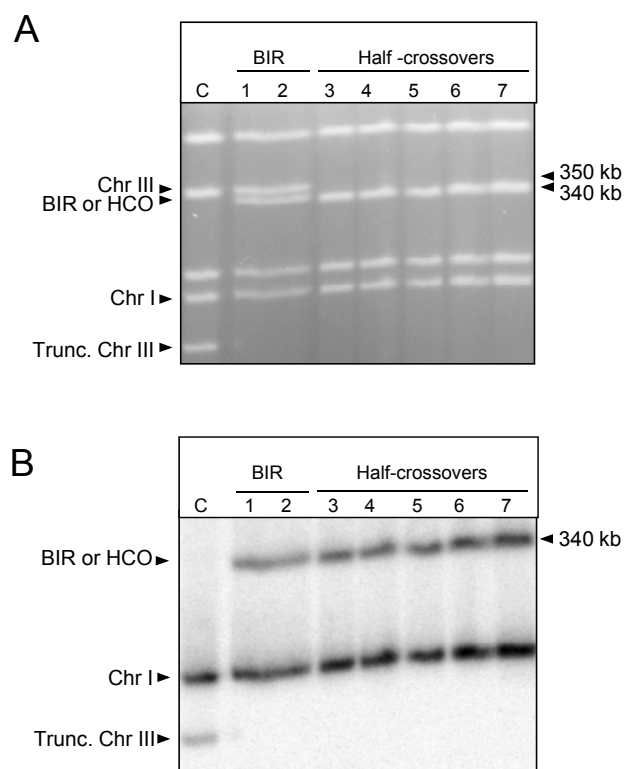


Figure 4.4. Structural analysis of HCO outcomes. (A) Ethidium bromide-stained PFGE gel of Ade^{-white}Leu⁻ (HCO) outcomes obtained from AM1014 (*pol32Δ*). (B) Southern blot analysis of the PFGE gel shown in (A) using an *ADE1*-specific probe that hybridizes to truncated chromosome III (trunc. Chr III) and to chromosome I (Chr I). Lane C contained DNA from AM1003-9 in which the HO site was not cleaved. Other lanes contained DNA from the following repair outcomes: 1 – Ade⁺Leu⁻ from AM1003-9 (WT BIR control); 2 - Ade⁺Leu⁻ from AM1014 (*pol32Δ* BIR control); 3-7 - Ade^{-white}Leu⁻ HCOs from AM1014 (*pol32Δ*). BIR controls contain both BIR repair product and full-length Chr III. HCOs contain only one BIR-sized fusion chromosome while the donor molecule is lost.

The majority (82%) of the HCO events recovered from *pol32Δ* cells (301/366 events) were Nat^r, while others (65/366 events) were Nat^s. We hypothesized that, in Nat^r events, chromosomal fusion occurred in the interval between *NAT* and the *MAT* locus, while in Nat^s events, the fusion occurred between *NAT* and the centromere. This hypothesis was tested by PCR analysis of Nat^r outcomes. Primers to detect the presence of the FS2 region, which exists only on the full-length copy of chromosome III in the disomic strain, were used in PCR reactions with either HCO outcomes or the uninduced wild type or *pol32Δ* derivative strains as DNA templates (see Table 2.2 and Figure 4.1 A for the positions and sequences of primers). As predicted, no bands were detected in any of the 8 Nat^r HCOs tested, whereas bands of the predicted sizes (approximately 664 bp and 660 bp for the combination of Primer 1 and Primer 2 and for the combination of Primer 1 and Primer 3, respectively; Figure 4.1 A) were confirmed both in AM1003-9 and AM1014, as well as in their respective BIR controls (not shown). This result was consistent with the predicted structure of the fusion chromosome, where the FS2 DNA sequences located centromere-proximal to the position of the fusion on the donor chromosome should be lost.

HCO events in wild type cells were extremely rare, but PFGE analysis of the events we were able to recover demonstrated their structure to be similar to that of HCO events obtained from *pol32Δ* cells. However, only 35% of HCOs in the wild-type strain (8/23 cases) were Nat^r. We believe that formation of HCOs in

our disomic system results from aberrant processing of BIR intermediates, which takes place at a significantly increased frequency in *po/32Δ* mutants.

Specifically, it is hypothesized that *po/32Δ* mutants are proficient at the strand-invasion step of BIR, but defective in initiation and/or progression of DNA synthesis associated with BIR (see also Section 4.5.2). Supportive of this hypothesis is the finding that HCO events were absent in *rad51Δ* mutants, which are defective at the earlier, strand-invasion step of BIR (Table 4.1). Rare HCOs in a *rad51Δ* background were reported by (Smith et al., 2009) using a plasmid transformation assay designed to select for such outcomes, though in this system it is possible these outcomes resulted from annealing of the transformed vector with a previously broken molecule (breaks would be persistent in a *rad51Δ* background due to the HR repair defect). Also, very rare HCO events were observed in a diploid system used to examine the effect of inverted repeats on BIR efficiency (Downing et al., 2008). In that system, approximately 10-fold more *rad51Δ* repair outcomes were analyzed compared to this study, and it is possible that very rare HCO outcomes may have been detected in our disomic system if the number of analyzed colonies had been greatly increased.

4.3. Checkpoint-deficient Mutants and BIR

The hypothesis that HCOs can result when BIR is interrupted after strand invasion but before completion of DNA synthesis (based on data from *po/32Δ*; see Section 4.2.1.2) raises the likely possibility that other genetic deficiencies

that impair the elongation step of BIR will increase HCO formation. Likewise, other cellular conditions can hinder BIR repair and may also alter repair outcomes. Because BIR is a long repair process that requires an extended G2/M arrest (Malkova et al., 2005), we investigated the effect of DNA damage checkpoint deficiency on BIR repair (see Section 2.4 for more information on the DNA damage checkpoint in *S. cerevisiae*). I hypothesized that failed DNA damage checkpoint response in either a *rad9Δ* or *rad24Δ* mutant background of the disomic BIR system (AM1003-9; see Figure 4.1) would decrease BIR efficiency. Furthermore, I expected that failed damage-induced arrest may increase half-crossover formation in one or both of these mutant strains.

Deletions of *RAD9* and *RAD24* were chosen because they represent two independent epistasis groups involved in DSB repair, and their deletion is known to confer different repair/checkpoint defects (de la Torre-Ruiz et al., 1998). Rad9p localizes to phosphorylated histones at the DSB site (Hammet et al., 2007) and promotes Mec1p-dependent phosphorylation of effector kinases Rad53p (Sun et al., 1998) and Chk1p (Blankley and Lydall, 2004). The effector kinases phosphorylate down-stream targets that result in cell cycle arrest and maintain pre-anaphase sister-chromatid interactions (Cohen-Fix and Koshland, 1997; Yamamoto et al., 1996). Deletion of *RAD9* results in a defective DNA damage checkpoint response (Weinert and Hartwell, 1988; Weinert and Hartwell, 1993) and increases both spontaneous and damage-induced GCR formation, including formation of NRTs (Fasullo et al., 1998). The *RAD24* epistasis group

senses DNA damage independently of the *RAD9* epistasis group, with Rad24p localizing to RPA-coated ssDNA (de la Torre-Ruiz et al., 1998; Majka et al., 2006). Rad24p is the DNA damage-specific member of the PCNA-like clamp loading complex (Green et al., 2000). Deletion of *RAD24* is shown to affect repair kinetics, and *rad24Δ* mutants also show improper choice of recombinational repair donor (Aylon and Kupiec, 2003; Grushcow et al., 1999).

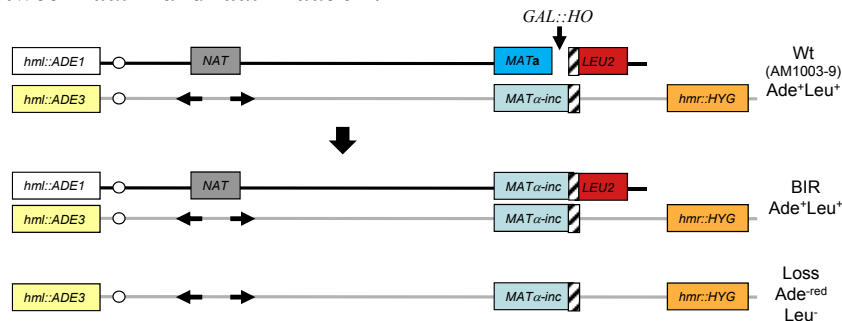
4.3.1. BIR efficiency is reduced in *rad9Δ* and *rad24Δ* mutants

To determine whether *rad9Δ* or *rad24Δ* cells was defective in BIR repair, either *RAD9* or *RAD24* was deleted from our disomic BIR system, grown overnight in glucose-free media, and plated on galactose-containing media to induce the HO-created DSB. A BIR deficiency, which manifests as a decrease in BIR repair events and coincident loss of the broken chromosome, was observed in both mutant strains. (Please note, I am showing the results obtained from one representative plating. Results obtained from several other platings were similar to those presented here (data not shown). The method I used to score the colonies evolved over time to best capture the events I observed, and only one experiment reflects the final scoring methodology I developed.) In *rad9Δ* and *rad24Δ* mutants, only 10.6% and 11.6% of colonies were fully Ade⁺Leu⁻, respectively (Table 4.2). In total, 79.9% and 82.3% of all colonies in *rad9Δ* and *rad24Δ* mutants, respectively, had ≥1 Ade^{-red}Leu⁻ sector, compared to only 10.8% in wild type (p<0.001 for both comparisons). Thus, failure of the cell to arrest

Table 4.2. BIR efficiency in strain AM1003-9 and its *rad9Δ*, *rad24Δ*, and *rad9Δrad50Δ* derivatives.

Genotype	Total colonies scored	Number of Colonies with Phenotype Indicated (%)						P-value
		Full BIR	Colonies with Loss of a Broken Chromatid				Other ^b	
			Ade ⁺ Leu ⁻	Ade ^{-red} Leu ⁻	Ade ^{+/-red} Leu ⁻	Other events with ≥1 Ade ^{-red} Leu ⁻ sector		
wt ^a	554	436 (78.7)	2 (0.3)	52 (9.4)	6 (1.1)	60 (10.8)	58 (10.5)	
<i>rad9Δ</i>	199	21 (10.6)	30 (15.1)	108 (54.3)	21 (10.6)	159 (79.9)	19 (9.5)	<0.001 ^c
<i>rad24Δ</i>	181	21 (11.6)	5 (2.8)	47(26.0)	97 (53.6)	149 (82.3)	11 (6.1)	<0.001 ^c
<i>rad9Δrad50Δ</i>	138	4 (2.9)	26 (18.8)	47 (34.1)	52 (37.7)	125 (90.6)	9 (6.5)	<0.001 ^c 0.1976 ^d

Abbreviations: Ade^{-red} = Ade⁻, His⁺ red colonies indicative of the *ade1 ADE3* genotype; BIR = break-induced replication; wt = wild type. Sectorized phenotypes are indicated by both phenotypes separated by a backslash. ^a Data for wild type are taken from a subset of platings performed for Deem et al., 2008. ^b Other events include GC (Ade⁺Leu⁺), HCOs (Ade^{-white}Leu⁻), and very rare outcomes such as Ade^{-red}Leu⁺. ^c P-value determined using chi-square comparison of BIR (Ade⁺Leu⁻) events versus all other events (loss and “other” events combined) between each mutant and wt. ^d P-value determined using chi-square comparison of BIR (Ade⁺Leu⁻) events versus all other events (loss and “other” events combined) between *rad9Δ* and *rad9Δrad50Δ*.



during DSB repair decreases the efficiency of BIR in our disomic system and results in loss of the broken chromatid or other repair outcomes (Figure 4.1). In the *rad9Δ* mutant, the number of colonies that lost the broken chromosome ($\text{Ade}^+ \text{Leu}^-$) was statistically significantly higher compared to both wild type and *rad24Δ* ($p < 0.001$ for both comparisons). *rad9Δ* mutants have been shown to resect broken chromosomes quickly (Lazzaro et al., 2008; Lydall and Weinert, 1995), which may increase chromosome loss; thus, a *rad9Δrad50Δ* double mutant was constructed to help stabilize the fragment (data presented for *rad9Δrad50Δ* are combined from two small, independent platings). In the double mutant, BIR efficiency continued to be statistically significantly reduced compared to wild type, and was not statistically significantly different from the *rad9Δ* single mutant (Table 4.2), indicating that deletion of the resection enzyme Rad50p did not prevent loss of the broken chromosome in *rad9Δ* mutants. However, in *rad9Δrad50Δ*, fewer $\text{Ade}^{+/-\text{red}} \text{Leu}^-$ colonies were observed compared to *rad9Δ*, and these events appear to be shifted into multiply sectored colonies, which reflects increased retention of the broken chromosome (see Section 4.3.2).

4.3.1.1. Physical characterization of BIR outcomes in *rad9Δ* and *rad24Δ* mutants

Previous physical analyses of $\text{Ade}^+ \text{Leu}^-$ outcomes in *pol32Δ* demonstrated that some of these events were GCRs versus molecules repaired by allelic BIR. It was determined that the proportion of $\text{Ade}^+ \text{Leu}^-$ outcomes that represented GCRs was elevated among events that had lost the *NAT* marker located

approximately 30 kb centromere-proximal to the DSB (see Section 4.2.1.1 and Figure 4.3). The proportion of Ade⁺Leu⁻ and Ade^{+/-red}Leu⁻ events that lost the NAT marker (became Nat^s) was statistically significantly higher in both the *rad9Δ* (65.4%) and *rad24Δ* (10.0%) mutants compared to wild type (4.4%; $p < 0.0001$ and $p = 0.0402$, respectively; Table 4.3), leading to the hypothesis that checkpoint mutants may have an increased incidence of GCRs among Ade⁺Leu⁻ events. This was tested by physical analyses of both Nat^r and Nat^s outcomes from *rad9Δ* and *rad24Δ* mutants. Consistent with the *pol32Δ* findings, many NAT^s Ade⁺Leu⁻ events in *rad9Δ* (9/14 analyzed (64%)) and *rad24Δ* (5/9 analyzed (56%)) mutants were actually GCR events, while half of NAT^r Ade⁺Leu⁻ outcomes in *rad9Δ* (2/4 analyzed) and 67% of *rad24Δ* outcomes (2/3 analyzed) represented allelic BIR repair events. These data suggest that *rad9Δ* and *rad24Δ* mutants are more prone to GCR formation than wild type.

When the percent of Nat^s events in *rad9Δ* (65.4%) and *rad24Δ* (10.0%; Table 4.3) is multiplied by the percent of Ade⁺Leu⁻ outcomes observed to be GCRs in each strain (64% and 56%, respectively; Figure 4.5), it can be estimated that 42% and 6% of all Ade⁺Leu⁻ BIR outcomes in *rad9Δ* and *rad24Δ* are actually GCR events.

In *rad9Δ*, the broken chromosome was frequently lost (Table 4.2) and, among repaired chromatids, the NAT marker was frequently lost (Table 4.3; Figure 4.1).

Elimination of the resection protein Rad50p in *rad9Δ* mutants did not decrease the frequency of chromosome loss compared to *rad9Δ* alone (90.6% compared to 79.9%, respectively; Table 4.2); however, among Ade⁺Leu⁻ or Ade^{+/-red}Leu⁻ BIR repair outcomes, *rad9Δrad50Δ* cells more frequently retained the *NAT* marker compared to *rad9Δ* alone (70.6% compared to 34.6, respectively; Table 4.3). Physical analyses on Ade⁺Leu⁻ outcomes from the double mutant have not yet been performed, but it is hypothesized that the increased frequency of NAT^r events suggests a decrease in the proportion of Ade⁺Leu⁻ events that represent GCRs.

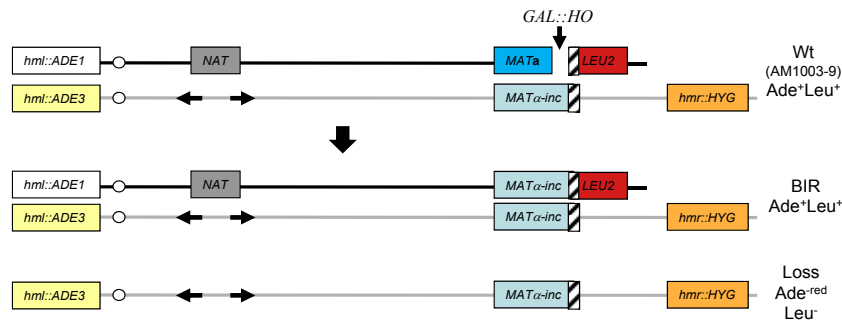
4.3.2. Sectoring of colonies in *rad9Δ* and *rad24Δ* mutants

A striking phenotype observed in both *rad9Δ* and *rad24Δ* mutants was that the colonies were highly sectoried. In *rad9Δ*, this manifested primarily as Ade^{+/-red}Leu⁻ events (Tables 4.2, 4.4), whereas in *rad24Δ*, over half of all colonies scored had ≥3 sectors (Table 4.4). In almost every case, ≥1 of the sectors in these multiple-sectoried colonies was Ade⁺Leu⁻, and ≥1 of the sectors was Ade^{-red}Leu⁻. (For this reason, Ade^{+/-red}Leu⁻ sectoried colonies are also considered in Table 4.4). This multiple-sectors phenotype was rarely observed in wild type cells and was not recorded.

Table 4.3. Analysis of retention of *NAT* marker among BIR repair outcomes.

Genotype	Total Ade ⁺ BIR colonies ^a	Number of Colonies with Phenotype Indicated (%)							P-value
		Nat ^r BIR Events				Nat ^s BIR Events			
		BIR Ade ⁺ Nat ^r Leu ⁻	BIR/Loss Ade ^{+/red} Nat ^{r/s} Leu ⁻	Total Nat ^r	BIR Ade ⁺ Nat ^s Leu ⁻	BIR/Loss Ade ^{+/red} Nat ^s Leu ⁻	Total Nat ^s		
wt ^b	574	518 (90.2)	31 (5.4)	549 (95.6)	6 (1.0)	19 (3.3)	25 (4.4)		
<i>rad9Δ</i>	130	16 (12.3)	29 (22.3)	45 (34.6)	5 (3.8)	80 (61.5)	85 (65.4)	<0.0001 ^c	
<i>rad24Δ</i>	70	19 (27.1)	44 (62.9)	63 (90.0)	2 (2.9)	5 (7.1)	7 (10.0)	0.0402 ^c , <0.0001 ^d	
<i>rad9Δrad50Δ</i>	51	4 (7.8)	32 (62.7)	36 (70.6)	0	15 (29.4)	15 (29.4)	<0.0001 ^{c,d} , 0.0063 ^e	

Abbreviations: Ade^{-red} = Ade⁻, His⁺ red colonies indicative of the *ade1 ADE3* genotype; BIR = break-induced replication; wt = wild type. Sectorized phenotypes are indicated by both phenotypes separated by a backslash. ^a Includes Ade⁺Leu⁻ and Ade^{+/red}Leu⁻ colonies indicative of full or partial BIR repair. ^b Data for wild type are taken from platings performed for Deem et al., 2008. ^c P-value determined using chi-square comparison of Nat^r versus Nat^s events between each mutant and wt. ^d P-value determined using chi-square comparison of Nat^r versus Nat^s events between each mutant and *rad9Δ*. ^e P-value determined using chi-square comparison of Nat^r versus Nat^s events between *rad9Δrad50Δ* mutant and *rad24Δ*.



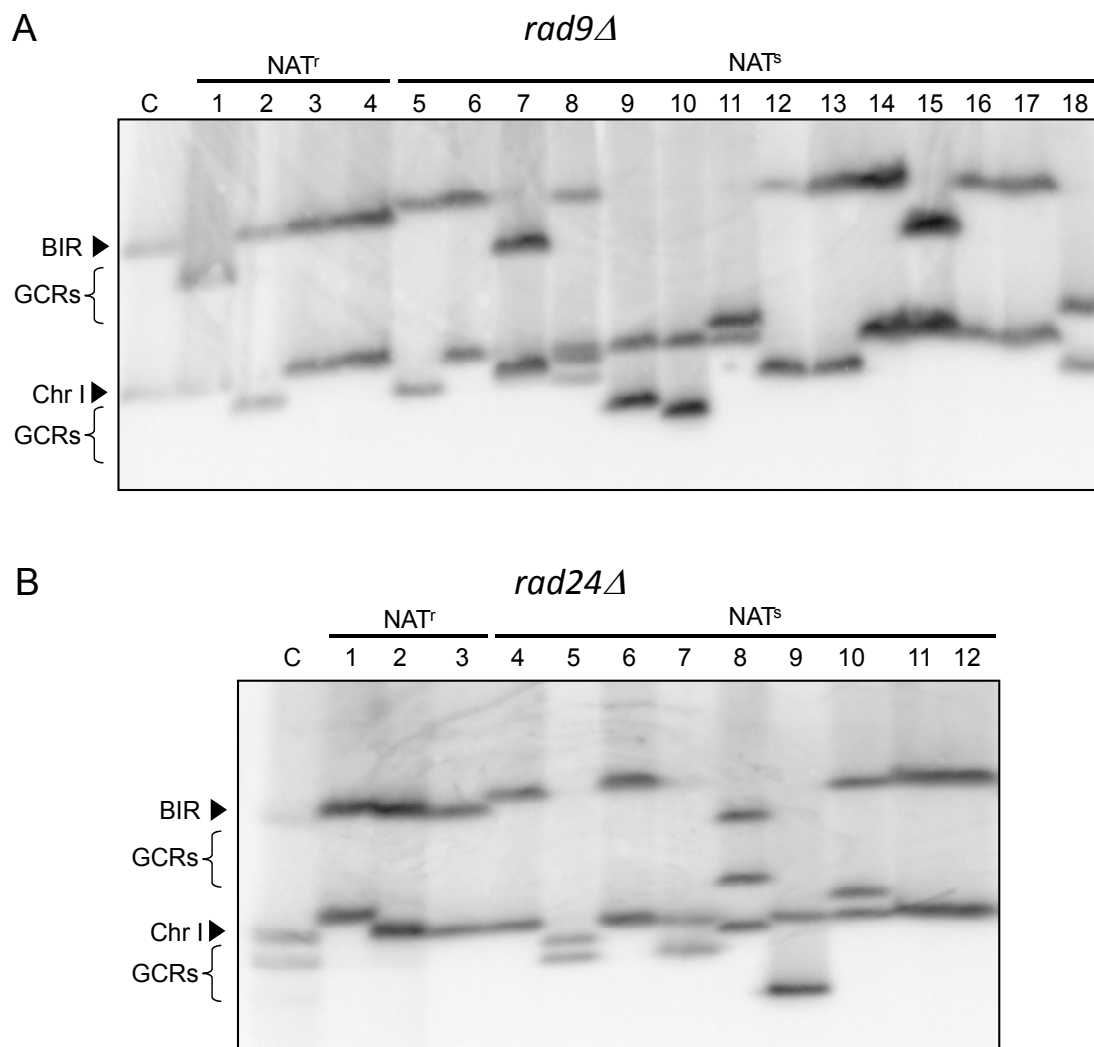


Figure 4.5. Structural analysis of Ade⁺Leu⁻ repair outcomes in *rad9Δ* and *rad24Δ*. Southern blot analysis of the PFGE gel of **(A)** *rad9Δ* and **(B)** *rad24Δ* outcomes using an *ADE1*-specific probe, which hybridizes to the copy of Chromosome (Chr) III that is cleaved by HO, as well as to Chr I. Lanes labeled C show DNA from a AM1003 timecourse after BIR repair. Other lanes contained DNA obtained from Nat^r or Nat^sAde⁺Leu⁻ repair outcomes from mutants as indicated. Bands indicative of BIR and GCR outcomes are indicated.

The multiple-sectors phenotype was also observed in the *rad9Δrad50Δ* double mutant, where statistically significantly more colonies were sectored compared to wild type ($p < 0.0001$; Table 4.4). While the double mutant was not statistically significantly different from the *rad9Δ* single mutant in terms of proportion of

Table 4.4. Effect of checkpoint deficiency on formation of sectored events.

Genotype	Total Colonies scored	Number of Colonies with Phenotype Indicated (%)				P-value
		Sectored colonies with Ade ⁺ Leu ⁻ and Ade ^{-red} Leu ⁻			Other ^c	
		Ade ^{+/-red}	Colonies with ≥3 sectors	Total sectored colonies		
wt ^a	684	51 (7.5)	ND ^b	51 (7.5)	633	
<i>rad9Δ</i>	199	108 (54.3)	20 (10.1)	128 (64.3)	71 (35.7)	<0.0001 ^c
<i>rad24Δ</i>	181	47(26.0)	93 (51.4)	140 (77.3)	41 (22.7)	<0.0001 ^c
<i>rad9Δrad50Δ</i>	138	47 (34.3)	43 (31.4)	90 (65.2)	48 (34.8)	<0.0001 ^c 0.8648 ^d

Abbreviations: Ade^{-red} = Ade⁻, His⁺ red colonies indicative of the *ade1 ADE3* genotype; wt = wild type. Sectored phenotypes are indicated by both phenotypes separated by a backslash. ^a Data for wild type are taken from platings performed for Deem et al., 2008. ^b Colonies with multiple sectors were rare in wt and were not recorded; however, they were sufficiently rare that their inclusion would not change the outcome of statistical analyses. ^c Other events include colonies with only a single event, as well as colonies with two sectors that contained one of the following:: GC (Ade⁺Leu⁺), HCO (Ade^{-white}Leu⁻), and very rare outcomes such as Ade^{-red}Leu⁺. ^c P-value determined using chi-square comparison of total sectored colonies versus “other” events between each mutant and wt. ^d P-value determined using chi-square comparison of total sectored colonies versus “other” events between *rad9Δ* and *rad9Δrad50Δ*.

sectored colonies, there was a shift from Ade^{+/-red}Leu⁻ colonies to colonies with ≥3 sectors in the double mutant (i.e., in the double mutant, the proportion of Ade^{+/-red}Leu⁻ colonies was statistically significantly lower than *rad9Δ*, while the proportion of sectors with ≥3 sectors was statistically significantly higher than *rad9Δ* ($p < 0.001$ for both comparisons)). This suggests that, in the double mutant,

the chromosome fragment more frequently persists through multiple cell divisions to repair in a later generation.

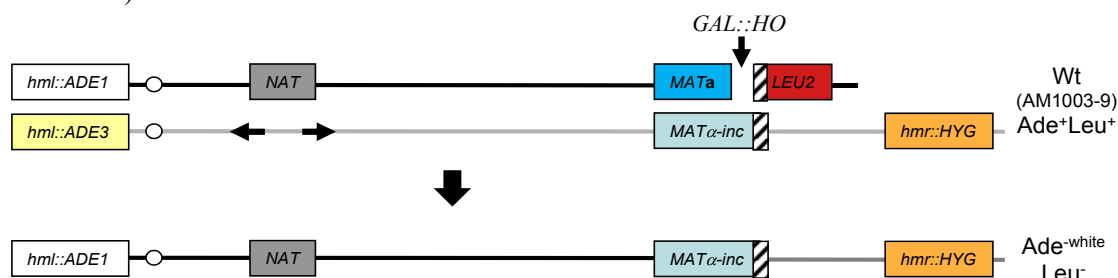
4.3.3. HCOs in *rad9Δ* and *rad24Δ* mutants

It was hypothesized that checkpoint mutants may have an increased number of HCO events because failure of the DNA damage checkpoint could allow BIR to initiate and form a heteroduplex molecule, but not allow enough time for BIR repair to complete. In the *rad24Δ* mutant, 11.6% of colonies had ≥ 1 HCO event (either the whole colony or ≥ 1 sector was Ade^{-white}Leu⁻), compared to only 3.4% colonies in wild type ($p < 0.0001$). In *rad9Δ* mutants, a trend toward higher HCO incidence was observed, with 8.0% of colonies exhibiting ≥ 1 HCO event ($p = 0.0058$). Interestingly, in the *rad9Δrad50Δ* double mutant, HCOs were statistically significantly increased both compared to wild type, as well as compared to *rad9Δ*. In these double mutants, colonies were more likely to have ≥ 3 sectors (see Table 4.3), suggesting the chromosome fragment persisted through several generations before repair. These HCO data demonstrate that, while stabilizing the chromosome fragment may allow for more frequent DSB repair, the repair outcomes themselves may be undesirable.

Table 4.5. HCOs in strain AM1003-9 and its *rad9Δ* and *rad24Δ* derivatives.

Genotype	Total colonies scored	Number of Colonies with Phenotype Indicated (%)		P-value
		HCO Ade ^{-white} Leu ^{-b}	Other ^c	
wt ^a	684	23 (3.4)	648 (96.6)	
<i>rad9Δ</i>	199	16 (8.0)	183 (92.0)	0.0058 ^d
<i>rad24Δ</i>	181	21 (11.6)	160 (88.4)	<0.0001 ^d
<i>rad9Δrad50Δ</i>	138	38 (27.5)	100 (72.5)	<0.0001 ^{d,e}

Abbreviations: HCO = half-crossover; Ade^{-white} = Ade⁻, His⁻ white colonies indicative of the *ade1 ade3* genotype; wt = wild type. Sectored phenotypes are indicated by both phenotypes separated by a backslash. ^a Data for wild type are taken from platings performed for Deem et al., 2008. ^b Includes full and partial HCOs in which part of the colony was Ade^{-white} while the other part(s) represented chromosome loss, BIR, or GC. ^c Other events include colonies with sectors of BIR (Ade⁺Leu⁻), GC (Ade⁺Leu⁺), loss (Ade^{-red}Leu⁻), and/or very rare outcomes such as Ade^{-red}Leu⁺. ^d P-value determined using chi-square comparison of HCO (Ade^{-white}Leu⁻) events versus “other” events between each mutant and wt. ^e P-value determined using chi-square comparison of HCO (Ade^{-white}Leu⁻) events versus “other” events between *rad9Δ* and *rad9Δrad50Δ*.



4.4. The Effect of Replication-inhibiting Drugs on BIR

Based on the hypothesis that interrupted BIR leads to half-crossover molecules (Deem et al., 2008), we sought to determine the effect of replication-inhibiting drugs on BIR and HCO formation. We hypothesized that introduction of a replication-inhibiting drug during BIR may interrupt DNA synthesis during BIR, resulting in an increase of HCO molecules. Because replication-inhibiting agents have varied mechanisms, several different agents were investigated by myself and other members of the lab, including methylmethanesulfonate (MMS), cis-

diamine-dichloro-platinum(II) (cisplatin), phleomycin, and hydroxyurea (HU).

Only my data are presented here.

To test the effect of replication-inhibiting drugs on formation of HCOs, the disomic strain (Figure 4.1) was grown to log phase in YEP-Lactate medium, incubated in galactose-containing media for 30 minutes (to induce the HO-created DSB), and then incubated with or without a replication-inhibiting drug for 7 hours and plated on YEPD rich medium. The time for drug incubation was selected based on the known kinetics of BIR, which initiates very slowly and takes up to 8 hours to complete (Malkova et al., 2005). Colonies were replica plated on Ade, His, and Leu drop-out media to analyze the fate of the broken chromosome.

Addition of 2.4 mM or 6 mM MMS during BIR repair statistically significantly increased the formation of HCO events ($\text{Ade}^{-\text{white}}\text{His}^{-}\text{Leu}^{-}$) to 16.2% and 20.4%, respectively, compared to cells with no drug treatment (5.5%). Preliminary experiments with cisplatin and phleomycin were highly variable and inconclusive. With respect to HU, my preliminary data (not shown) suggest a BIR defect in which BIR repair is less frequent compared to a no-drug control and the broken chromosome is frequently lost; however, these initial experiments were inconclusive with regard to the effect on HCOs. The effects of cisplatin and HU on BIR and HCO formation are being investigated by other members of the lab,

as this may provide important insight into the BIR replication fork and its response to depletion of dNTP pools.

Table 4.6. Replication-inhibiting drugs used in BIR studies.

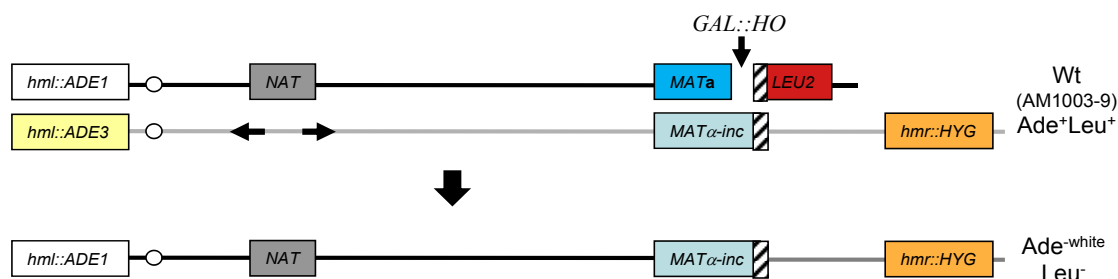
Drug	Biological Activity	Rationale	Selected References
MMS	DNA alkylating agent	Addition of an alkyl group to DNA is repaired by BER, which creates a single-strand break. If the replication fork encounters the single-strand break, a DSB can result	(Lundin et al.; Murakami-Sekimata et al., 2010; Paulovich and Hartwell, 1995; Xiao et al., 1996)
Cisplatin	DNA cross-linking agent	Cross-linking may create a physical barrier that results in disassembly of the replisome. Cisplatin may also be removed from DNA by NER, resulting in a single-strand break that could be converted to a DSB.	(Dronkert and Kanaar, 2001; Frankenberg-Schwager et al., 2005; Lippert, 1992; McHugh et al., 2000)
Phleomycin	DNA intercalating agent; oxidative damage	Oxidative damage results in single-strand breaks in DNA that can be converted to a DSB.	(Fasullo et al., 2005; Koy JF, 1995; Moore, 1989; Sleight, 1976)
HU	Inhibits RNR; depletes nucleotide pools	Elimination of dNTPs pauses the replication fork due to lack of substrate for the polymerase elongation reaction.	(Eklund et al., 2001; Slater, 1973)

MMS = methylmethane sulfonate; DNA = deoxyribonucleic acid; BER = base excision repair; DSB = double-strand break; NER = nucleotide excision repair; HU = hydroxyurea.

Table 4.7. Effect of MMS on HCO formation in cells undergoing BIR repair.

Drug (Conc)	Total Colonies scored	Colonies with		Estimated Viability	Number of experiments	P-value ^b
		HCO Ade ^{-white} Leu ^{-a}	% HCOs			
None	4776	263	5.5	90.2% ± 25.1%*	16	
MMS (2.4 mM)	852	138	16.2	23.5% ± 11.1%	5	<0.0001
MMS (6 mM)	1225	200	16.3	13.8% ± 6.0%*	7	<0.0001

Abbreviations: HCO = half-crossover; Ade^{-white} = Ade⁻, His⁻ white colonies indicative of the *adel1 ade3* genotype; MMS = methylmethane sulfonate. Data from independent experiments were determined to be similar to each other and therefore combined. ^a Includes both fully Ade^{-w}Leu⁻ colonies as well as colonies with ≥1 Ade-wLeu- sector. ^d P-value determined using Chi-square comparison of HCO (Ade^{-w}Leu⁻) events versus “other” events between each mutant and wt. ^b P-value determined using Chi-square comparison of HCO (Ade^{-w}Leu⁻) events versus all other events between each treatment group and no-treatment.



4.5. Discussion

BIR is an important process of DNA metabolism. While BIR effectively repairs DSBs, it may do so with a cost for the cell, as BIR is implicated in formation of NRTs (Bosco and Haber, 1998; Malkova et al., 2005) and GCRs (Le et al., 1999; Lydeard et al., 2007; Teng et al., 2000; Teng and Zakian, 1999). This chapter describes a BIR defect in cells deficient in a gene encoding a third non-essential subunit of polymerase delta, *POL32*, as well as in various mutants that impair the DNA damage checkpoint response. In addition, the initial characterization of *pol32Δ* mutants led to the discovery of HCOs that are analogous to NRTs observed in mammalian cells. NRTs were described in mammalian tumor cells

as a pathway of telomere acquisition by broken chromosomes that results in the donor molecule losing genetic information – including its telomere – and becoming unstable (Chang et al., 2001; Difilippantonio et al., 2002; Gollin, 2001; Ingvarsson, 1999; Rudolph et al., 2001; Sabatier et al., 2005; Sprung et al., 1999). This destabilization of the donor makes NRTs especially devastating because the events are self-perpetuating and result in cascades of genomic destabilization events, including NRTs, chromosome loss, and multiple rearrangements (Sabatier et al., 2005).

4.5.1. *pol32Δ*, *rad9Δ*, and *rad24Δ* are defective in BIR repair

In contrast to recent findings by Lydeard et al. (2007), who showed BIR to be completely *POL32*-dependent in an ectopic BIR system in yeast, this study of allelic BIR indicated that *POL32*-independent BIR still occurred in a significant portion of cells (Table 4.1, Deem et al., 2008). Physical characterization of Ade⁺Leu⁻ BIR outcomes indicated that some of these events actually represented GCRs. Isogenic wild type and *pol32Δ* strains that contained a *URA3* marker approximately 3 kb centromere-proximal to the DSB site were used to show that *pol32Δ* mutants lost the *URA3* marker more frequently compared to wild type, leading to the hypothesis that more extensive homology is important to facilitate BIR repair in this background (Deem et al., 2008).

DNA damage checkpoint-deficient mutants also displayed a BIR defect, with decreased BIR repair and increased loss of the broken chromosome. However, the defect differed between *rad9Δ* and *rad24Δ*. In *rad24Δ* mutants, over half of the colonies displayed ≥ 3 sectors, with ≥ 1 Ade⁺Leu⁻ sector in nearly every case. This was not unexpected, as the faulty checkpoint could result in cell division prior to DSB repair followed by missegregation of the centromeric fragment that persists for several generations before successful repair. In *rad9Δ*, multiple-sectored colonies were not as frequent; rather, the primary BIR defect in this background was loss of the broken chromosome. Potentially, the frequent loss of the chromosome is related to the known role of Rad9p to protect uncapped telomere ends from resection, though an analogous role for Rad9p at DSB ends has not yet been confirmed (Lydall and Weinert, 1995). If Rad9p does, in fact, confer protection to the DSB ends, the increased loss of the broken chromosome in *rad9Δ* could be explained by rapid resection of the broken chromosome that does not allow sufficient time for repair. This idea is consistent with the fact that the *rad9Δ* mutant also displayed frequent loss of the *NAT* marker approximately 30 kb upstream of the DSB among Ade⁺Leu⁻ repair events. Elimination of Rad50p in the *rad9Δ* background to slow resection resulted in more multiple-sector colonies such as those seen in *rad24Δ*, which could reflect an increase in DSB repair that results from delayed degradation of the chromosome fragment. Since the *rad9Δrad50Δ* double mutant was created, a great deal about post-DSB resection has been elucidated, and the effects of *exo1Δ* and/or *sgs1Δ* on DSB

repair in *rad9Δ* should be considered in future research (Gravel et al., 2008; Mimitou and Symington, 2008; Zhu et al., 2008).

As with *pol32Δ*, physical analysis of Ade⁺Leu⁻ outcomes in both *rad9Δ* and *rad24Δ* confirmed that many of these events were in fact GCRs, and that the proportion of GCRs was higher among NAT^s events compared to NAT^r events. The observation of GCR formation in checkpoint mutants is not new (Aylon and Kupiec, 2003; Fasullo et al., 1998), but this investigation allows us to estimate that a very high proportion of Ade⁺Leu⁻ repair events in *rad9Δ*, approximately 54%, may represent GCRs, with a lower incidence of GCRs in *rad24Δ*.

4.5.2. Interrupted BIR leads to HCOs

In *pol32Δ*, it was observed that, in addition to chromosome loss, a significant portion of the BIR defect was accounted for by an increase in HCO molecules. Because Pol32p is involved in the elongation step of BIR, the finding of increased HCOs in the *pol32Δ* mutant led to the hypothesis that HCOs result from aberrant processing of BIR intermediates. This hypothesis is consistent with an observation made in mouse tumors where duplications were observed at the sites of NRTs (Difilippantonio et al., 2002), suggesting that NRTs could form as the result of interrupted BIR repair. According to this model, *pol32Δ* mutants would be prone to HCO outcomes because they are proficient in BIR initiation

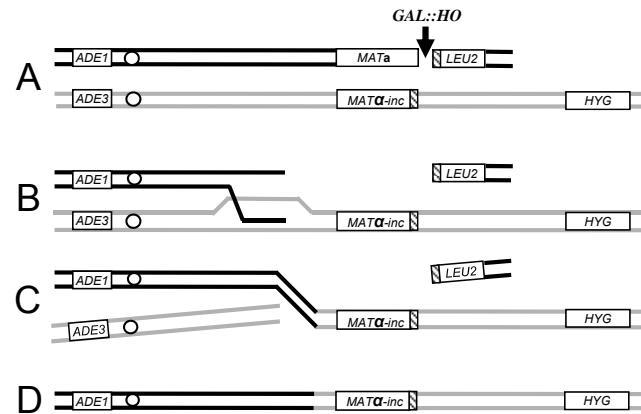


Figure 4.6. Hypothetical mechanism of HCO formation. After induction of a DSB at *MATa* (A) and successful strand invasion (B), BIR progression is interrupted leading to accumulation of a strand invasion intermediate. Resolution of this intermediate (C) leads to formation of a fusion (HCO) chromosome containing parts of donor and recipient molecules (D), accompanied by loss of the other chromosome fragments.

(Lydeard et al., 2007), but deficient in elongation and completion of the repair process. The heteroduplex intermediate created in *pol32Δ* could either dissociate to allow the broken chromosome to be completely resected, or it could be resolved enzymatically or physically to produce HCO molecules (Figure 4.6).

As a result of this HCO model, it was hypothesized that a deficiency in the DNA damage checkpoint may also increase HCO formation among cells undergoing BIR repair. Compared to wild type, a trend toward increased HCOs was observed in *rad9Δ*, while a statistically significant increase was observed in *rad24Δ*. Interestingly, in the *rad9Δrad50Δ* double mutant, HCOs were significantly more frequent than in both wild type and *rad9Δ*. This finding could indicate that, in some backgrounds, persistence of a broken chromosome fragment is more deleterious than complete resection of the fragment, as a persistent fragment may ultimately damage other parts of the genome. Finally, based on that observation of multiple-sectored colonies in both the *rad9Δ* and *rad24Δ* mutants, as well as the relatively frequent occurrence of both Ade⁺Leu⁻ and Ade^{-white}Leu⁻ sectors within these colonies (data not shown), I hypothesize that further physical analyses may identify some Ade⁺Leu⁻ sectors to represent cells in which a HCO molecule formed and the resultant *ADE3*-containing fragment stabilized through formation of a GCR. This can be examined by PFGE and confirmation as a single, 340-kb band that hybridizes to an *ADE1* probe, along with a band of any size (other than 350 kb) that hybridizes to an *ADE3*

probe. My initial attempts to identify such outcomes were inconclusive due to poor quality of DNA samples and Southern blots.

Our disomic system to study BIR was also used to investigate the effect of replication-inhibiting drugs on BIR repair. Of particular interest in these investigations was the formation of HCOs, as it was hypothesized that these drugs, if introduced during BIR repair, may interrupt BIR elongation to form HCO molecules. This may result from a physical block of the replication fork, the BIR replication fork encountering a single-strand break in the donor template, or by eliminating dNTPs needed for DNA synthesis. A statistically significant increase in HCO formation was observed among cells undergoing BIR repair that were pulse treated with either 2.4 mM or 6 mM MMS. Due to their varied effects on DNA and replication, cisplatin, phleomycin, and HU were also tested for effects on HCO formation, but preliminary data from these compounds remains inconclusive.

4.5.3. Summary

Our disomic system in yeast is an efficient tool to study allelic BIR repair. This chapter describes the BIR defects of *pol32Δ*, *rad9Δ*, *rad24Δ*, and *rad9rad50Δ*. In all cases, the BIR defect is characterized by decreased BIR efficiency and an increase in loss of the chromosome. Furthermore, in all mutants except *rad9Δ*, the BIR defect is also characterized by an increase in HCOs. Addition of MMS to cells repairing DSBs by BIR also increased HCO formation. Thus, the disomic

system used in this research is an important and powerful tool to further examine one possible mechanism of HCO formation: interrupted BIR. As NRT research in mammalian cells has proven to be very difficult, this yeast system provides a valuable tool to further characterize such genome-destabilizing events that are associated with aging and cancer.

CHAPTER 5. FRAMESHIFT MUTAGENESIS ASSOCIATED WITH BREAK-INDUCED REPLICATION

5.1. Introduction

Genetic information is preserved through generations by chromosome duplication during S-phase DNA replication, which is highly accurate due to the fidelity of replicative polymerases and efficient elimination of replication errors by polymerase-coupled proofreading activity and post-replicative mismatch repair (MMR). Aside from scheduled DNA replication during S-phase, DNA synthesis is also a part of various types of DNA repair, such as nucleotide-excision repair, base-excision repair, and DSB repair. It has been shown that short-patch synthesis associated with repair of various kinds of DNA damage is highly error-prone (Eckardt and Haynes, 1977; Hicks et al., 2010; James and Kilbey, 1977; James et al., 1978; Strathern et al., 1995), making these events important contributors to a cell's overall mutation rate.

DSBs as a source of hypermutability have been documented for several repair events, including GC and SSA in vegetative cells (Hicks et al., 2010; Holbeck and Strathern, 1997; McGill et al., 1998; Rattray et al., 2002; Strathern et al., 1995; Yang et al., 2008), and DSB repair in meiosis and non-dividing cells (He et al., 2006; Magni, 1963). Also, increased mutability has been associated with

senescence in telomerase-deficient cells (Meyer and Bailis, 2007), where shortened chromosome ends behave similarly to DSB ends. At least two mechanisms were demonstrated to contribute to DSB-induced mutagenesis. First, unrepaired lesions accumulated in tracts of single-stranded DNA that form after a DSB result in error-prone restoration of the duplex molecule (Yang et al., 2008). A similar pathway was shown to be responsible for hypermutagenesis associated with recovery of dysfunctional telomeres (Yang et al., 2008). Second, it has been demonstrated that copying of a donor sequence associated with GC is mutagenic (Hicks et al., 2010; Paques et al., 1998; Paques et al., 2001; Strathern et al., 1995), which could be explained by inefficient MMR during GC (Hicks et al., 2010; McGill et al., 1998), or by an unusual, conservative mode of synthesis that proceeds without formation of a replication fork (Wang et al., 2004).

This study was designed to determine the mutation rate associated with the processive DNA replication that occurs during BIR. While BIR can replicate replicon-sized portions of DNA, in stark contrast to S-phase replication, BIR is initiated at a DSB site rather than at a replication origin. Unlike other forms of DSB repair, BIR is believed to proceed in the context of a replication fork (Lydeard et al., 2007), and the establishment of the BIR fork requires almost all of the proteins required for initiation of normal replication (Lydeard et al., 2010). However, several observations indicate that the BIR replication fork may differ from an S-phase replication fork in several important ways. For example, it has

been shown that, in *S. cerevisiae*, BIR requires Pol32p, a subunit of Pol δ (Deem et al., 2008; Lydeard et al., 2007; Smith et al., 2009) that is dispensable for yeast S-phase DNA replication. Further, the roles of the main replicative polymerases may differ between BIR and S-phase replication. Thus, for BIR initiation, only Pol α -primase and Pol δ are essential, while Pol ϵ is involved only in later steps of BIR, and up to 25% of BIR events can complete in the absence of Pol ϵ (Lydeard et al., 2007). Also, BIR initiation is very slow (takes approximately 4 hours (Deem et al., 2008; Jain et al., 2009; Malkova et al., 2005)) and is associated with frequent template switching that subsides after the first 10 kb of synthesis (Smith et al., 2007), which led to speculation that there may be slow assembly of an unstable replication fork that shifts to a more stable version later in synthesis. Alternatively, initiation of BIR might be slow due to a “recombination execution checkpoint” that regulates the initiation of DNA synthesis during BIR (Jain et al., 2009). All of these unique features of BIR led us to test whether it is more mutagenic than S-phase replication.

Here it is demonstrated that DNA synthesis associated with BIR is highly error-prone, as the frequency of frameshift mutations associated with BIR is dramatically increased compared to normal DNA replication. These results indicate that BIR mutagenesis results from several problems, including increased polymerase error rate and reduced efficiency of mismatch repair.

5.2. Characterization of BIR Frameshift Mutagenesis

5.2.1. Experimental System

To assay the accuracy of BIR, a modified version of our disomic experimental system in *S. cerevisiae* was used (Figure 5.1 A; see Also Figure 4.1 A for original system), wherein a galactose-inducible DSB is initiated at the *MATa* locus of the truncated, recipient copy of chromosome III, while the donor copy of chromosome III contains an uncleavable *MATa-inc* allele and serves as the template for DSB repair (Deem et al., 2008). Elimination of all but 46 bp of homology on one side of the break on the recipient molecule via replacement with *LEU2* and telomeric sequences results in efficient DSB repair through BIR in this strain (Figure 5.1 B, C). Initiation of BIR in this system is preceded by extensive 5'-to-3' resection of the *GAL::HO*-induced DSB at *MATa*, followed by strand invasion of the 3' single-strand end into the donor chromosome at a position proximal to *MATa-inc* (Figure 5.1 B; (Chung et al., 2010)). To study the accuracy of BIR, the level of frameshift mutagenesis was assayed using reversion frameshift reporters in our disomic strain. The frameshift reporters used allowed detection of mutations that occurred during BIR even in the presence of the original wild type gene (an essential feature because the wild type template allele remains after BIR repair) and also allowed investigation of different aspects of BIR replication (similar to (Tran et al., 1997), see below). Frameshifts comprise a significant fraction (10%-20%) of all spontaneous mutations (Giroux et al., 1988; Lawrence, 1984; Lee GS, 1988) and are the most deleterious type of point mutations, as they almost always eliminate gene

function. In contrast, >90% of base substitutions are silent (Lang and Murray, 2008). Notably, an increase in the rate of frameshifts typically correlates with an increase in base substitutions (reviewed in (Kunkel and Bebenek, 2000; McCulloch and Kunkel, 2008)).

Figure 5.1. Experimental system to study BIR-associated mutagenesis. (A) Chromosome (Chr) III in a modified version of disomic experimental strain AM1003 (Deem et al., 2008) used to study BIR. A DSB is created at *MATa* by a galactose-inducible HO gene. The *MATa*-containing copy of Chr III is truncated by insertion of *LEU2* fused to telomere sequences, leaving only 46 bp of homology with the donor sequence (hatched rectangle). The *MAT α -inc*-containing copy is full-length and is resistant to cutting by HO. In this strain, the majority of DSBs introduced at *MATa* are repaired by BIR initiated by strand invasion centromere-proximal to *MAT α -inc* followed by copying of the donor chromosome to the end. To assess mutagenesis associated with BIR, frameshift *lys2::Ins* reporters (see text for details) were inserted into donor Chr. III at one of three positions located at different distances from *MAT α -inc* (*MAT*, 16, or 36 kb). **(B)** After 5'-to-3' resection, BIR proceeds through 1-ended invasion of the broken molecule into the homologous donor chromosome. BIR-associated copying of approximately 100 kb of DNA from the donor chromosome results in an α -mating, *Leu⁻* phenotype. **(C)** Frameshift mutations associated with BIR are detected by the *Lys⁺* phenotype, which arises when an error in DNA copying that restores the *LYS2* reading frame is made in a second copy of the *lys2::Ins* reporter. The example depicts a *Lys⁺* BIR event in the reporter at the 16-kb position. **(D)** Sequence of the 61-, 64-, and 70-bp inserts of the *lys2::Ins(A₄)*, *lys2::Ins(A₇)*, and *lys2::Ins(A₁₄)* constructs, respectively, and flanking *LYS2* sequences. Asterisks indicate the location of the poly-A run; Grey box shades the 6-bp direct repeats that flank the inserted sequence; nucleotides in underlined italics represent a mutation hotspot (right side) and its -1-bp quasipalindromic sequence (left side).

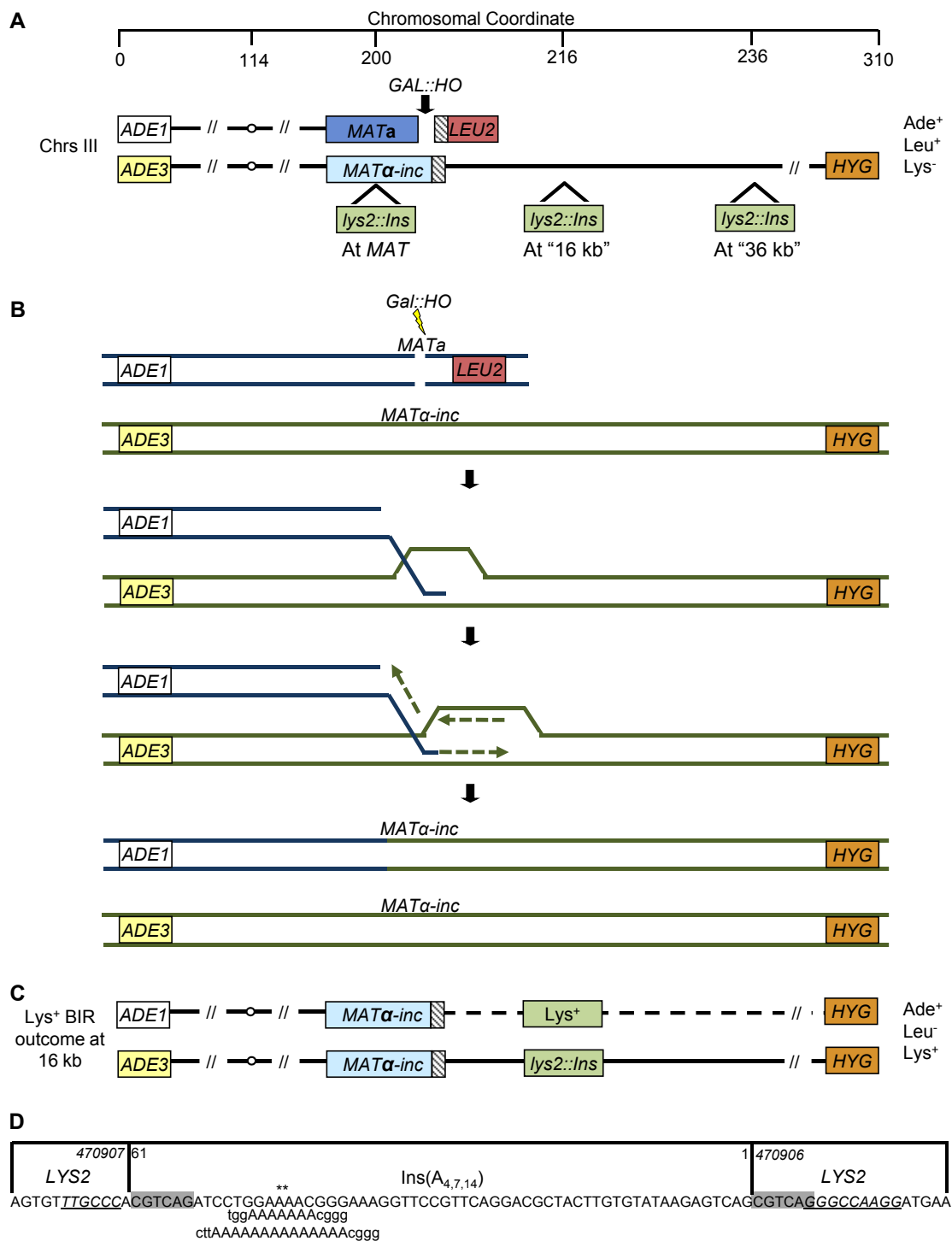


Figure 5.1. Experimental system to study BIR-associated mutagenesis.

Three different frameshift reporters were employed: A_4 , A_7 , and A_{14} (Tran et al., 1997), which are all alleles of the *LYS2* gene with an insertion of approximately 60 bp that includes a homonucleotide run of four adenines (A_4), seven adenines (A_7), or fourteen adenines (A_{14}) (Figure 5.1 D). Insertion of any of the three alleles results in a “+1” shift in the reading frame and a Lys^- phenotype, while a Lys^+ phenotype is restored by a frameshift mutation that occurs in an approximately 71-bp region of the allele (that includes the inserted sequence) and restores the reading frame. A series of isogenic strains was created with insertion of the described reporter alleles into one of three positions on the donor (*MAT α -inc*-containing) chromosome (Figure 5.1 A): 1) at *MAT α -inc* (“*MAT*”), 2) 16 kb centromere-distal from *MAT α -inc* in the region between *RSC6* and *THR4* (“16 kb”), and 3) 36 kb centromere-distal to *MAT α -inc* in the region between *SED4* and *ATG15* (“36 kb”). In all strains, *LYS2* was fully deleted from its native location in chromosome II (see Section 3.1.1 for details regarding strain construction).

BIR-associated mutagenesis was measured by plating appropriate dilutions of cell suspensions to obtain single colonies on rich media (YPD) and lysine drop-out media after a 7-hr incubation in liquid galactose-containing media. The majority of cells undergoing DSB repair remained in G2/M arrest for the duration of the experiment (Figure 5.2 (FACS analysis performed by Ruchi Mathur) and data not shown), consistent with repair of most DSBs by BIR, which exhibits delayed initiation associated with a long G2/M checkpoint arrest (Malkova et al.,

2005). Coherently, the majority of colonies grown with or without selection (on lysine omission media or YEPD, respectively) repaired the DSB by BIR and displayed either an Ade⁺Leu⁻ or Ade^{+/-}Leu⁻ phenotype (Table 5.2), which were previously confirmed to result from BIR repair of both or one of two sister chromatids, respectively (Deem et al., 2008). BIR efficiency in wild type and mutant strains is shown in Table 5.1.

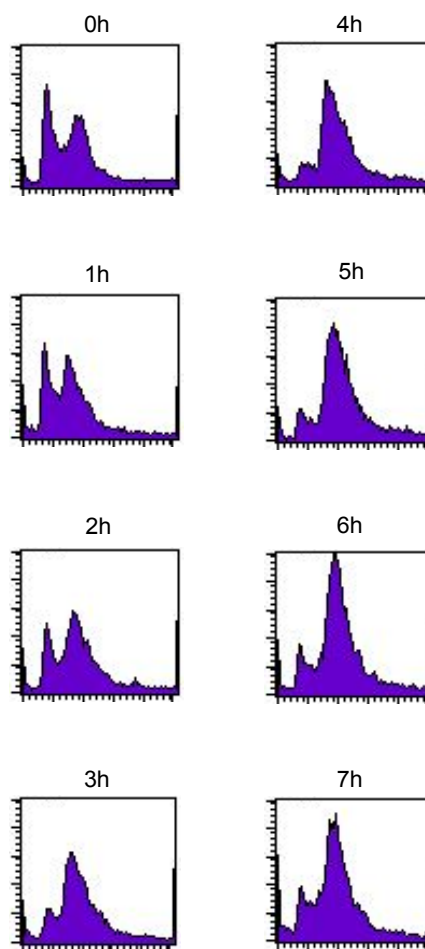


Figure 5.2. Arrest of wild type cells during mutagenesis experiments. FACS analysis of wild type cells with the *lys2::Ins(A₄)* reporter at the 36-kb position before (0h) and after (1h, 2h, 3h, 4h, 5h, 6h, 7h) addition of galactose.

Table 5.1. BIR efficiency in wild type and mutant strains.^a

Genotype	BIR efficiency (%) ^b	
	Median	CI or range ^c [# of repeats]
wt	77.5	(61.8 - 93.0) [7]
<i>msh2Δ</i>	82.5	(70.2 - 91.8) [7]
<i>mlh1Δ</i>	67.4	(47.0 - 74.0) [3]
<i>pol3-5DV</i>	67.0	(54.7 - 75.4) [9]
<i>pol2-4</i>	76.3	(60.0 - 92.3) [7]
<i>rev3Δ</i>	70.4	(66.7 - 77.0) [5]
<i>rad30Δ</i>	71.4	(58.8 - 82.7) [6]
<i>dun1Δ</i> *	64.0	(53.7 - 69.2) [7]
<i>sml1Δ</i> *	69.1	(52.9 - 76.9) [13]
<i>msh3Δ</i>	81.0	(66.0 - 89.0) [5]
<i>pol2-4msh3Δ</i>	ND	ND
<i>pol3-5DVmsh3Δ</i>	71.5	(52.6 - 96.3) [6]

^a Data shown represent combined data from strains with A₄ at the 16- and 36-kb positions. ^b BIR efficiency of wild type and mutant strains was calculated as described in Experimental Procedures. ^c For strains with ≥6 repetitions, 95% CI of the median is indicated. For strains with <6 repetitions, the median range is indicated. *Median is statistically significantly different from wild type (p<0.05), as determined using the Mann-Whitney U test. Abbreviations: BIR, break-induced replication; CI, confidence interval; ND = not done.

5.2.2. Rate of Frameshift Mutagenesis during BIR

For all three reporters at all three locations, the rate of Lys⁺ frameshifts was much higher after DSB repair compared to the spontaneous Lys⁺ rate (Figure 5.3; Table 5.2; see Materials and Methods for details regarding rate calculations). Specifically, for all A₄ and A₇ strains, the rate of frameshift mutagenesis associated with DSB repair (7h) exceeded the Lys⁺ reversion rate before the DSB (0h) by 100- to 550-fold. Because most strains with a DSB site exhibited residual DSB formation even before addition of galactose (data not shown), isogenic no-DSB controls were used to estimate more accurately the rate of spontaneous mutagenesis (see Materials and Methods for details). Using these no-DSB control strains lacking the HO cut site, a 780- to 2800-fold increase in frameshift mutagenesis was observed during BIR compared to spontaneous frameshift mutations. In all strains containing A₁₄, in which spontaneous events were approximately 1100- to 2500-fold more frequent compared to A₄, the rate of frameshift mutagenesis associated with DSB repair remained 25- to 300-fold higher than the rate of spontaneous events. Similar to unselected colonies, the majority of Lys⁺ DSB repair outcomes resulted from BIR (Table 5.2); thus, the substantial increase in frameshift mutagenesis observed in strains with DSBs compared to their no-DSB isogenic controls can be attributed to DNA synthesis during BIR. In control strains that contained the A₄, A₇, or A₁₄ reporters in the native *LYS2* position on chromosome II, no increase in the rates of Lys⁺ was observed after 7 hours in galactose (Figure 5.3; Table 5.2), which confirmed that the increased frameshift mutagenesis was specific for the chromosome

undergoing BIR. Taken together, our data show that frameshift mutagenesis during BIR is increased 25- to 2800-fold compared to spontaneous mutagenesis.

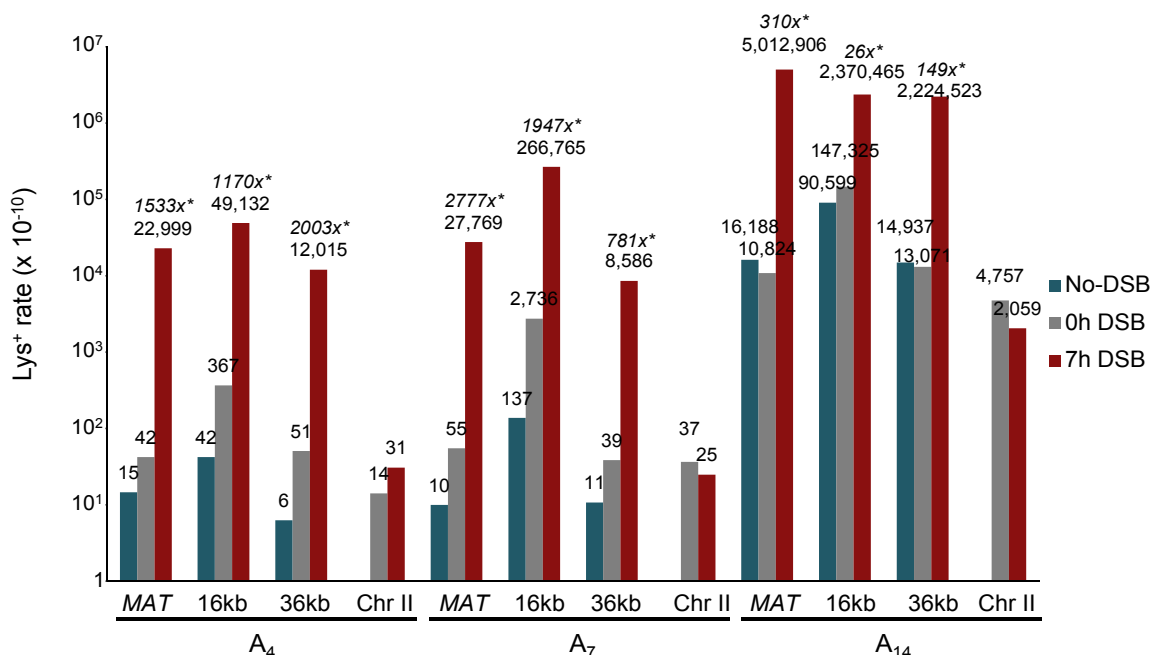


Figure 5.3. BIR-associated mutagenesis determined by frameshift reporters at three chromosomal positions. The rate of Lys⁺ revertants was measured before addition of galactose (0h) and 7 hours after incubation in galactose-containing media (7h) in wild type and its various mutant derivatives containing frameshift reporters A₄, A₇, or A₁₄ in the donor chromosome at *MATα-inc* ("MAT") or approximately 16 or 36 kb centromere-distal to the DSB site. The rate of Lys⁺ revertants in strains with a DSB site in Chr III but containing frameshift reporters in the native *LYS2* position on chromosome II is also shown. Rates of spontaneous Lys⁺ mutagenesis were determined using isogenic no-DSB controls ("no-DSB"). Medians of mutation rates are plotted in log₁₀ scale. See Table S1 for ranges of variation and numbers of repeats. Statistically significant differences from the rate of spontaneous events are indicated by *. The fold increase of the BIR mutation rate compared to spontaneous events is indicated in italics.

Table 5.2. The rate of spontaneous and DSB-associated Lys⁺ mutations.

				Rate of Lys ⁺ (x10 ⁻¹⁰) ^a						
				Before galactose (0h)		After galactose (frequency (7h -0h))				
Position	Construct	HO Site	Relevant Genotype	CI or Range ^b		CI or Range ^b		Fold over ^c	Fold over wt (p-value) ^d	% BIR ^e
				Median	[# Repeats]	Median	[# Repeats]	No-DSB Control		
<i>MAT</i>	A ₄	DSB	WT	42	(25 - 81) [9]	22,999	(18,058 - 30,416) [9]	1,533	NA	96.3 (2.1)
<i>MAT</i>	A ₄	DSB	<i>msh2Δ</i>	353	(243 - 1,346) [12]	43,279	(35,579 - 54,757) [12]	163	1.9 (0.0095)	79.1 (6.6)
<i>MAT</i>	A ₄	DSB	<i>mlh1Δ</i>	770	(551 - 1,261) [7]	78,052	(47,071 - 164,969) [7]	121	3.4 (0.0007)	84.3 (10.5)
<i>MAT</i>	A ₄	DSB	<i>pol3-5DV</i>	256	(99 - 822) [9]	74,124	(52,370 - 91,275) [9]	988	3.2 (0.0005)	90.5 (4.4)
<i>MAT</i>	A ₄	DSB	<i>pol2-4</i>	49	(40-103) [8]	22,119	(14,850-52,436) [8]	1,382	NS	96.6 (0.7)
<i>MAT</i>	A ₄	DSB	<i>rev3Δ</i>	21	(13 - 33) [6]	7,692	(2,745 - 12,153) [6]	2,564	0.3 (0.0004)	96.5 (0)
<i>MAT</i>	A ₄	DSB	<i>rad30Δ</i>	57	(38 - 65) [6]	30,620	(16,447 - 35,988) [6]	2,784	NS	93.0 (4.0)
<i>MAT</i>	A ₄	DSB	<i>dun1Δ</i>	26	(15 - 147) [7]	5,695	(3,031 - 9,959) [7]	475	0.2 (0.0002)	86.4 (11.4)
<i>MAT</i>	A ₄	DSB	<i>sml1Δ</i>	44	(33 - 131) [6]	32,652	(28,439 - 41,467) [6]	3,628	1.4 (0.0176)	91.3 (5.2)
<i>MAT</i>	A ₄	DSB	<i>msh3Δ</i>	52	(36 - 68) [10]	19,161	(4,243 - 31,481) [10]	1,916	NS	86.5 (11.2)
<i>MAT</i>	A ₄	DSB	<i>pol2-4 msh3Δ</i>	90	(16 - 194) [6]	32,743	(19,470 - 75,269) [6]	712	NS ^f (0.0016 [†] , 0.007 [§])	ND
<i>MAT</i>	A ₄	DSB	<i>pol3-5DV msh3Δ</i>	596	(474 - 1,004) [6]	121,012	(107,698 - 141,069) [6]	349	5.3 (0.0004, 0.0002 [†] , 0.0004 [‡])	85.0 (15.0)
<i>MAT</i>	A ₄	No	WT	15	(4 - 16) [7]	0	(0 - 12) [7]	NA	NA	4.0 (4.0)
<i>MAT</i>	A ₄	No	<i>msh2Δ</i>	265	(114 - 3,418) [6]	0	(0 - 102) [6]	NA	17.7 (0.0034)	0 (0)
<i>MAT</i>	A ₄	No	<i>mlh1Δ</i>	645	(215 - 1,404) [6]	0	(0 - 272) [6]	NA	43.0 (0.0034)	4.5 (1.8)
<i>MAT</i>	A ₄	No	<i>pol3-5ΔV</i>	75	(40 - 105) [9]	61	(0 - 205) [9]	NA	5.0 (0.0010)	0 (0)
<i>MAT</i>	A ₄	No	<i>pol2-4</i>	16	(7 - 28) [5]	0	(0 - 55) [5]	NA	NS	0 (0)
<i>MAT</i>	A ₄	No	<i>rev3Δ</i>	3	(1 - 5) [4]	1	(0 - 1) [4]	NA	0.2 (0.0179)	0 (0)
<i>MAT</i>	A ₄	No	<i>rad30Δ</i>	11	(8 - 15) [10]	6	(0 - 27) [10]	NA	NS	0 (0)
<i>MAT</i>	A ₄	No	<i>dun1Δ</i>	12	(9 - 24) [6]	2	(0 - 19) [6]	NA	NS	ND
<i>MAT</i>	A ₄	No	<i>sml1Δ</i>	9	(6 - 12) [6]	14	(0 - 32)[6]	NA	NS	0 (0)
<i>MAT</i>	A ₄	No	<i>msh3Δ</i>	10	(7 - 39) [6]	13	(0 - 30) [6]	NA	NS	0 (0)

Position	Construct	HO Site	Relevant Genotype	Rate of Lys ⁺ (x10 ⁻¹⁰) ^a				Fold over ^c No-DSB Control	Fold over wt (p-value) ^d	% BIR ^e
				Before galactose (0h)		After galactose (frequency (7h -0h))				
				Median	CI or Range ^b [# Repeats]	Median	CI or Range ^b [# Repeats]			
<i>MAT</i>	A ₄	No	<i>pol2-4 msh3Δ</i>	46	(16 - 212) [8]	0	(0 - 22) [5]	NA	3.1 (0.0015, 0.0016 [†] , 0.007 [§])	ND
<i>MAT</i>	A ₄	No	<i>pol3-5DV msh3Δ</i>	347	(33 - 896) [11]	162	(0 - 3778) [11]	NA	23.1 (0.0006, 0.0030 [†] , 0.0030 [‡])	0 (0)
<i>MAT</i>	A ₇	DSB	WT	55	(31 - 80) [9]	27,769	(21,700 - 30,220) [9] (1,351,974 - 5,649,194)	2,777	NA	91.4 (4.8)
<i>MAT</i>	A ₇	DSB	<i>msh2Δ</i>	121,231	(70,337 - 467,001) [7]	1,834,678	[7]	7	66.1 (0.0002)	88.9 (6.7)
<i>MAT</i>	A ₇	DSB	<i>pol3-5DV</i>	136	(93 - 162) [10]	90,216	(68,881 - 161,880) [10]	1,432	3.2 (<0.0001)	86.7 (4.4)
<i>MAT</i>	A ₇	DSB	<i>pol2-4</i>	54	(31 - 116) [6]	57,731	(21,092 - 85,871) [6]	4,811	2.1 (0.0496)	96.2 (1.0)
<i>MAT</i>	A ₇	DSB	<i>rev3Δ</i>	20	(15 - 150) [7]	13,282	(6,638 - 39,278) [7]	1,476	0.48 (0.0115)	98.0 (0.7)
<i>MAT</i>	A ₇	DSB	<i>rad30Δ</i>	53	(26 - 73) [6]	24,483	(11,015 - 54,849) [6]	1,883	NS	89.4 (1.8)
<i>MAT</i>	A ₇	DSB	<i>msh3Δ</i>	52	(33 - 87) [10]	101,201	(23,881 - 187,343) [10]	7,785	3.6 (0.0440)	88.6 (3.6)
<i>MAT</i>	A ₇	DSB	<i>pol2-4 msh3Δ</i>	41	(29 - 149) [6]	28,158	(25,740 - 115,258) [6]	217	NS	ND
<i>MAT</i>	A ₇	DSB	<i>pol3-5DV msh3D</i>	2,110	(1,061 - 9,328) [9]	413,703	(242,689 - 1,321,030) [9]	345	14.9 (<0.0001 <0.0001 [†] , <0.0001 [‡])	90.0 (4.0)
<i>MAT</i>	A ₇	No	WT	10	(5 - 28) [6]	0	- [6]	NA	NA	0 (0)
<i>MAT</i>	A ₇	No	<i>msh2Δ</i>	263,769	(72,228 - 489,915) [6]	0	- [6]	NA	26377.0 (0.0022)	0 (1.7)
<i>MAT</i>	A ₇	No	<i>pol3-5DV</i>	63	(33 - 107) [6]	0	(0 - 286) [6]	NA	6.3 (0.0022)	0 (0.9)
<i>MAT</i>	A ₇	No	<i>pol2-4</i>	12	(6 - 13) [5]	10	(0 - 21) [5]	NA	NS	18.2 (0)
<i>MAT</i>	A ₇	No	<i>rev3Δ</i>	9	(3 - 33) [8]	0	(0 - 17) [8]	NA	NS	7.1 (0)
<i>MAT</i>	A ₇	No	<i>rad30Δ</i>	13	(4 - 224) [6]	3	(0 - 11)[6]	NA	NS	ND

				Rate of Lys ⁺ (x10 ⁻¹⁰) ^a						
				Before galactose (0h)		After galactose (frequency (7h -0h))				
								Fold over ^c		
Position	Construct	HO Site	Relevant Genotype	Median	CI or Range ^b [# Repeats]	Median	CI or Range ^b [# Repeats]	No-DSB Control	Fold over wt (p-value) ^d	% BIR ^e
<i>MAT</i>	A ₇	No	<i>msh3Δ</i>	13	(9 - 168) [8]	0	(0 - 29) [8]	NA	NS	0 (0)
<i>MAT</i>	A ₇	No	<i>pol2-4 msh3Δ</i>	130	(105 - 154) [2]	560	(455 - 665) [2]	NA	ND	ND
<i>MAT</i>	A ₇	No	<i>pol3-5DV msh3Δ</i>	1,200	(624 - 2,322) [6]	0	(0 - 542) [6]	NA	120.0 (0.0022, 0.0007 [†] , 0.0022 [‡])	ND
(3,208,725 - 6,143,645)										
<i>MAT</i>	A ₁₄	DSB	WT	10,824	(3,156 - 24,267) [9]	5,012,906	[9]	310	NA	93.2 (6.1)
<i>MAT</i>	A ₁₄	No	WT	16,188	(4,868 - 28,917) [6]	0	(0 - 12,250) [6]	NA	NA	4.2 (4.2)
16 kb	A ₄	DSB	WT	367	(166 - 615) [10]	49,132	(24,012 - 83,090) [10]	1,170	NA	91.2 (7.1)
16 kb	A ₄	DSB	<i>msh2Δ</i>	12,296	(5,470 - 20,584) [7]	370,115	(275,661 - 479,013) [7]	60	7.5 (0.0001)	73.9 (16.6)
16 kb	A ₄	DSB	<i>pol3-5DV</i>	713	(328 - 1,174) [7]	194,587	(159,505 - 254,883) [7]	432	4.0 (0.0001)	94.8 (3.3)
16 kb	A ₄	DSB	<i>pol2-4</i>	198	(113 - 495) [6]	46,030	(24,247 - 64,527) [6]	836	NS	97.1 (0)
16 kb	A ₄	DSB	<i>rev3Δ</i>	244	(82 - 550) [7]	18,049	(5,327 - 24,374) [7]	668	0.4 (0.0004)	94.1 (4.9)
16 kb	A ₄	DSB	<i>rad30Δ</i>	197	(161 - 306) [5]	62,360	(31,104 - 73,402) [5]	904	NS	97.6 (0)
16 kb	A ₄	DSB	<i>dun1Δ</i>	196	(36 - 352) [6]	20,330	(10,599 - 51,278) [6]	239	0.4 (0.031)	84.0 (12.3)
16 kb	A ₄	DSB	<i>sml1Δ</i>	645	(231 - 930) [6]	90,507	(61,618 - 209,507) [6]	526	1.8 (0.011)	96.4 (1.8)
16 kb	A ₄	DSB	<i>msh3Δ</i>	362	(238- 589) [7]	109,716	(96,350 - 150,870) [7]	459	2.2 (0.0012)	88.1 (8.4)
16 kb	A ₄	DSB	<i>pol2-4 msh3Δ</i>	645	(514 - 1,847) [6]	205,523	(97,944 - 234,082) [6]	587	4.2 (0.0005, 0.0035 [†] , 0.0022 [‡])	ND
16 kb	A ₄	DSB	<i>pol3-5DV msh3Δ</i>	4,717	(2,377 - 15,538) [6]	371,070	(282,924 - 557,955) [6]	78	7.6 (0.0002, 0.0012 [†] , 0.0012 [‡])	71.3 (18.1)
16 kb	A ₄	No	WT	42	(38 - 99) [6]	5	(0 - 52) [6]	NA	NA	8.0 (0)
16 kb	A ₄	No	<i>msh2Δ</i>	6163	(4,677- 8147) [9]	13,972	(0 - 94,394) [9]	NA	146.7 (0.0004)	1.2 (1.2)

Rate of Lys ⁺ (x10 ⁻¹⁰) ^a										
				Before galactose (0h)		After galactose (frequency (7h -0h))		Fold over ^c		
Position	Construct	HO Site	Relevant Genotype	Median	CI or Range ^b [# Repeats]	Median	CI or Range ^b [# Repeats]	No-DSB Control	Fold over wt (p-value) ^d	% BIR ^e
16 kb	A ₄	No	<i>pol3-5DV</i>	450	(208 - 765) [5]	1,918	(0 - 7,850) [5]	NA	10.7 (0.0043)	4.9 (0)
16 kb	A ₄	No	<i>pol2-4</i>	55	(25 - 101) [6]	341	(49 - 2,256) [6]	NA	NS	29 (0)
16 kb	A ₄	No	<i>rev3Δ</i>	27	(16 - 81) [6]	9	(0 - 67) [6]	NA	0.6 (0.0410)	19.5 (0)
16 kb	A ₄	No	<i>rad30Δ</i>	69	(51 - 132) [7]	0	(0 - 74) [7]	NA	NS	16.7 (0)
16 kb	A ₄	No	<i>dun1Δ</i>	85	(32 - 110) [9]	52	(0 - 99) [9]	NA	NS	0 (0)
16 kb	A ₄	No	<i>sml1Δ</i>	172	(57- 254) [4]	0	(0 - 17)[4]	NA	NS	0 (0)
16 kb	A ₄	No	<i>msh3Δ</i>	239	(195 - 280) [6]	0	- [6]	NA	5.7 (0.0012)	0 (0)
16 kb	A ₄	No	<i>pol2-4</i> <i>msh3Δ</i>	350	(164 - 660) [8]	16	(0 - 918) [5]	NA	8.3 (0.0007, 0.0426 [†] , 0.007 [§])	ND
16 kb	A ₄	No	<i>pol3-5DV</i> <i>msh3Δ</i>	4771	(2,490- 11,007) [6]	5,699	(0 - 16,834) [6]	NA	113.6 (0.0022, 0.0022 [†] , 0.0043 [‡])	0 (0)
16 kb	A ₇	DSB	WT	2,736	(975 - 10,447) [8]	266,765	(161,398 - 323,714) [8]	1,947	NA	92.6 (6.6)
16 kb	A ₇	DSB	<i>msh2Δ</i>	2,276,298	(882,761 - 3,976,321) [10]	9,567,052	(2,465,474 - 47,976,249) [10]	3	35.9 (<0.0001)	84.0 (6.0)
16 kb	A ₇	DSB	<i>pol3-5DV</i>	4,745	(3,963 - 13,357) [9]	585,823	(415,737 - 771,709) [9]	347	2.2 (0.0055)	93.0 (1.2)
16 kb	A ₇	DSB	<i>pol2-4</i>	2,516	(1,084 - 14,935) [6]	299,554	(194,602 - 1,529,399) [6]	844	1.1 (0.036)	96.0 (0.4)
16 kb	A ₇	DSB	<i>rev3Δ</i>	1,249	(1,019 - 1,779) [9]	200,142	(125,984 - 392,259) [9]	590	NS	99.1 (0.2)
16 kb	A ₇	DSB	<i>rad30Δ</i>	2,151	(869 - 8,129) [6]	206,091	(136,858 - 306,281) [6]	517	NS	96.5 (1.9)
16 kb	A ₇	DSB	<i>msh3Δ</i>	14,461	(10,380 - 29,155) [7]	630,667	(162,052 - 1,960,118) [7]	252	NS	82.1 (12.2)
16 kb	A ₇	DSB	<i>pol2-4</i> <i>msh3Δ</i>	ND	ND	ND	ND	ND	ND	ND
16 kb	A ₇	DSB	<i>pol3-5DV</i> <i>msh3Δ</i>	93,738	(34,515 - 134,072) [6]	1,871,658	(1,347,373 - 4,292,566) [6]	30	7.0 (0.0007, 0.0140 [†] , 0.0004 [‡])	73.5 (12.6)

Rate of Lys ⁺ (x10 ⁻¹⁰) ^a										
				Before galactose (0h)		After galactose (frequency (7h -0h))		Fold over ^c		
Position	Construct	HO Site	Relevant Genotype	Median	CI or Range ^b [# Repeats]	Median	CI or Range ^b [# Repeats]	No-DSB Control	Fold over wt (p-value) ^d	% BIR ^e
16 kb	A ₇	No	WT	137	(120 - 339) [6]	157	(0 - 1,491) [6]	NA	NA	0 (0)
16 kb	A ₇	No	<i>msh2Δ</i>	2,884,399	(1,633,488 - 3,366,307) [12]	0	- [12]	NA	21054.0 (0.0009)	0 (0)
16 kb	A ₇	No	<i>pol3-5DV</i>	1,690	(746 - 2,655) [6]	1,035	(0 - 4,684) [6]	NA	12.3 (0.0022)	0.6 (0)
16 kb	A ₇	No	<i>pol2-4</i>	355	(183 - 973) [8]	475	(0 - 3,460) [8]	NA	2.6 (0.0047)	5.4 (0)
16 kb	A ₇	No	<i>rev3Δ</i>	339	(237 - 654) [10]	885	(0 - 2,185) [10]	NA	2.5 (0.0047)	0.1 (0)
16 kb	A ₇	No	<i>rad30Δ</i>	399	(90 - 645) [8]	120	(0 - 517) [8]	NA	NS	8.7 (0)
16 kb	A ₇	No	<i>msh3Δ</i>	2,505	(1,198 - 3,379) [6]	2,757	(1,398 - 7,138) [6]	NA	18.3 (0.0022)	0 (1.7)
16 kb	A ₇	No	<i>pol2-4 msh3Δ</i>	1,855	(1811 - 10,024) [3]	ND	ND	NA	13.5 (0.024, 0.0121 [§])	ND
16 kb	A ₇	No	<i>pol3-5DV msh3Δ</i>	61,821	(41,789 - 209,839) [6]	37,205	(0 - 1,286,693) [6]	NA	451.2 (0.0022, 0.0022 [†] , 0.0022 [‡])	0 (1.5)
(1,275,755 - 4,181,943)										
16 kb	A ₁₄	DSB	WT	147,325	(47,905 - 668,125) [6]	2,370,465	[6]	26	NA	90.2 (6.8)
16 kb	A ₁₄	No	WT	90,599	(73,797 - 338,588) [8]	0	(0 - 498,176) [8]	NA	NA	0 (0)
36 kb	A ₄	DSB	WT	51	(37 - 71) [9]	12,015	(5,158 - 14,123) [9]	2,003	NA	95.2 (3.1)
36 kb	A ₄	DSB	<i>msh2Δ</i>	2,581	(1,233 - 5,824) [11]	131,304	(93,629 - 175,262) [11]	61	10.9 (0.0002)	92.2 (2.9)
36 kb	A ₄	DSB	<i>mlh1Δ</i>	1,263	(809 - 7,104) [6]	55,701	(25,767 - 64,380) [6]	32	4.6 (0.0004)	85.3 (5.9)
36 kb	A ₄	DSB	<i>pol3-5DV</i>	224	(119 - 262) [13]	66,896	(58,853 - 92,282) [13]	1,487	5.6 (0.0001)	92.7 (5.9)
36 kb	A ₄	DSB	<i>pol2-4</i>	60	(44 - 84) [7]	8,280	(5,014 - 11,517) [7]	690	NS	97.5 (1.0)
36 kb	A ₄	DSB	<i>rev3Δ</i>	30	(22 - 61) [9]	8,592	(6,080 - 11,757) [9]	2,148	NS	93.2 (2.7)
36 kb	A ₄	DSB	<i>rad30Δ</i>	63	(34 - 157) [7]	10,739	(9,662 - 21,157) [7]	1,790	NS	92.3 (7.3)
36 kb	A ₄	DSB	<i>dun1Δ</i>	17	(12 - 51) [10]	2,208	(954 - 3,499) [10]	116	0.2 (0.0021)	98.0 (2.0)
36 kb	A ₄	DSB	<i>sml1Δ</i>	23	(21 - 37) [9]	10,040	(4,595 - 246,470) [9]	558	NS	92.5 (2.5)
36 kb	A ₄	DSB	<i>msh3Δ</i>	114	(26 - 161) [6]	28,269	(14,056 - 37,574)[6]	1,488	2.4 (0.0016)	91.7 (6.2)

Rate of Lys ⁺ (x10 ⁻¹⁰) ^a										
				Before galactose (0h)		After galactose (frequency (7h -0h))				
Position	Construct	HO Site	Relevant Genotype	CI or Range ^b		CI or Range ^b		Fold over ^c	Fold over wt (p-value) ^d	% BIR ^e
				Median	[# Repeats]	Median	[# Repeats]	No-DSB Control		
36 kb	A ₄	DSB	<i>pol2-4 msh3Δ</i>	165	(47 - 430) [6]	17,468	(11,514 - 51,646) [6]	1,165	1.5 (0.0496, 0.0023 [§])	ND
36 kb	A ₄	DSB	<i>pol3-5DV msh3Δ</i>	521	(224 - 5,197) [8]	229,358	(140,694 - 340,488) [8]	717	19.1 (0.0006, 0.0024 [†] , 0.0003 [‡])	78.7 (15.7)
36 kb	A ₄	No	WT	6	(5 - 12) [9]	2	(0 - 10) [9]	NA	NA	ND
36 kb	A ₄	No	<i>msh2Δ</i>	2,143	(1,034 - 4,230) [6]	0	(0 - 7,770) [6]	NA	357.2 (0.0011)	0 (7.0)
36 kb	A ₄	No	<i>mlh1Δ</i>	1,731	(1,087 - 2,003) [6]	85	(0 - 3,971) [6]	NA	288.5 (0.0011)	2.5 (1.3)
36 kb	A ₄	No	<i>pol3-5DV</i>	45	(15 - 295) [6]	45	(23 - 365) [6]	NA	7.5 (0.0042)	4.2 (2.1)
36 kb	A ₄	No	<i>pol2-4</i>	12	(6 - 20) [4]	0	(0 - 9) [4]	NA	2.0 (0.005)	27.3 (0)
36 kb	A ₄	No	<i>rev3Δ</i>	4	(2 - 7) [6]	8	(0 - 21) [6]	NA	NS	10 (0)
36 kb	A ₄	No	<i>rad30Δ</i>	6	(4 - 17) [6]	8	(0 - 21) [6]	NA	NS	4 (0)
36 kb	A ₄	No	<i>dun1Δ</i>	19	(9 - 116) [7]	14	(0 - 21) [7]	NA	3.2 (0.0066)	0 (0)
36 kb	A ₄	No	<i>sml1Δ</i>	18	(14 - 26) [6]	0	(0 - 55) [6]	NA	3.0 (0.0140)	0 (0)
36 kb	A ₄	No	<i>msh3Δ</i>	19	(4 - 75) [6]	24	(0 - 193) [6]	NA	NS	1.2 (0)
36 kb	A ₄	No	<i>pol2-4 msh3Δ</i>	15	(8 - 54) [8]	0	(0 - 78) [5]	NA	2.5 (0.0118, 0.004 [§])	ND
36 kb	A ₄	No	<i>pol3-5DV msh3Δ</i>	320	(254 - 611) [6]	0	(0 - 504) [6]	NA	53.3 (0.0011, 0.0022 [†] , 0.0152 [‡])	0 (0)
36 kb	A ₇	DSB	WT	39	(16 - 119) [8]	8,586	(6,217 - 22,002) [8]	781	NA	96.9 (1.3)
36 kb	A ₇	DSB	<i>msh2Δ</i>	1,103,095	(804,278 - 1,583,201) [13]	10,605,324	(4,291,667 - 15,077,381) [13]	14	1235.2 (0.0002)	98.1 (1.9)
36 kb	A ₇	DSB	<i>pol3-5DV</i>	215	(137 - 409) [12]	77,636	(72,667 - 132,734) [12]	3,697	9.0 (0.0002)	97.1 (2.2)
36 kb	A ₇	DSB	<i>pol2-4</i>	41	(17 - 68) [9]	14,800	(8,945 - 34,547) [9]	1,644	1.7 (0.0152)	95.2 (4.8)
36 kb	A ₇	DSB	<i>rev3Δ</i>	37	(12 - 67) [8]	8,417	(3,659 - 12,472) [8]	842	NS	97.3 (0)

Rate of Lys ⁺ (x10 ⁻¹⁰) ^a										
<div><div>Before galactose (0h)</div><div>After galactose (frequency (7h -0h))</div></div>										
Position	Construct	HO Site	Relevant Genotype	CI or Range ^b		CI or Range ^b		Fold over ^c	Fold over wt (p-value) ^d	% BIR ^e
				Median	[# Repeats]	Median	[# Repeats]	No-DSB Control		
36 kb	A ₇	DSB	<i>rad30Δ</i>	74	(23 - 121) [6]	10,965	(6,818 - 22,531) [6]	1,371	NS	99.1 (0)
36 kb	A ₇	DSB	<i>msh3Δ</i>	44	(28 - 93) [6]	31,311	(21,560 - 186,879) [6]	3,479	3.6 (0.0013)	95.6 (1.1)
36 kb	A ₇	DSB	<i>pol2-4 msh3Δ</i>	55	(41 - 100) [6]	43,217	(40,766 - 53,031) [6]	1,964	5.0 (0.0007, 0.0004 [§])	ND
36 kb	A ₇	DSB	<i>pol3-5DV msh3Δ</i>	483	(146 - 2,890) [7]	291,652	(42,813 - 474,104) [7]	704	34.0 (0.0003, 0.0047 [†] , 0.0127 [‡])	92.4 (3.8)
36 kb	A ₇	No	WT	11	(2 - 14) [8]	7	(0 - 22) [8]	NA	NA	4.8 (0)
36 kb	A ₇	No	<i>msh2Δ</i>	745,078	(289,360 - 918,023) [6]	0	- [6]	NA	67734.4 (0.0007)	0 (0)
36 kb	A ₇	No	<i>pol3-5DV</i>	21	(4 - 35) [6]	41	(15 - 126) [6]	NA	1.9 (0.0293)	5.3 (0)
36 kb	A ₇	No	<i>pol2-4</i>	9	(4 - 15) [6]	0	(0 - 19) [6]	NA	NS	25.0 (0)
36 kb	A ₇	No	<i>rev3Δ</i>	10	(4 - 17) [6]	0	(0 -25) [6]	NA	NS	ND
36 kb	A ₇	No	<i>rad30Δ</i>	8	(6 - 19) [11]	16	(0 - 21) [11]	NA	NS	0 (0)
36 kb	A ₇	No	<i>msh3Δ</i>	9	(5 - 44) [10]	1	(0 - 94) [10]	NA	NS	ND
36 kb	A ₇	No	<i>pol2-4 msh3Δ</i>	22	(10 - 54) [7]	45	(12 - 46) [4]	NA	2 (0.0037, 0.0330 [†] , 0.0082 [§])	ND
36 kb	A ₇	No	<i>pol3-5DV msh3Δ</i>	414	(133 - 947) [7]	313	(0 - 1,443) [7]	NA	37.6 (0.0003, 0.0001 [†] , 0.0012 [‡])	0 (12.9)
36 kb	A ₁₄	DSB	WT	13,071	(4,184 - 56,583) [8]	2,224,523	(713,783 - 11,515,027) [8]	149	NA	98.4 (1.6)
36 kb	A ₁₄	No	WT	14,937	(5,862 - 78,194) [6]	0	(0 - 5,809) [6]	NA	NA	1.1 (0)

				Rate of Lys ⁺ (x10 ⁻¹⁰) ^a						
				Before galactose (0h)		After galactose (frequency (7h -0h))				
								Fold over ^c		
Position	Construct	HO Site	Relevant Genotype	Median	CI or Range ^b [# Repeats]	Median	CI or Range ^b [# Repeats]	No-DSB Control	Fold over wt (p-value) ^d	% BIR ^e
Chr II, native	A ₄	Yes	WT	14	(8 - 48) [6]	31	(0 - 69) [6]	NA	NA	ND
Chr II, native	A ₇	Yes	WT	37	(8 - 170) [6]	25	(0 - 329) [6]	NA	NA	ND
Chr II, native	A ₁₄	Yes	WT	4,757	(3,346 - 34,711) [6]	2,059	(0 - 7,860) [6]	NA	NA	ND

^a Rates calculated at 0h based on 0h frequencies using the Drake equation (see Materials and methods for details). At 7 hrs, rates were calculated as (7h frequency - 0h frequency); differences <0 are reported as "0". ^b For strains with ≥6 experiments, the 95% CI of the median is given. For the strains with <6 experiments, the median range is given. A dash indicates cases where both the minimum and maximum values were 0. ^c Statistically significant elevation of 7h median rate in strains with a DSB over 0h median rate in isogenic no-DSB controls. Significance determined using the Mann-Whitney U test at the p≤0.05 level. ^d Statistically significant elevation of: 7h median rate of mutant compared to 7h median rate of WT in strains with a DSB; 0h median rate of mutant compared to 0h median of WT in no-DSB control strains; parentheses = p-values determined using the Mann-Whitney U test; [†]Significant difference of 7h *pol3-5DVmsh3Δ* median rate from 7h *msh3Δ* median rate in strains with a DSB and 0h *pol3-5DVmsh3Δ* median rate from 0h *msh3Δ* median rate in no-DSB control strains [‡]Significant difference of 7h *pol3-5DVmsh3Δ* median rate from the 7h *pol3-5DV* median rate in strains with a DSB and 0h *pol3-5DVmsh3Δ* median rate from 0h *pol3-5DV* median rate in no-DSB control strains [§] Significant difference of 7h *pol2-4msh3Δ* median rate from the 7h *pol2-4* median rate in strains with a DSB and 0h *pol2-4msh3Δ* median rate from 0h *pol2-4* median rate in no-DSB control strains ^e Percent BIR for 7h Lys⁺ colonies for strains with a DSB site and for 0h Lys⁺ colonies for no-DSB controls; parentheses = percent partial BIR (colonies containing ≥1 Ade⁺Leu⁻ sector). For strains with a DSB, 35 - 1000 colonies were analyzed from 2 - 5 independent experiments; for no-DSB controls, 6 - 200 colonies were analyzed from 2 - 5 independent experiments. Lys⁺ BIR events observed in no-DSB controls could result from extremely rare HO-induced DSBs at *MATα-inc* or from spontaneous BIR. Abbreviations: ND, not determined; NS, not significant; NA, not applicable. [†]Statistically significant elevation not observed between mutant and WT, but was detected for other comparisons.

5.2.3. Sequencing Analysis of BIR Mutations

Lys⁺ BIR outcomes were primarily 1-bp deletions, the majority of which (70-100%) occurred in ≥ 2 homonucleotide runs (Table 5.3; Figure 5.4). With data for all strains combined, the majority of Lys⁺ mutations concentrated in two hotspots: 1) the poly-A run, which is known to provoke replication slippage, and 2) the sequence GGGCCAAGG (Table 5.3; Figures 5.1 D, 5.4), which could also promote replication slippage within one of its small homonucleotide runs. Alternatively, the second hot spot could result from template switching involving the first seven nucleotides of this hotspot (GGGCCAA) and its -1-bp quasipalindromic copy (TTGCCC) located approximately 70 bp away (Figures 5.1 D, 5.4; see Section 5.4 for details). As expected, the proportion of 1-bp deletions in the poly-A run increased with the length of the run, with only 3%, 20%, and 0% of frameshifts occurring in the poly-A run of the A₄ reporter at the *MAT*, 16-, and 36-kb positions, respectively, and 100% of frameshifts occurring in the A₁₄ run at all three positions (Table 5.3 and Figure 5.4). The proportion of frameshifts in the A₇ run varied somewhat across reporter positions. The spectra of Lys⁺ frameshift mutations were generally similar for BIR-induced compared to spontaneous mutations for each given reporter (Table 5.3 and Figure 5.4). One exception was the increase in 2-bp insertions observed in A₄ and A₇ no-DSB control strains at the 16-kb position.

Table 5.3. Spectrum of BIR-associated and spontaneous Lys⁺ mutations in MMR⁺ and *msh2Δ* strains.

Position	Reporter	HO site	Genotype	1-bp deletions			Other mutations ^a	Total
				Poly-A run	Other ≥2-nt runs (HS)	Not in run		
<i>MAT</i>	A ₄	DSB	WT	1	37 (35)	2	8	48
<i>MAT</i>	A ₄	No	WT	0	12 (12)	0	2	14
16 kb	A ₄	DSB	WT	10	33 (13)	6	10	59
16 kb	A ₄	No	WT	0	5 (2)	1	8	14
36kb	A ₄	DSB	WT	0	35 (32)	15	2	52
36kb	A ₄	No	WT	0	8 (8)	0	2	10
<i>MAT</i>	A ₇	DSB	WT	4	57 (57)	10	5	76
<i>MAT</i>	A ₇	No	WT	0	8 (8)	6	1	15
16 kb	A ₇	DSB	WT	47	3 (3)	1	1	52
16 kb	A ₇	No	WT	13	2 (1)	0	5	20
36kb	A ₇	DSB	WT	4	26 (26)	3	3	36
36kb	A ₇	No	WT	0	7 (7)	2	4	13
<i>MAT</i>	A ₁₄	DSB	WT	24	0 (0)	0	0	24
<i>MAT</i>	A ₁₄	No	WT	9	0 (0)	0	0	9
16 kb	A ₁₄	DSB	WT	24	0 (0)	0	1	25
16 kb	A ₁₄	No	WT	18	0 (0)	0	2	20
36kb	A ₁₄	DSB	WT	14	0 (0)	0	0	14
36kb	A ₁₄	No	WT	8	0 (0)	0	0	8
<i>MAT</i>	A ₄	DSB	<i>msh2Δ</i>	1	10 (10)	1	0	12
<i>MAT</i>	A ₄	No	<i>msh2Δ</i>	0	8 (8)	3	1	12
16 kb	A ₄	DSB	<i>msh2Δ</i>	10*	0 (0)	0	0	10
16 kb	A ₄	No	<i>msh2Δ</i>	12	0 (0)	1	0	13
36kb	A ₄	DSB	<i>msh2Δ</i>	5*	12 (12)	0	0	17
36kb	A ₄	No	<i>msh2Δ</i>	3	8 (8)	1	0	12
<i>MAT</i>	A ₇	DSB	<i>msh2Δ</i>	4*	6 (6)	1	0	11
<i>MAT</i>	A ₇	No	<i>msh2Δ</i>	18	0 (0)	0	1	19
16 kb	A ₇	DSB	<i>msh2Δ</i>	9	0 (0)	0	0	9
16 kb	A ₇	No	<i>msh2Δ</i>	17	0 (0)	0	0	17
36kb	A ₇	DSB	<i>msh2Δ</i>	9*	7 (7)	0	0	16
36kb	A ₇	No	<i>msh2Δ</i>	18	6 (6)	1	0	25

^a Other mutations include insertions and >1-bp deletions, as well as 1-bp deletions accompanied by base substitutions; * Percentage of 1-bp deletions occurring in the poly-A run is statistically significantly different from the isogenic wild type strain using Fisher's Exact Test (p<0.05). Abbreviations: bp, base pair; nt, nucleotide; HS, the GGGCCAAGG frameshift hotspot shown in Fig. 1D and Table S1; DSB, double-strand break; WT, wild type.

Figure 5.4. Spectrum of BIR-associated and spontaneous Lys⁺ mutations in MMR⁺ and *msh2Δ* strains. A part of the *LYS2* coding sequence bearing insertion of approximately 61 bp (*Ins*; positions 1 - 61) is shown. In the sequence: gray box indicates direct repeats flanking the 61-bp insert; ** indicates the location of the A₄, A₇, or A₁₄ poly-adenine run; Underlined, italics indicates the GGGCCAAGG frameshift hotspot (see text for details), for which a partial -1-bp quasipalindromic copy (TTGCCC, also underlined, italics) is located approximately 70 bp away. In the table: numbers indicate 1-bp deletions at the positions depicted on the top; parentheses indicate larger deletions (del) and insertions (ins); “Comp del” indicates reversions to Lys⁺ resulting from complete deletion of *Ins*(A₄), (A₇), or (A₁₄) that occurred by template switching involving direct repeats (gray boxes) flanking the insertion; “Other” indicates complex events where 1-bp deletions were associated with a nearby base substitution; [†] indicates cases where the percentage of -1-bp deletions occurring in the poly-A run is statistically significantly different from the isogenic wild type strain using Fisher’s Exact Test (p<0.05).



5.3. Genetic Control of BIR Frameshift Mutagenesis

5.3.1. The Role of Translesion DNA Synthesis

It was hypothesized that involvement of translesion DNA synthesis during BIR, whether due to a defective replisome or DNA template damage (as discussed in (Northam et al., 2010; Pavlov et al., 2006b; Strathern et al., 1995; Yang et al., 2008)), may contribute to the increased rate of BIR frameshift mutations. To address this, the activity of either of two translesion polymerases was eliminated. Specifically, BIR-associated mutagenesis in A_4 and A_7 strains with deletion of *RAD30* (encoding DNA Pol η) or deletion of *REV3* (encoding the catalytic subunit of DNA Pol ζ) was measured at all three positions (Figure 5.5; Table 5.2). While *rad30* Δ mutants showed no change in the rate of frameshift mutations compared to wild type at any position, deletion of *REV3* did result in a small but statistically significant decrease (2x to 3x) in mutations at *MAT* and for A_4 at 16 kb. No change was observed in the other *rev3* Δ strains. (Importantly, BIR efficiency in *rev3* Δ mutants was similar to that observed in wild type (Table 5.1 and data not shown)).

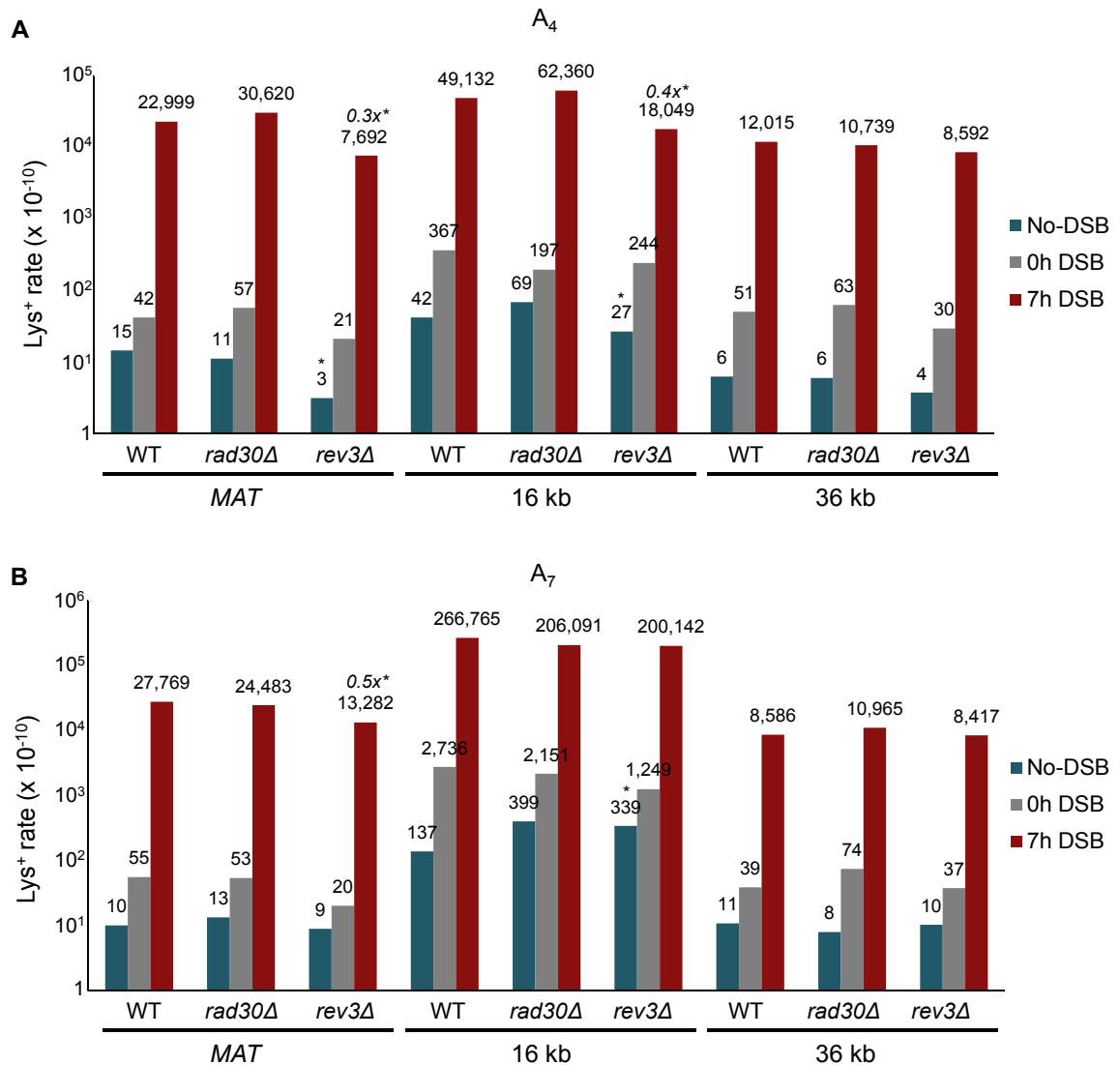


Figure 5.5. The role of translesion polymerases in BIR-associated mutagenesis. The rate of Lys⁺ revertants was measured before addition of galactose (0h) and 7 hours after incubation in galactose-containing media (7h) in wild type and its *rad30Δ* (Pol η-deficient) and *rev3Δ* (Pol ζ-deficient) mutant derivatives containing frameshift reporters **(A)** A₄ or **(B)** A₇ at the MAT, 16-kb, and 36-kb chromosomal positions. Statistically significant differences from the rate of wild type events are indicated by *. The fold increase of BIR mutation rate in mutants compared to wild type (in cases of a statistically significant change) is indicated in italics. Other abbreviations and statistical details are similar to those provided in the legend to Figure 5.3.

To differentiate the role of *REV3* in BIR from its role in damage-induced mutagenesis, *rev3Δ* no-DSB control strains containing A₇ at the 36-kb position (where there was no effect of *rev3Δ* on BIR mutagenesis) were exposed to 20 J/m² of UV light (Figure 5.6). This exposure resulted in an approximately 10-fold increase in Lys⁺ events compared to the frequency of spontaneous events. Consistent with the observation of Abdulovic and Jinks-Robertson (Abdulovic and Jinks-Robertson, 2006), the UV-induced increase in mutagenesis was largely *REV3*-dependent in our system. Thus, it is concluded that BIR-induced mutagenesis differs from UV-induced mutagenesis in its dependency on Pol ζ, while the latter strongly depends on Pol ζ, the former is only modestly dependent on Pol ζ and only at some chromosomal positions.

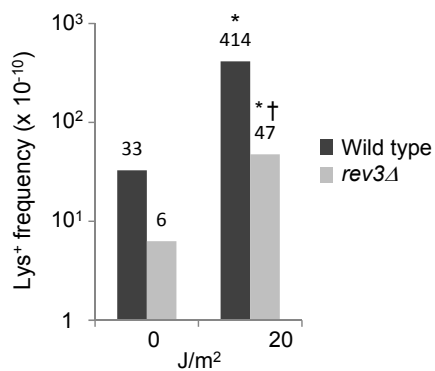


Figure 5.6. Effect of UV damage on frameshift mutagenesis. Lys⁺ frequency was measured in no-DSB controls of wild type and *rev3Δ* mutants containing the A₇ reporter at the 36-kb position after exposure to 0 or 20 J/m² UV light. * indicates statistically significantly different from no exposure; † indicates statistically different from wild type.

5.3.2. The Role of MMR

MSH2 was eliminated from all A_4 and A_7 strains to test whether MMR corrects frameshift errors made during BIR. In all cases, a significant increase in frameshift mutagenesis was observed during BIR in *msh2Δ* strains compared to their isogenic wild type strains, suggesting that MMR corrects a large number of BIR frameshift errors (Figure 5.7; Table 5.2). The mutation rate observed during BIR in MMR-deficient mutants significantly exceeded the level of spontaneous mutagenesis observed in MMR-deficient no-DSB controls, confirming that MMR deficiency further increased the already high rate of BIR mutagenesis. Strains containing A_7 reporters were more sensitive to MMR deficiency and showed higher increases in the rate of frameshifts compared to increases for the corresponding A_4 strains. This effect is similar to the effect of *msh2Δ* during normal replication, where MMR is especially important to correct errors in long homonucleotide runs (Greene and Jinks-Robertson, 1997, 2001; Tran et al., 1997). Also, consistent with Tran *et al.* (Tran et al., 1997), who reported a dramatic shift of spontaneous frameshifts to the poly-A run in MMR-deficient A_7 strains, a significantly higher percentage of mutations occurring in the poly-A run in MMR-deficient A_7 strains at the *MAT* and 36-kb positions was observed compared to isogenic MMR-proficient strains (Table 5.3; Figure 5.4). At the 16-kb position, where most events in the wild type A_7 strain were in the poly-A run, it was confirmed that MMR deficiency caused mutation events to shift to the poly-A run in the A_4 strain. The ability of MMR to correct BIR errors was further supported by data from *mlh1Δ* mutants, which were tested at the *MAT* and 36-kb

positions with the A_4 reporter (Figure 5.7; Table 5.2). Our data thus suggest that BIR occurs in the context of functional MMR machinery, and that long homonucleotide runs are especially susceptible to failure of MMR, as is the case during normal DNA replication.

Figure 5.7. The role of MMR in BIR-associated mutagenesis. The rate of Lys⁺ revertants was measured before addition of galactose (0h) and 7 hours after incubation in galactose-containing media (7h) in wild type and its various MMR⁻ containing frameshift reporters **(A)** A₄ or **(B)** A₇ at the *MAT*, 16-kb, and 36-kb chromosomal positions. Statistically significant differences from wild type are indicated by *. The fold increase of BIR mutation rate in mutants compared to wild type (in cases of a statistically significant change) is indicated in italics. Other abbreviations and statistical details are similar to those provided in the legend to Figure 5.3.

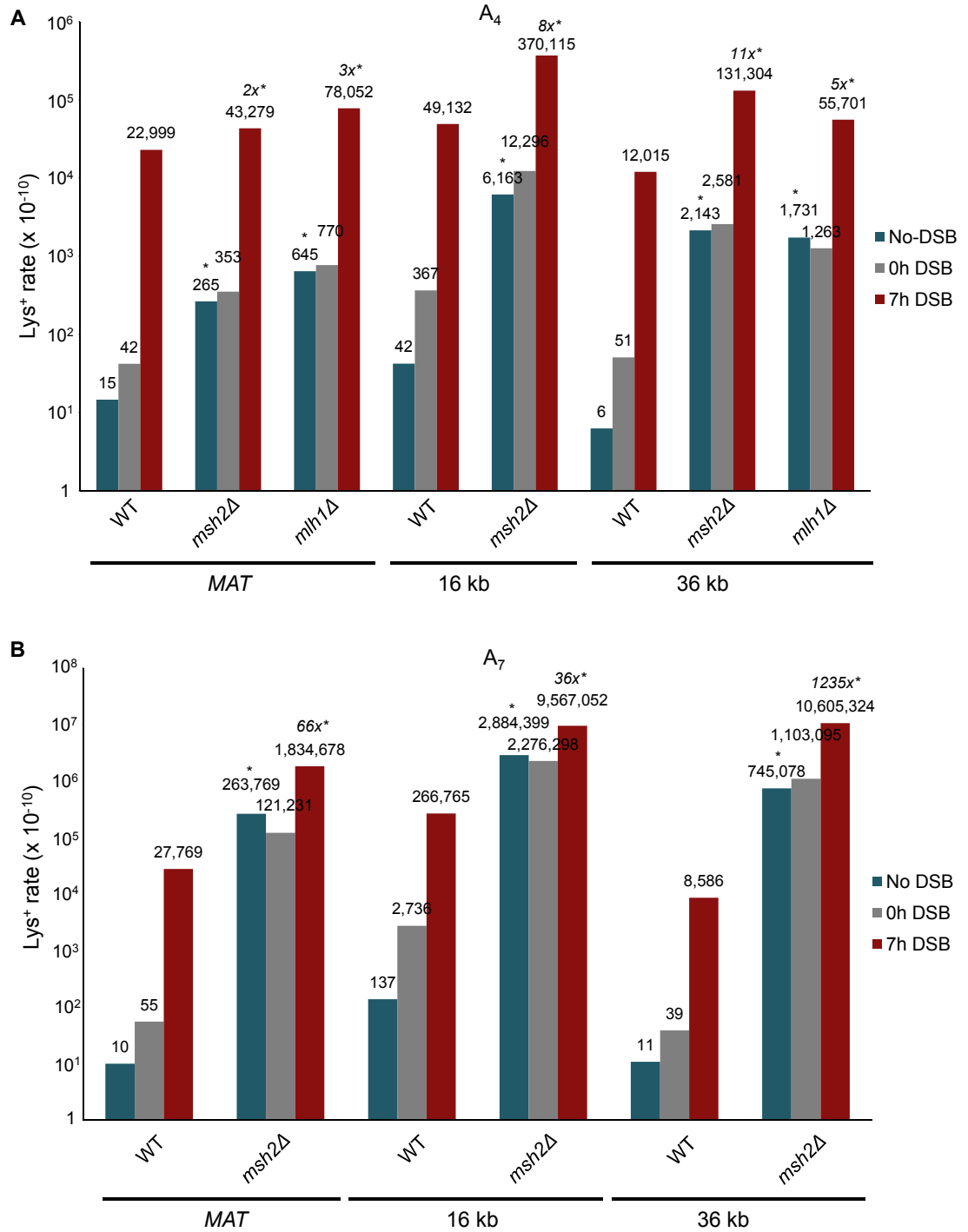


Figure 5.7. The role of MMR in BIR-associated mutagenesis.

To better characterize the role of MMR in correction of BIR-induced replication errors, mutation rates in experimental MMR-deficient strains were compared to their no-DSB controls. This comparison showed that, prior to MMR correction, the level of polymerase errors was significantly higher during BIR compared to normal DNA replication for all constructs (Table 5.4). Based on the percent of these errors that was repaired by MMR (calculated in Table 5.4), the efficiency of MMR in BIR was 98%, 97%, and 99.9% for A_7 strains at the *MAT*, 16-, and 36-kb positions, respectively, and approached 99.9% for all positions during normal DNA replication. MMR also repaired a high percentage of BIR errors in A_4 strains (47%, 87%, and 91% at the *MAT*, 16-, and 36-kb positions, respectively), but this was somewhat lower than the efficiency of MMR during normal DNA replication for these strains (94%, 99%, and 99.7% at the *MAT*, 16-, and 36-kb positions, respectively). These data suggest that, although MMR operates during BIR, the percentage of MMR-repaired polymerase errors is often lower for BIR than for normal replication.

Table 5.4. Efficiency of MMR during BIR repair.

Position	Reporter	Type of DNA Synthesis	Polymerase Errors				Fold increase in errors before vs. after MMR repair ^e
			Total Before MMR Repair (per 10 ¹⁰) ^a	Total After MMR Repair (per 10 ¹⁰) ^b	Total Repaired by MMR (per 10 ¹⁰) ^c	% repaired by MMR ^d	
<i>MAT</i>	A ₄	S-phase	265	15	250	94.34	17.6
<i>MAT</i>	A ₄	BIR (BIR/S-phase)	43,279 (163)	22,999 (1,533)	20,280	46.86	1.8
16 kb	A ₄	S-phase	6,163	42	6,121	99.32	147.0
16 kb	A ₄	BIR (BIR/S-phase)	370,115 (60)	49,132 (1,170)	320,983	86.73	7.5
36 kb	A ₄	S-phase	2,143	6	2,137	99.72	357.2
36 kb	A ₄	BIR (BIR/S-phase)	131,304 (61)	12,015 (2,003)	119,289	90.85	10.9
<i>MAT</i>	A ₇	S-phase	263,769	10	263,759	99.996	26,376.9
<i>MAT</i>	A ₇	BIR (BIR/S-phase)	1,834,678 (7)	27,769 (2,777)	1,806,909	98.486	66.1
16 kb	A ₇	S-phase	2,884,399	137	2,884,262	99.995	21,054.0
16 kb	A ₇	BIR (BIR/S-phase)	9,567,052 (3)	266,765 (1,947)	9,300,287	97.211	35.9
36 kb	A ₇	S-phase	745,078	11	745,067	99.999	67,734.4
36 kb	A ₇	BIR (BIR/S-phase)	10,605,324 (14)	8,586 (781)	10,596,738	99.919	1,235.2

^a Rate of Lys⁺ frameshifts in *msh2Δ*; ^b Rate of Lys⁺ frameshifts in wt; ^c (Total before MMR repair) - (Total after MMR repair); ^d (Total repaired by MMR)/(Total before MMR repair); ^e (Total before MMR repair)/(Total after MMR repair). Abbreviations: BIR, break-induced replication; MMR, mismatch repair.

5.3.3. The Role of Polymerase Proofreading

Our previous analysis indicated that BIR is associated with a significantly higher level of polymerase errors than normal replication. To determine the role of proofreading activity during BIR, *pol3-5DV* and *pol2-4*, both exonuclease-deficient mutations, were introduced into A_4 and A_7 strains at all three chromosomal locations to eliminate the proofreading activity of Pol δ and Pol ϵ , respectively.

5.3.3.1. Pol ϵ proofreading

In S-phase, Pol ϵ is primarily responsible for DNA synthesis on the leading strand of the replication fork (Larrea et al., 2010; Nick McElhinny et al., 2008). The exact role of Pol ϵ in BIR is not completely understood, though it appears to be involved in later steps of BIR, and BIR can complete in the absence of Pol ϵ in approximately 25% of cases. Previous characterization of the *pol2-4* mutation showed that it conferred approximately 6- and 60-fold increases in spontaneous frameshift mutations with the A_4 and A_7 reporters, respectively (Tran et al., 1997). In our strain background, however, no increase in spontaneous mutagenesis was observed in 5 of the 6 strains tested (a statistically significant increase compared to wild type was detected in the A_7 strain at 16 kb; Figure 5.8; Table 5.2). The effects of *pol2-4* on BIR mutagenesis were somewhat inconsistent, with small but statistically significant increases compared to wild type only in strains with the A_7 reporter, which is consistent with the increased sensitivity of the A_7 reporter to *pol2-4* (Tran et al., 1997). Our strain background, however, is less sensitive to

the *pol2-4* mutation even with respect to spontaneous frameshift mutation events.

The effect of proofreading can only be accurately assessed in the absence of MMR, as some redundancy exists between the two activities. Thus, one possible explanation for the lack of effect in *pol2-4* mutants was that, in our system, MMR corrects errors left by Pol ϵ with very high efficiency. To test this, *msh2 Δ pol2-4* double mutants were constructed in strains at all 3 positions containing either the *A₄* or *A₇* reporter. *pol2-4msh2 Δ* double mutants grew poorly in lactate, and did not survive our BIR experiments (*gal::HO* induction and plating), precluding any conclusions regarding the role of *pol2-4* during BIR from these strains. To determine if any effect of *pol2-4* on spontaneous mutagenesis could be measured in these strains, *pol2-4msh2 Δ* no-cuts were grown in YEPD. These strains also displayed poor growth and low plating viability (between 17% and 33% for the 16- and 36-kb positions; viability at *MAT* was not measured) and, even among survivors, no increase in mutagenesis compared to *msh2 Δ* was observed (data not shown).

Due to the viability issues of the *pol2-4msh2 Δ* double mutant in our strain background, *pol2-4msh3 Δ* double mutants were constructed in the *A₄* and *A₇* reporter strains at all three positions (although experiments were not run for the 16-kb *A₇* DSB strain; Figure 5.8; Table 5.2). *pol2-4msh3 Δ* double mutants grew

well in lactate and did not lose viability after addition of galactose (data not shown). In the strain background studied in Tran et al. (1997), both MMR and Pol ϵ proofreading can correct frameshift mutations in short (<8 bp) runs. If this were true in our strain background, the expected outcome of the *pol2-4msh3 Δ* double mutant in the case of a *pol2-4* effect on BIR mutagenesis is a synergistic increase in mutagenesis compared to *pol2-4* and *msh3 Δ* alone. However, in our strains, effects of the double mutant on spontaneous and BIR mutagenesis were inconsistent. For spontaneous events, statistically significant increases compared to both *pol2-4* and *msh3 Δ* were observed at *MAT* and 16-kb in the *A₄* reporter and at 36 kb with the *A₇* reporter. For BIR mutagenesis, statistically significant increases compared to both *pol2-4* and *msh3 Δ* were only detected at 16 kb with the *A₄* reporter. (For both spontaneous and BIR mutagenesis, there were instances where *pol2-4msh3 Δ* was statistically significant from only one of the single mutants.) Importantly, because it was clear early on that the *pol2-4msh3 Δ* construct was not able to provide new information on *pol2-4* mutagenesis in our strain background, some strains had a low number of repeated experiments, which is a relevant consideration for some of the statistical conclusions made here (see Table 5.2).

Figure 5.8. The role of Pol ϵ proofreading in BIR-associated mutagenesis.

The rate of Lys⁺ revertants was measured before addition of galactose (0h) and 7 hours after incubation in galactose-containing media (7h) in wild type and its various MMR- and Pol ϵ proofreading-deficient derivatives containing frameshift reporters **(A)** A₄ or **(B)** A₇ at the *MAT*, 16-kb, and 36-kb chromosomal positions. Statistically significant differences from wild type are indicated by *. The fold increase of BIR mutation rate in mutants compared to wild type (in cases of a statistically significant change) is indicated in italics. Statistically significant differences from *msh3Δ* are indicated by [†]. Statistically significant differences from *pol2-4* are indicated by [‡]. Other abbreviations and statistical details are similar to those provided in the legend to Figure 5.3.

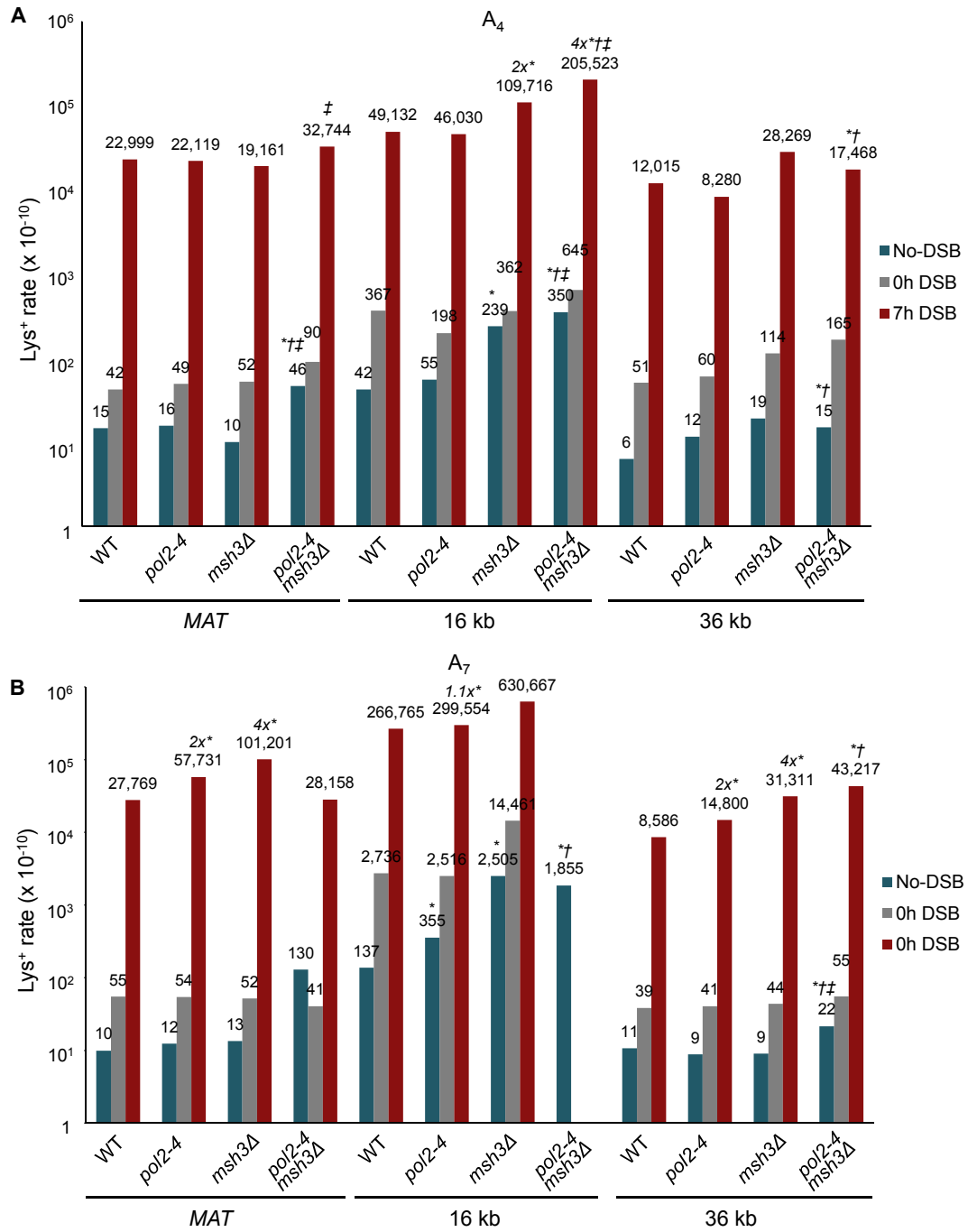


Figure 5.8. The role of Pol ϵ proofreading in BIR-associated mutagenesis.

These results bring into question the role of Pol ϵ and/or its proofreading activity in our strain background. One possibility is the Pol ϵ and/or its proofreading activity are not functional in our strain, even during normal replication. This seems unlikely based on the extreme decrease in viability observed in our *pol2-4msh2 Δ* mutant strain, which shows that deletion of Pol ϵ proofreading has a severe, negative impact on the strain. A more likely explanation is that *pol2-4* is not a strong frameshift mutator in this strain, which could either be the result of Pol ϵ making very few frameshift mutations, or Pol ϵ proofreading inefficiently correcting frameshift mutations in particular. Support for the latter hypothesis comes both from spontaneous mutation rates reported for *msh2 Δ* mutants by Tran et al. (1997) compared to those in this study. Specifically, compared to wild type, Tran et al. (1997) reported approximately 9- and 155-fold increases in spontaneous frameshift mutations for *msh2 Δ* mutants, compared to between 18- to 357-fold and 21,054- to 67,734-fold increases for A₄ and A₇, respectively, in this study (Figure 5.7). This result suggests that the majority of errors in our experimental system are normally repaired by MMR, while in the system studied by Tran et al. (1997) they are repaired by both proofreading and MMR. Indeed, spontaneous frameshift mutations reported by Tran et al. (1997) for the *pol2-4msh2 Δ* double mutant were approximately 307- and 940-fold higher than wild type for the A₄ and A₇ constructs, respectively, while in our system no increase compared to the *msh2 Δ* single mutant was observed. Thus, the increase in spontaneous mutagenesis in our *msh2 Δ* strains more closely approximates the

increases reported for the *pol2-4msh2Δ* double mutant the strain background investigated by Tran et al. (1997), and may indicate that *msh2Δ* phenocopies a double mutant due to inefficient frameshift error correction by Pol ε proofreading in our strain background. Taken together, these data point to efficient -1 bp frameshift correction by MMR, but inefficient correction of these loops by Pol ε proofreading, which complicates any conclusions regarding the role of Pol ε or its proofreading activity on BIR mutagenesis. Future investigation of the role of Pol ε using a reporter to detect base substitutions may provide more details regarding the role of Pol ε proofreading to correct errors that may be made by Pol ε during BIR.

5.3.3.2. Pol δ Proofreading

Unlike Pol ε, Pol δ is required at all stages of BIR synthesis (Lydeard et al., 2007). Fitting with previous characterization of defective Pol δ proofreading (Tran et al., 1999), *pol3-5DV* strains consistently showed an increase in spontaneous mutagenesis compared to wild type (Figure 5.9; Table 5.2). BIR mutagenesis in *pol3-5DV* strains was also increased above the already high mutagenesis observed in wild type strains (a 3- to 6-fold increase for A_4 and a 2- to 9-fold increase for A_7). Also, the frameshift mutation spectrum of Lys^+ outcomes in *pol3-5DV* strains was similar to that in their respective wild type strains (data not shown). These results indicate that the proofreading activity of Pol δ is capable of correcting polymerase errors made during BIR.

Figure 5.9. The role of Pol δ proofreading in BIR-associated mutagenesis.

The rate of Lys⁺ revertants was measured before addition of galactose (0h) and 7 hours after incubation in galactose-containing media (7h) in wild type and its various MMR⁻ and Pol δ proofreading-deficient derivatives containing frameshift reporters **(A)** A₄ or **(B)** A₇ at the *MAT*, 16-kb, and 36-kb chromosomal positions. Statistically significant differences from wild type are indicated by *. The fold increase of BIR mutation rate in mutants compared to wild type (in cases of a statistically significant change) is indicated in italics. Statistically significant differences from *msh3 Δ* are indicated by [†]. Statistically significant differences from *pol3-5DV* are indicated by [‡]. Other abbreviations and statistical details are similar to those provided in the legend to Figure 5.3.

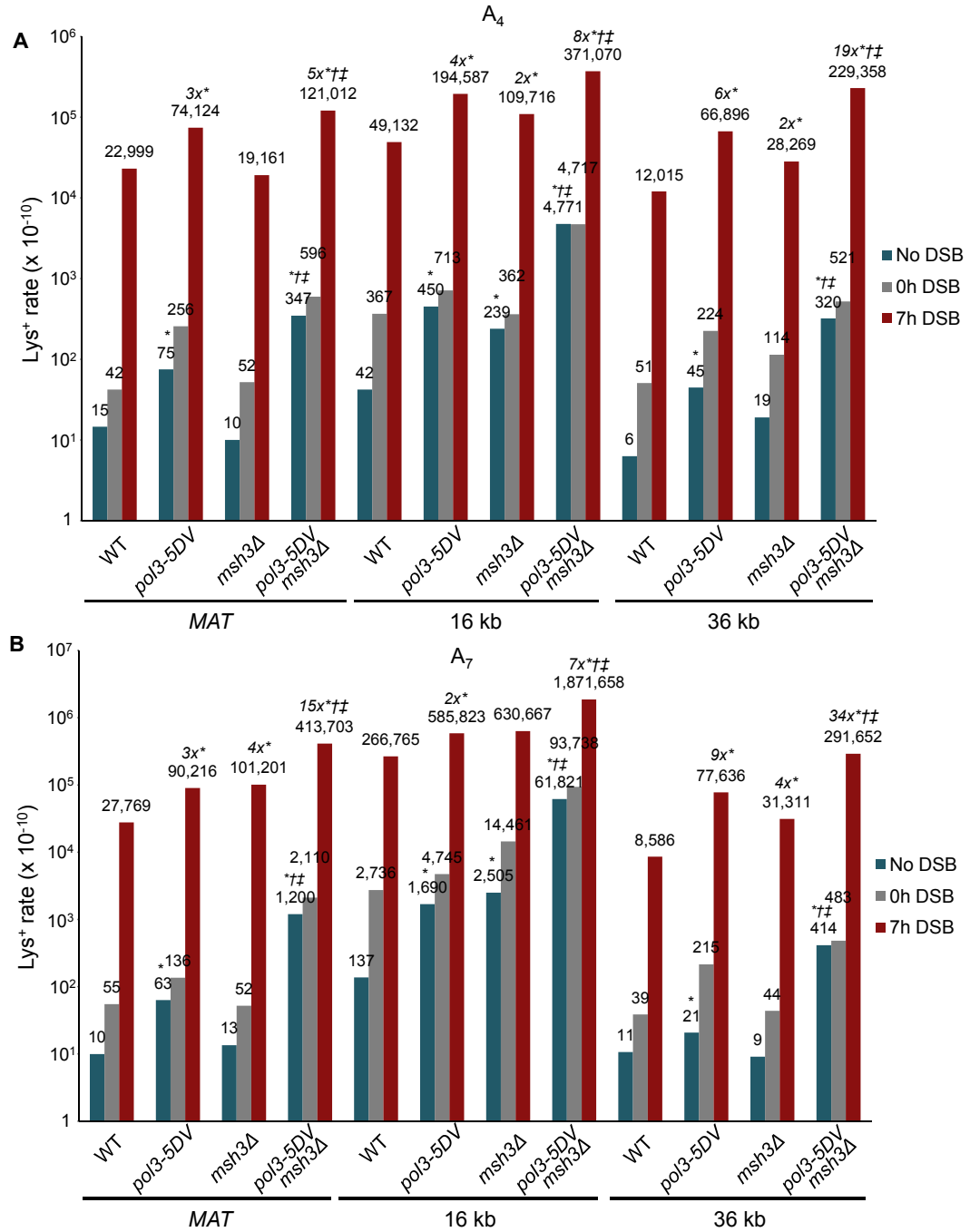


Figure 5.9. The role of Pol δ proofreading in BIR-associated mutagenesis.

As with Pol ϵ , the role of Pol δ proofreading activity can be accurately estimated only in the absence of MMR due to redundancy between the two activities. However, haploid *pol3-5DV* mutants are inviable in combination with full MMR deficiency; thus, *MSH3* (which is known to result in a partial MMR defect) was deleted in *pol3-5DV* strains to better understand the effect of Pol δ proofreading activity. The growth rate of *pol3-5DVmsh3 Δ* double mutant was similar to wild type (Figure 5.10) and its viability was not reduced following 7-hr incubation in galactose (data not shown). Synergistic increases in BIR frameshift mutagenesis were observed in *pol3-5DVmsh3 Δ* double mutants compared to their respective single-mutant strains at all positions (Figure 5.9; Table 5.2). However, the increase in mutagenesis that resulted from synergism between *pol3-5DV* and *msh3 Δ* was generally higher for spontaneous events compared to BIR events, which may indicate decreased efficiency of Pol δ proofreading during BIR. Finally, because the increase in mutagenesis was observed in a mutant lacking the exonuclease activity of Pol δ , many replication errors during BIR must be produced by Pol δ (Jin et al., 2005), although it cannot be excluded that DNA synthesis errors by other polymerases contribute as well (Nick McElhinny et al., 2006; Pavlov et al., 2006a).

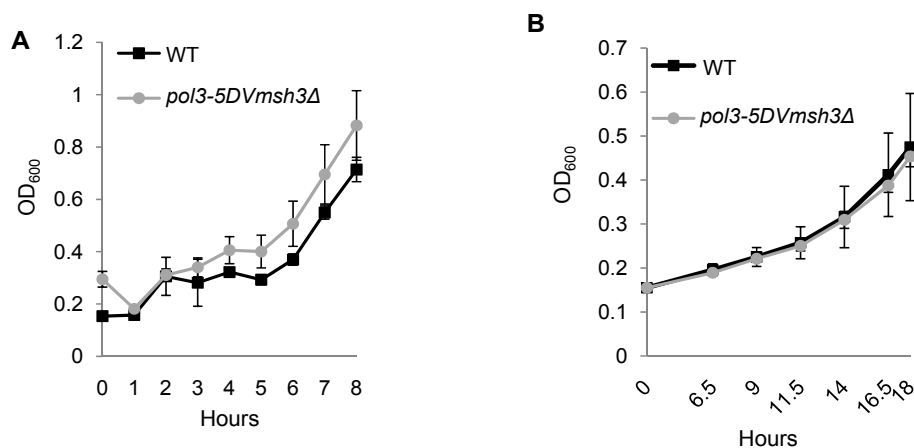


Figure 5.10. Growth characteristics of wild type and its *pol3-5DVmsh3Δ* derivatives. Strains with the *lys2::Ins(A₄)* reporter at the 36-kb position were analyzed. **(A)** Growth curve of wild type and its *pol3-5DVmsh3Δ* derivative measured by OD₆₀₀ in YEPD and **(B)** YEP-Lactate. Each data point represents mean and standard deviation from three independent cultures for each strain.

5.3.4. The Role of Pif1p Helicase

Pif1p is a ssDNA-dependent 5'-to-3' helicase with roles in both mitochondrial and nuclear DNA metabolism (Foury and Kolodynski, 1983; Lahaye A, 1991; Schulz and Zakian, 1994; Zhou JQ, 2002). In the nucleus, Pif1p plays multiple roles, including impeding telomerase-dependent telomere addition to DSBs (Makovets and Blackburn, 2009; Mangahas et al., 2001; Myung et al., 2001a; Schulz and Zakian, 1994; Zhou et al., 2000) and processing of long Okazaki fragments (Budd et al., 2006; Pike et al., 2009; Rossi et al., 2008). Nuclear Pif1p function can be eliminated either via complete deletion of *PIF1* or through a site-specific mutation (*pif1-m2*; (Schulz and Zakian, 1994)), both of which show a BIR defect and an increase in half-crossover formation (Gregorz Ira and Anna Malkova, personal communication), confirming a role for Pif1p in BIR repair. To determine whether Pif1p may play a role in BIR mutagenesis, the *pif1-m2* mutation was introduced into strains containing the A_4 reporter at the *MAT* and 36-kb positions (Figure 5.11; Table 5.4). Due to the known BIR defect in these strains, the rate of frameshift mutations was determined only among those cells that successfully repaired the broken chromosome through either BIR or GC (by finding the frequency of Ade^+Lys^+ events among only Ade^+ events). Frameshift mutations were approximately 2- and 5-fold less likely in *pif1-m2* strains compared to their respective wild type strains at *MAT* and 36 kb, respectively (Figure 5.11; Table 5.5), implicating Pif1p in BIR mutagenesis.

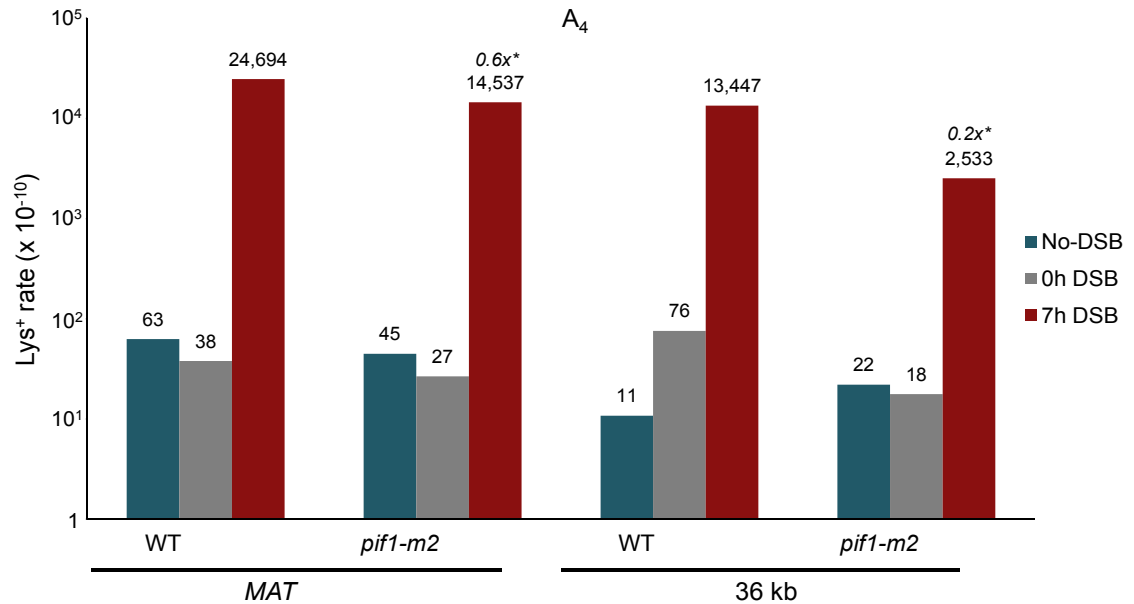


Figure 5.11. The role Pif1p helicase in BIR-associated mutagenesis. The rate of Lys⁺ revertants was measured before addition of galactose (0h) and 7 hours after incubation in galactose-containing media (7h) in wild type and its *pif1-m2* mutant derivatives containing the A₄frameshift reporter at the *MAT* and 36-kb chromosomal positions. Statistically significant differences from the rate of wild type events are indicated by *. The fold increase of BIR mutation rate in mutants compared to wild type (in cases of a statistically significant change) is indicated in italics. Other abbreviations and statistical details are similar to those provided in the legend to Figure 5.3.

Table 5.5. The rate of spontaneous and DSB-associated Lys⁺ mutations in *pif1-m2*.

				Rate of Ade ⁺ Lys ⁺ (x10 ⁻¹⁰) ^a					
				Before galactose		After galactose			
				(0h)		(frequency (7h -0h))			
		HO	Relevant	Median Range		Median Range		Fold over ^b	Fold over wt
Position	Construct	Site	Genotype	Median	[# Repeats]	Median	[# Repeats]	No-DSB Control	(p-value) ^c
<i>MAT</i>	A ₄	DSB	wt	38	(32 - 54) [3]	24,694	(23,581 - 29,234) [3]	797	NA
<i>MAT</i>	A ₄	DSB	<i>pif1-m2</i>	27	(18 - 36) [5]	14,537	(11,786 - 16,162) [5]	661	0.6 (0.0357)
36 kb	A ₄	DSB	wt	76	(34 - 112) [4]	13,447	(11,598 - 18,388) [4]	1,222	NA
36 kb	A ₄	DSB	<i>pif1-m2</i>	18	(12 - 23) [6]	2,533	(2,153 - 4,350) [6]	115	0.2 (0.0095)
<i>MAT</i>	A ₄	No	wt	31	(25 - 42) [3]	ND	ND	NA	NA
<i>MAT</i>	A ₄	No	<i>pif1-m2</i>	22	(14 - 29) [4]	ND	ND	NA	NS
36 kb	A ₄	No	wt	11	(7 - 54) [4]	ND	ND	NA	NA
36 kb	A ₄	No	<i>pif1-m2</i>	22	(7 - 35) [4]	ND	ND	NA	NS

^a Rates calculated at 0h based on 0h frequencies using the Drake equation (see Materials and methods for details). At 7 hrs, rates were calculated as (7h frequency - 0h frequency). ^b Statistically significant elevation of 7h median rate in strains with a DSB over 0h median rate in isogenic no-DSB controls. Significance determined using the Mann-Whitney U test at the p≤0.05 level. ^c Statistically significant elevation of: 7h median rate of mutant compared to 7h median rate of WT in strains with a DSB; 0h median rate of mutant compared to 0h median of WT in no-DSB control strains; parentheses = p-values determined using the Mann-Whitney U test. Abbreviations: ND, not determined; NS, not significant; NA, not applicable.

5.3.5. The Role of dNTP Levels

Increased dNTP levels are known to decrease the fidelity of DNA polymerases and are associated with increased mutation rates. In collaboration with the laboratory of Dr. Andrei Chabes at Umeå University, Sweden, it was shown that our strains undergo ribonucleotide reductase-dependent dNTP increases during BIR repair, as well as during S-phase replication. Furthermore, it was determined that deletion of *DUN1*, which up-regulates dNTP levels during the DNA damage checkpoint response by activating ribonucleotide reductase (RNR) genes, attenuated the post-DSB dNTP increases, while deletion of *SML1*, which represses RNR activity, resulted in constitutively increased dNTP levels in normally cycling cells with no additional effect during BIR (Figure 5.12; (Deem et al., 2011)). The findings in these mutants were consistent with the known roles of Dun1p and Sml1p in dNTP regulation during normal DNA replication and in the DNA damage checkpoint response. To investigate the role of increased nucleotide pools in BIR-related mutagenesis, the level of frameshift mutagenesis was measured in *dun1Δ* and *sml1Δ* A₄ strains (Figure 5.13; Table 5.2). BIR mutagenesis decreased by 4.0-, 2.4-, and 5.4-fold at the *MAT*, 16-, and 36-kb positions, respectively, in *dun1Δ* compared to wild type. The efficiency of BIR in *dun1Δ* cells was slightly reduced (a 1.2-fold reduction at all positions; Table 5.1 and data not shown) compared to wild type. This decrease in BIR efficiency

G2/M Checkpoint

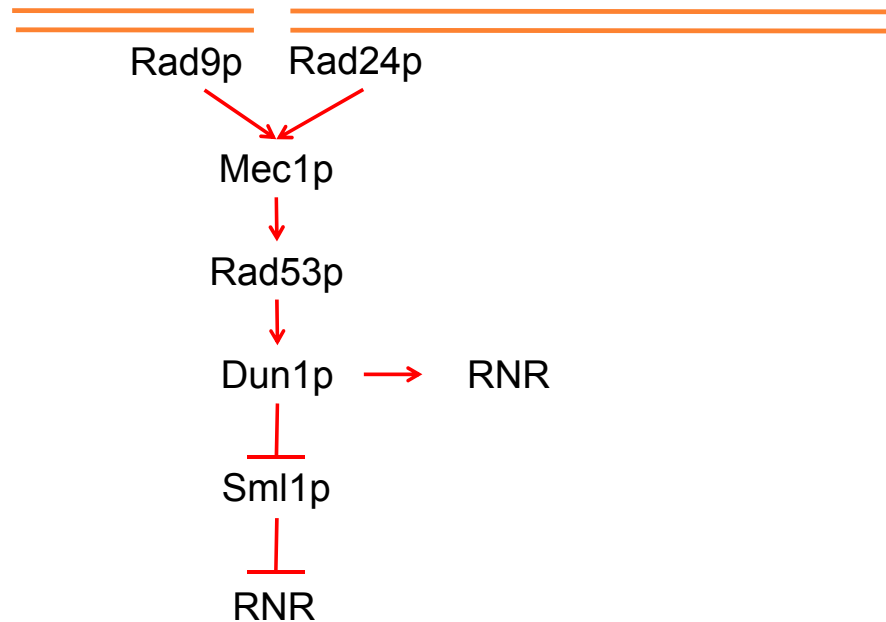


Figure 5.12. Role of DNA damage checkpoint response on dNTP levels. The DNA damage checkpoint is initiated by sensor proteins Rad9p and Rad24p that phosphorylate downstream targets. Phosphorylated Dun1p activates various RNR genes and simultaneously degrades Sml1p, an inhibitor of RNR, resulting in a spike in dNTP levels. Abbreviations: RNR = ribonucleotide reductase.

results most likely from a checkpoint response deficit in *dun1Δ*, which may lead to premature recovery from G2 arrest of cells undergoing BIR repair and, therefore, to increased loss of the broken chromosome due to mis-segregation (similar to observations described for other checkpoint mutants in Section 4.2). To accommodate this, the data were re-calculated to determine the rate of Lys⁺ events per BIR event. These results confirm that the *dun1Δ* mutation reduced the rate of frameshift mutations by 3.3-, 2.0-, and 4.8-fold at the *MAT*, 16-, and 36-kb positions, respectively. Conversely, *smf1Δ* mutants did not display any change in the rate of mutations associated with BIR at the 36-kb position, but did show small, 1.4- and 1.8-fold increases at *MAT* and 16 kb.

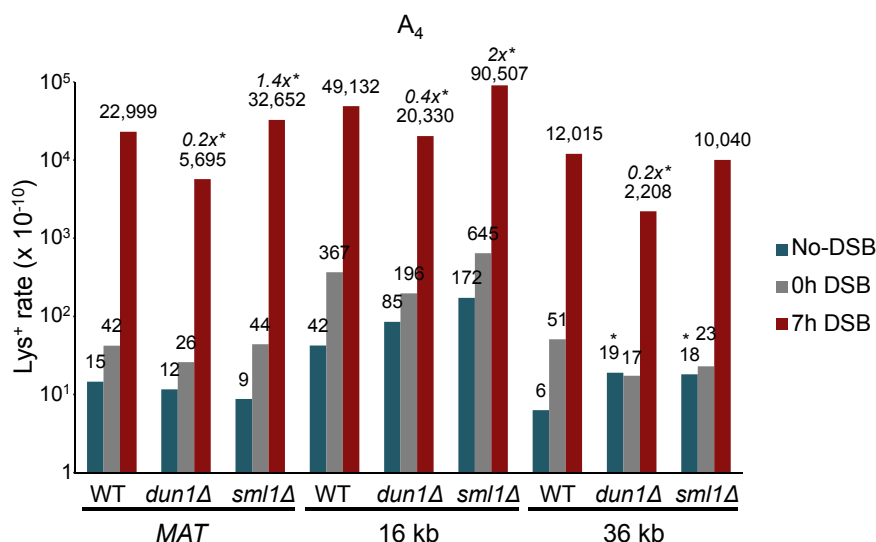


Figure 5.13. Effect of mutations affecting dNTP levels on BIR-associated mutagenesis. The rate of Lys⁺ revertants was measured before addition of galactose (0h) and 7 hours after incubation in galactose-containing media (7h) in wild type and its *dun1*Δ and *sml1*Δ derivatives containing the A_4 frameshift reporter at the *MAT*, 16-kb, and 36-kb chromosomal positions. Statistically significant differences from the rate of wild type events are indicated by *. The fold increase of BIR mutation rate in mutants compared to wild type (in cases of a statistically significant change) is indicated in italics. Other abbreviations and statistical details are similar to those provided in the legend to Fig. 5.3.

We propose that increased dNTP pools contribute to the high mutagenesis associated with BIR. However, the fact that mutagenesis during BIR remained approximately 100- to 500-fold higher than during normal DNA synthesis even in *dun1Δ* mutants suggests that a large portion of BIR-related mutations may be independent of dNTP levels (see Discussion).

5.4. Discussion

Mutations arise from two sources: uncorrected replication errors left by a replication fork copying an undamaged template and error-prone copying of damaged DNA by a translesion polymerase. The role of translesion-synthesis polymerases Pol η and Pol ζ in BIR mutagenesis was investigated and it was determined that hypermutability during BIR is independent of Pol η , while modestly dependent on Pol ζ at some chromosomal positions. The activity of Pol ζ is known to be highly mutagenic in yeast, with the majority of damage-induced and over half of spontaneous mutations ascribed to Pol ζ , whereas lesion bypass by Pol η can be error-free or error-prone depending on the type of lesion and experimental assay employed (reviewed in (Abdulovic et al., 2006; Pavlov et al., 2006b)). Here, elimination of Pol η did not affect BIR-related mutagenesis. At the 36-kb position, where BIR is fast and stable, BIR-mutagenesis was also Pol ζ -independent. In contrast, UV-induced mutagenesis at the 36-kb position was largely Pol ζ -dependent (consistent with data in (Abdulovic and Jinks-Robertson, 2006)), emphasizing the difference in the role of

Pol ζ in BIR versus damage-induced mutagenesis. Interestingly, a small but significant reduction in BIR mutations occurred at *MAT* in strains with the Pol ζ mutation. One possible explanation is that the slow initiation of BIR in this region (Jain et al., 2009; Malkova et al., 2005) results in persistent ssDNA in the D-loop, which leads to higher mutagenesis, presumably by accumulating endogenous damage in ssDNA. Previously, increased spontaneous mutagenesis in regions of artificially created transient ssDNA at DSBs and uncapped telomeres was shown to significantly decrease in the absence of Pol ζ (Yang et al., 2008). Pol ζ dependence was also observed at the 16-kb position in the A₄ strain. This location may be more difficult for replication machinery to traverse, as evidenced by the overall increased rate of mutations (both spontaneous and BIR-related) at this position compared to others. Lack of Pol ζ dependence for the A₇ construct at the 16-kb position could be explained by additional mutations in the poly-A run, which could be Pol ζ -independent. Overall, it is concluded that BIR-associated frameshift mutagenesis is independent of Pol η , while modestly dependent on Pol ζ at some chromosomal positions.

These data demonstrate that MMR operates during BIR, but is often less efficient at correcting BIR-related versus spontaneous errors. This could indicate a decreased efficiency of MMR to correct any individual error made during BIR, or that the amount of errors during BIR is sufficiently high to overwhelm MMR repair capabilities. Alternatively, it could indicate that BIR mutants result from both

MMR-dependent and MMR-independent pathways, as has been proposed for spontaneous mutations (Tran et al., 1995). This final possibility is supported by our observation of higher effects of *msh2Δ* in A₇ versus A₄ strains, because the increased number of errors in A₇ results from replication slippage in the poly-A run, which is efficiently repaired by MMR (Tran et al., 1997). The varying ratio of MMR-dependent to MMR-independent mutation events may explain the varying effect of *msh2Δ* across the three chromosomal locations on both BIR-associated and spontaneous mutagenesis (Table 2), as well as the context-dependence of MMR previously observed by (Hawk et al., 2005) for spontaneous mutagenesis.

Because it was shown that Pol ε participates in DNA synthesis during BIR, *pol2-4* mutants were created to test the effect of Pol ε on BIR mutagenesis. This mutation behaved differently in our background compared to previous reports, and the expected increase in spontaneous mutagenesis could not be detected in our strains (Tran et al., 1997). Attempts to combine the *pol2-4* mutation with mutations that confer an MMR defect resulted in either non-viable strains (*pol2-4msh2Δ*) or inconsistent effects on both spontaneous and BIR mutagenesis (*pol2-4msh3Δ*). The most likely explanation is that *pol2-4* is not a strong frameshift mutator in our strain background, and further investigation of Pol ε proofreading during BIR is needed using a reporter that can detect base substitutions, or in a different strain background.

In *pol3-5DV* mutants, in which Pol δ proofreading was inactivated, we observed a further increase in the mutation rate compared to wild type, suggesting that Pol δ proofreading activity operates during BIR. This result implicates Pol δ as one polymerase responsible for many BIR elongation errors (Jin et al., 2005), although other polymerases may contribute as well (see discussions regarding Pol ϵ and the *pol2-4* mutation herein) (Nick McElhinny et al., 2006; Pavlov et al., 2006a). The synergistic increase in BIR mutations observed in *pol3-5DVmsh3 Δ* double mutants further supports the involvement of Pol δ proofreading during BIR. However, the efficiency of Pol δ proofreading of BIR errors appeared somewhat lower compared to S-phase replication. Furthermore, this synergism suggests that Pol δ introduces mutagenic errors during BIR replication associated with MMR, versus during other repair-related synthesis. As a final point, collaborators at Umeå University also tested the effect of the *pol3-5DV* mutation on dNTP levels both during BIR and in no-DSB controls and confirmed that this mutation did not affect dNTP levels in either case (Deem et al., 2011), consistent with the prior conclusion that the observed effects of *pol3-5DV* on BIR-induced mutagenesis resulted directly from the proofreading defect.

The *pif1-m2* mutation, which eliminates the nuclear Pif1p function, has been shown to impart a BIR defect in which both chromosome loss and HCOs are increased (Gregorz Ira and Anna Malkova, personal communication). Here, *pif1-m2* is also shown to play a role in BIR mutagenesis, as 2- to 5-fold

decreases in BIR mutagenesis were observed at *MAT* and 36 kb, respectively. Pif1p is not a component of the S-phase replisome; rather, it is recruited to the replication fork on an “as-needed” basis (reviewed in Bochman et al. 2010 DNA Repair). The exact role of Pif1p in BIR repair is not known, but the *pif1-m2* mutation did not affect the rate of spontaneous mutations. Possibly, Pif1p plays a larger role in the BIR replication fork compared to the S-phase replication fork. Alternatively, Pif1p may participate in only a subset of BIR replication forks that are more mutagenic than forks that do not contain Pif1p.

Previously, it was established that BIR proceeds under conditions of G2/M cell-cycle arrest resulting from the DNA damage checkpoint response (Deem et al., 2008; Malkova et al., 2005) and hypothesized that cells with chromosome(s) undergoing BIR repair may induce RNR and dNTP levels in a manner similar to other damage-induced checkpoint responses ((Chabes et al., 2003), and reviewed in (Elledge et al., 1993)). This hypothesis was tested in collaboration with the lab of Dr. Andrei Chabes at Umeå University, Sweden, who employed my strain with the *A₄* reporter at the 16-kb position to measure dNTP pools before galactose induction of the DSB (0 hrs), and 3 and 6 hours after galactose addition (Figure 5). (BIR-associated DNA synthesis is initiated approximately 4-6 hours after galactose addition (Deem et al., 2008; Malkova et al., 2005)). This collaboration yielded two important findings (Deem et al., 2011). First, it was demonstrated that a single DSB undergoing BIR repair triggers a complete checkpoint response which includes both cell cycle arrest and Dun1p-dependent

induction of RNR. This differentiates BIR repair in G2/M from the truncated checkpoint response observed, for example, in yeast undergoing DSB repair in G1 (Janke et al., 2010). Second, eliminating G2/M checkpoint-dependent increases in the dNTP pool in *dun1Δ* mutants decreased BIR mutagenesis, suggesting that increased dNTPs contribute to BIR-induced mutagenesis. Nevertheless, even in *dun1Δ*, BIR mutagenesis remained at least 100-fold higher than the spontaneous level of mutations, which indicates that elevated dNTP pools alone cannot explain the decrease in replication fidelity. These findings are consistent with previous work that has shown elevated dNTP levels to be mildly mutagenic in the presence of MMR (Chabes et al., 2003; Kumar et al., 2010), and it is proposed that the role of elevated dNTP pools in this system is to further increase the number of errors made by an already error-prone fork.

5.4.1. Conclusions

In summary, it is proposed that the high level of BIR-associated frameshift mutagenesis is due to uncorrected errors left by a mutagenic replication fork. These data suggest that undamaged template DNA is copied by a BIR fork that contains multiple deficiencies, including decreased Pol δ replication fidelity in the presence of elevated dNTP pools and reduced MMR efficiency, which act synergistically to markedly increase frameshift mutagenesis. In addition, the Pif1p helicase contributes to BIR mutagenesis and may play a more significant role in the BIR replisome than it does during S-phase. This proposed mechanism is generally similar to the mechanism recently suggested to generate

mutations during GC repair (Hicks et al., 2010). What is unexpected is to observe such similar mutation mechanisms between GC, which proceeds through synthesis-dependent strand annealing that does not assemble a replication fork (Wang et al., 2004), and BIR, which proceeds in the context of a replication fork (Lydeard et al., 2007; Lydeard JR, 2010). Future investigations will focus on defining the BIR replication fork to better understand its mutagenic nature. One important aspect of this work is to more clearly define the possible role of Pol ϵ and its proofreading activity in the BIR fork and any potential role(s) for BIR mutagenesis.

Based on its widespread involvement in various processes, we propose that BIR may significantly contribute to the mutation rate and spectrum of many cell types, which is relevant to both disease development and selective adaptation. It may also provide an additional mechanism for so-called “mutation showers” reported to contribute to up to 1% of all mutations in the mouse genome (Wang et al., 2007). BIR-associated mutagenesis may have an especially important role in tumorigenesis, because human cancer cells may both activate BIR at an elevated rate and be MMR-deficient (reviewed in (Kolodner, 1995)). Also, several human tumor-suppressor genes contain homonucleotide runs (Huang et al., 1996; Markowitz et al., 1995; Parsons et al., 1995; Souza et al., 1996), which we demonstrated confer hypermutability in the context of BIR in MMR-deficient cells.

REFERENCES

REFERENCES

- Abdulovic, A., Kim, N., and Jinks-Robertson, S. (2006). Mutagenesis and the three R's in yeast. *DNA Repair (Amst)* 5, 409-421.
- Abdulovic, A.L., and Jinks-Robertson, S. (2006). The in vivo characterization of translesion synthesis across UV-induced lesions in *Saccharomyces cerevisiae*: insights into Pol zeta- and Pol eta-dependent frameshift mutagenesis. *Genetics* 172, 1487-1498.
- Agarwal, R., Tang, Z., Yu, H., and Cohen-Fix, O. (2003). Two Distinct Pathways for Inhibiting Pds1 Ubiquitination in Response to DNA Damage. *Journal of Biological Chemistry* 278, 45027-45033.
- Aguilera A., R.R., ed. (2007). *Molecular Genetics of Recombination*, 1st edn (Springer).
- Alani, E., Cao, L., and Kleckner, N. (1987). A Method for Gene Disruption That Allows Repeated Use of *USR3* Selection in the Construction of Multiply Disrupted Yeast Strains. *Genetics* 116, 541-545.
- Alani, E., Subbiah, S., and Kleckner, N. (1989). The Yeast *RAD50* Gene Encodes a Predicted 153-kD Protein Containing a Purine Nucleotide-Binding Domain and Two Large Heptad-Repeat Regions. *Genetics* 122, 47-57.
- Alexeev, A., Mazin, A., and Kowalczykowski, S.C. (2003). Rad54 protein possesses chromatin-remodeling activity stimulated by the Rad51-ssDNA nucleoprotein filament. *Nat Struct Biol* 10, 182-186.
- Amitani, I., Baskin, R.J., and Kowalczykowski, S.C. (2006). Visualization of Rad54, a Chromatin Remodeling Protein, Translocating on Single DNA Molecules. *Molecular Cell* 23, 143-148.
- Andersen, S.L., and Sekelsky, J. (2010). Meiotic versus mitotic recombination: Two different routes for double-strand break repair. *BioEssays*.

Asai, T., Bates, D.B., and Kogoma, T. (1994). DNA replication triggered by double-stranded breaks in *E. coli*: Dependence on homologous recombination functions. *Cell* 78, 1051-1061.

Asai, T., Sommer, S., Bailone, A., and Kogoma, T. (1993). Homologous recombination-dependent initiation of DNA replication from DNA damage-inducible origins in *Escherichia coli*. *Embo J* 12, 3287-3295.

Aylon, Y., and Kupiec, M. (2003). The checkpoint protein Rad24 of *Saccharomyces cerevisiae* is involved in processing double-strand break ends and in recombination partner choice. *Mol Cell Biol* 23, 6585-6596.

Aylon, Y., Liefshitz, B., and Kupiec, M. (2004). The CDK regulates repair of double-strand breaks by homologous recombination during the cell cycle. *EMBO J* 23, 4868-4875.

Bardwell, A.J., Bardwell, L., Tomkinson, A.E., and Friedberg, E.C. (1994). Specific cleavage of model recombination and repair intermediates by the yeast Rad1-Rad10 DNA endonuclease. *Science* 265, 2082-2085.

Barlow, J.H., Lisby, M., and Rothstein, R. (2008). Differential Regulation of the Cellular Response to DNA Double-Strand Breaks in G1. *Molecular Cell* 30, 73-85.

Blankley, R.T., and Lydall, D. (2004). A domain of Rad9 specifically required for activation of Chk1 in budding yeast. *J Cell Sci* 117, 601-608.

Bleuit, J.S., Xu, H., Ma, Y., Wang, T., Liu, J., and Morrical, S.W. (2001). Mediator proteins orchestrate enzyme-ssDNA assembly during T4 recombination-dependent DNA replication and repair. *Proc Natl Acad Sci U S A* 98, 8298-8305.

Bonilla, C.Y., Melo, J.A., and Toczyski, D.P. (2008). Colocalization of Sensors Is Sufficient to Activate the DNA Damage Checkpoint in the Absence of Damage. *Molecular Cell* 30, 267-276.

Bosco, G., and Haber, J.E. (1998). Chromosome break-induced DNA replication leads to nonreciprocal translocations and telomere capture. *Genetics* 150, 1037-1047.

Budd, M.E., Reis, C.C., Smith, S., Myung, K., and Campbell, J.L. (2006). Evidence Suggesting that Pif1 Helicase Functions in DNA Replication with the Dna2 Helicase/Nuclease and DNA Polymerase $\{\delta\}$. *Mol Cell Biol* 26, 2490-2500.

Bugreev, D.V., Mazina, O.M., and Mazin, A.V. (2006). Rad54 protein promotes branch migration of Holliday junctions. *Nature* 442, 590-593.

Chabes, A., Georgieva, B., Domkin, V., Zhao, X., Rothstein, R., and Thelander, L. (2003). Survival of DNA damage in yeast directly depends on increased dNTP levels allowed by relaxed feedback inhibition of ribonucleotide reductase. *Cell* 112, 391-401.

Chang, S., Khoo, C., and DePinho, R.A. (2001). Modeling chromosomal instability and epithelial carcinogenesis in the telomerase-deficient mouse. *Semin Cancer Biol* 11, 227-239.

Chen, D.-C., Yang, B.-C., and Kuo, T.-T. (1992). One-step transformation of yeast in stationary phase. *Current Genetics* 21, 83-84.

Chen, S.-h., Smolka, M.B., and Zhou, H. (2007). Mechanism of Dun1 Activation by Rad53 Phosphorylation in *Saccharomyces cerevisiae*. *Journal of Biological Chemistry* 282, 986-995.

Chung, W.H., Zhu, Z., Papusha, A., Malkova, A., and Ira, G. (2010). Defective resection at DNA double-strand breaks leads to de novo telomere formation and enhances gene targeting. *PLoS Genet* 6, e1000948.

Cohen-Fix, O., and Koshland, D. (1997). The anaphase inhibitor of *Saccharomyces cerevisiae* Pds1p is a target of the DNA damage checkpoint pathway. *Proceedings of the National Academy of Sciences of the United States of America* 94, 14361-14366.

Colleaux, L., D'Auriol, L., Galibert, F., and Dujon, B. (1988). Recognition and cleavage site of the intron-encoded omega transposase. *Proceedings of the National Academy of Sciences of the United States of America* 85, 6022-6026.

Daley, J.M., Palmbo, P.L., Wu, D., and Wilson, T.E. (2005). Nonhomologous end joining in yeast. *Annual Review of Genetics* 39, 431-451.

Davis, A.P., and Symington, L.S. (2004). RAD51-dependent break-induced replication in yeast. *Mol Cell Biol* 24, 2344-2351.

de la Torre-Ruiz, M.-A., Green, C.M., and Lowndes, N.F. (1998). RAD9 and RAD24 define two additive, interacting branches of the DNA damage checkpoint pathway in budding yeast normally required for Rad53 modification and activation. *EMBO J* 17, 2687-2698.

Deem, A., Barker, K., Vanhulle, K., Downing, B., Vayl, A., and Malkova, A. (2008). Defective break-induced replication leads to half-crossovers in *Saccharomyces cerevisiae*. *Genetics* 179, 1845-1860.

Deem, A., Keszthelyi, A., Blackgrove, T., Vayl, A., Coffey, B., Mathur, R., Chabes, A., and Malkova, A. (2011). Break-Induced Replication Is Highly Inaccurate. *PLoS Biol* 9, e1000594.

Difilippantonio, M.J., Petersen, S., Chen, H.T., Johnson, R., Jasin, M., Kanaar, R., Ried, T., and Nussenzweig, A. (2002). Evidence for replicative repair of DNA double-strand breaks leading to oncogenic translocation and gene amplification. *J Exp Med* 196, 469-480.

Dixon, W.J., and Massey, F.J. (1969). *Introduction to Statistical Analysis*. McGraw-Hill, New York.

Downing, B., Morgan, R., VanHulle, K., Deem, A., and Malkova, A. (2008). Large inverted repeats in the vicinity of a single double-strand break strongly affect repair in yeast diploids lacking Rad51. *Mutat Res* 645, 9-18.

Downs, J.A., Allard, S., Jobin-Robitaille, O., Javaheri, A., Auger, A., Bouchard, N., Kron, S.J., Jackson, S.P., and Côté, J. (2004). Binding of Chromatin-Modifying Activities to Phosphorylated Histone H2A at DNA Damage Sites. *Molecular Cell* 16, 979-990.

Drake, J.W. (1991). A constant rate of spontaneous mutation in DNA-based microbes. *Proc Natl Acad Sci U S A* 88, 7160-7164.

Dronkert, M.L.G., and Kanaar, R. (2001). Repair of DNA interstrand cross-links. *Mutation Research/DNA Repair* 486, 217-247.

Dunn, B., Szauter, P., Pardue, M.L., and Szostak, J.W. (1984). Transfer of yeast telomeres to linear plasmids by recombination. *Cell* 39, 191-201.

Eckardt, F., and Haynes, R.H. (1977). Kinetics of mutation induction by ultraviolet light in excision-deficient yeast. *Genetics* 85, 225-247.

Eklund, H., Uhlin, U., Färnegårdh, M., Logan, D.T., and Nordlund, P. (2001). Structure and function of the radical enzyme ribonucleotide reductase. *Progress in Biophysics and Molecular Biology* 77, 177-268.

Elledge, S.J., Zhou, Z., Allen, J.B., and Navas, T.A. (1993). DNA damage and cell cycle regulation of ribonucleotide reductase. *Bioessays* 15, 333-339.

Elledge, S.J., Zhou Z., Allen J. B., Navas T. A. (2003). DNA damage and cell cycle regulation of ribonucleotide reductase. *BioEssays* 15, 333-339.

Enserink, J.M., Smolka, M.B., Zhou, H., and Kolodner, R.D. (2006). Checkpoint proteins control morphogenetic events during DNA replication stress in *Saccharomyces cerevisiae*. *J Cell Biol* 175, 729-741.

Fasullo, M., Bennett, T., Ahching, P., and Koudelik, J. (1998). The *Saccharomyces cerevisiae* RAD9 Checkpoint Reduces the DNA Damage-Associated Stimulation of Directed Translocations. *Mol Cell Biol* 18, 1190-1200.

Fasullo, M., Giallanza, P., Dong, Z., Cera, C., and Bennett, T. (2001). *Saccharomyces cerevisiae* rad51 mutants are defective in DNA damage-associated sister chromatid exchanges but exhibit increased rates of homology-directed translocations. *Genetics* 158, 959-972.

Fasullo, M., St. Amour, C., and Zeng, L. (2005). Enhanced stimulation of chromosomal translocations and sister chromatid exchanges by either HO-induced double-strand breaks or ionizing radiation in *Saccharomyces cerevisiae* yku70 mutants. *Mutation Research/Fundamental and Molecular Mechanisms of Mutagenesis* 578, 158-169.

Fishman-Lobell, J., and Haber, J.E. (1992). Removal of nonhomologous DNA ends in double-strand break recombination: the role of the yeast ultraviolet repair gene RAD1. *Science* 258, 480-484.

Formosa, T., and Alberts, B.M. (1986a). DNA synthesis dependent on genetic recombination: characterization of a reaction catalyzed by purified bacteriophage T4 proteins. *Cell* 47, 793-806.

Formosa, T., and Alberts, B.M. (1986b). Purification and characterization of the T4 bacteriophage uvsX protein. *J Biol Chem* 261, 6107-6118.

Foury, F., and Kolodnyski, J. (1983). pif mutation blocks recombination between mitochondrial rho⁺ and rho⁻ genomes having tandemly arrayed repeat units in *Saccharomyces cerevisiae*. *Proceedings of the National Academy of Sciences of the United States of America* 80, 5345-5349.

Frankenberg-Schwager, M., Kirchermeier, D., Greif, G., Baer, K., Becker, M., and Frankenberg, D. (2005). Cisplatin-mediated DNA double-strand breaks in replicating but not in quiescent cells of the yeast *Saccharomyces cerevisiae*. *Toxicology* 212, 175-184.

- Gambus, A., Jones, R.C., Sanchez-Diaz, A., Kanemaki, M., van Deursen, F., Edmondson, R.D., and Labib, K. (2006). GINS maintains association of Cdc45 with MCM in replisome progression complexes at eukaryotic DNA replication forks. *Nat Cell Biol* 8, 358-366.
- George, J.W., and Kreuzer, K.N. (1996). Repair of Double-Strand Breaks in Bacteriophage T4 by a Mechanism That Involves Extensive DNA Replication. *Genetics* 143, 1507-1520.
- George, J.W., Stohr, B.A., Tomso, D.J., and Kreuzer, K.N. (2001). The tight linkage between DNA replication and double-strand break repair in bacteriophage T4. *Proc Natl Acad Sci U S A* 98, 8290-8297.
- Giroux, C.N., Mis, J.R., Pierce, M.K., Kohalmi, S.E., and Kunz, B.A. (1988). DNA sequence analysis of spontaneous mutations in the SUP4-o gene of *Saccharomyces cerevisiae*. *Mol Cell Biol* 8, 978-981.
- Gollin, S.M. (2001). Chromosomal alterations in squamous cell carcinomas of the head and neck: window to the biology of disease. *Head Neck* 23, 238-253.
- Gravel, S., Chapman, J.R., Magill, C., and Jackson, S.P. (2008). DNA helicases Sgs1 and BLM promote DNA double-strand break resection. *Genes & Development* 22, 2767-2772.
- Green, C.M., Erdjument-Bromage, H., Tempst, P., and Lowndes, N.F. (2000). A novel Rad24 checkpoint protein complex closely related to replication factor C. *Current Biology* 10, 39-42.
- Greene, C.N., and Jinks-Robertson, S. (1997). Frameshift intermediates in homopolymer runs are removed efficiently by yeast mismatch repair proteins. *Mol Cell Biol* 17, 2844-2850.
- Greene, C.N., and Jinks-Robertson, S. (2001). Spontaneous frameshift mutations in *Saccharomyces cerevisiae*: accumulation during DNA replication and removal by proofreading and mismatch repair activities. *Genetics* 159, 65-75.
- Grushcow, J.M., Holzen, T.M., Park, K.J., Weinert, T., Lichten, M., and Bishop, D.K. (1999). *Saccharomyces cerevisiae* Checkpoint Genes MEC1, RAD17 and RAD24 Are Required for Normal Meiotic Recombination Partner Choice. *Genetics* 153, 607-620.
- Guthrie, C., and Fink, G.R. (1991). *Guide to Yeast Genetics and Molecular Biology*. (San Diego: Academic Press).

Haber, J.E. (2006). Transpositions and translocations induced by site-specific double-strand breaks in budding yeast. *DNA Repair* 5, 998-1009.

Haber, J.E., and Hearn, M. (1985). Rad52-independent mitotic gene conversion in *Saccharomyces cerevisiae* frequently results in chromosomal loss. *Genetics* 111, 7-22.

Hammet, A., Magill, C., Heierhorst, J., and Jackson, S.P. (2007). Rad9 BRCT domain interaction with phosphorylated H2AX regulates the G1 checkpoint in budding yeast. *EMBO Rep* 8, 851-857.

Harrison, J.C., and Haber, J.E. (2006). Surviving the Breakup: The DNA Damage Checkpoint. *Annual Review of Genetics* 40, 209-235.

Hawk, J.D., Stefanovic, L., Boyer, J.C., Petes, T.D., and Farber, R.A. (2005). Variation in efficiency of DNA mismatch repair at different sites in the yeast genome. *Proc Natl Acad Sci U S A* 102, 8639-8643.

He, A.S., Rohatgi, P.R., Hersh, M.N., and Rosenberg, S.M. (2006). Roles of *E. coli* double-strand-break-repair proteins in stress-induced mutation. *DNA Repair (Amst)* 5, 258-273.

Hicks, W.M., Kim, M., and Haber, J.E. (2010). Increased Mutagenesis and Unique Mutation Signature Associated with Mitotic Gene Conversion. *Science* 329, 82-85.

Hirano, Y., and Sugimoto, K. (2006). ATR Homolog Mec1 Controls Association of DNA Polymerase [zeta]-Rev1 Complex with Regions near a Double-Strand Break. *Current Biology* 16, 586-590.

Holbeck, S.L., and Strathern, J.N. (1997). A role for REV3 in mutagenesis during double-strand break repair in *Saccharomyces cerevisiae*. *Genetics* 147, 1017-1024.

Holmes, A.M., and Haber, J.E. (1999). Double-strand break repair in yeast requires both leading and lagging strand DNA polymerases. *Cell* 96, 415-424.

Hopfner, K.-P., Craig, L., Moncalian, G., Zinkel, R.A., Usui, T., Owen, B.A.L., Karcher, A., Henderson, B., Bodmer, J.-L., McMurray, C.T., *et al.* (2002). The Rad50 zinc-hook is a structure joining Mre11 complexes in DNA recombination and repair. *Nature* 418, 562-566.

Huang, J., Papadopoulos, N., McKinley, A.J., Farrington, S.M., Curtis, L.J., Wyllie, A.H., Zheng, S., Willson, J.K., Markowitz, S.D., Morin, P., *et al.* (1996). APC mutations in colorectal tumors with mismatch repair deficiency. *Proc Natl Acad Sci U S A* 93, 9049-9054.

Ingvarsson, S. (1999). Molecular genetics of breast cancer progression. *Semin Cancer Biol* 9, 277-288.

Ira, G., Malkova, A., Liberi, G., Foiani, M., and Haber, J.E. (2003). Srs2 and Sgs1-Top3 suppress crossovers during double-strand break repair in yeast. *Cell* 115, 401-411.

Ira, G., Pellicioli, A., Balijja, A., Wang, X., Fiorani, S., Carotenuto, W., Liberi, G., Bressan, D., Wan, L., Hollingsworth, N.M., *et al.* (2004). DNA end resection, homologous recombination and DNA damage checkpoint activation require CDK1. *Nature* 431, 1011-1017.

Ira, G., Satory, D., and Haber, J.E. (2006). Conservative inheritance of newly synthesized DNA in double-strand break-induced gene conversion. *Mol Cell Biol* 26, 9424-9429.

Ivanov, E.L., and Haber, J.E. (1995). RAD1 and RAD10, but not other excision repair genes, are required for double-strand break-induced recombination in *Saccharomyces cerevisiae*. *Mol Cell Biol* 15, 2245-2251.

Jackson, A.L., and Loeb, L.A. (2001). The contribution of endogenous sources of DNA damage to the multiple mutations in cancer. *Mutation Research/Fundamental and Molecular Mechanisms of Mutagenesis* 477, 7-21.

Jain, S., Sugawara, N., Lydeard, J., Vaze, M., Tanguy Le Gac, N., and Haber, J.E. (2009). A recombination execution checkpoint regulates the choice of homologous recombination pathway during DNA double-strand break repair. *Genes Dev* 23, 291-303.

James, A.P., and Kilbey, B.J. (1977). The timing of UV mutagenesis in yeast: a pedigree analysis of induced recessive mutation. *Genetics* 87, 237-248.

James, A.P., Kilbey, B.J., and Prefontaine, G.J. (1978). The timing of UV mutagenesis in yeast: continuing mutation in an excision-defective (*rad1-1*) strain. *Mol Gen Genet* 165, 207-212.

Janke, R., Herzberg, K., Rolfsmeier, M., Mar, J., Bashkirov, V.I., Haghazari, E., Cantin, G., Yates, J.R., 3rd, and Heyer, W.D. (2010). A truncated DNA-damage-signaling response is activated after DSB formation in the G1 phase of *Saccharomyces cerevisiae*. *Nucleic Acids Res.*

Jaskelioff, M., Van Komen, S., Krebs, J.E., Sung, P., and Peterson, C.L. (2003). Rad54p is a chromatin remodeling enzyme required for heteroduplex DNA joint formation with chromatin. *J Biol Chem* 278, 9212-9218.

Jensen, R.E., and Herskowitz, I. (1984). Directionality and regulation of cassette substitution in yeast. *Cold Spring Harb Symp Quant Biol* 49, 97-104.

Jin, Y.H., Garg, P., Stith, C.M., Al-Refai, H., Sterling, J.F., Murray, L.J., Kunkel, T.A., Resnick, M.A., Burgers, P.M., and Gordenin, D.A. (2005). The multiple biological roles of the 3'→5' exonuclease of *Saccharomyces cerevisiae* DNA polymerase delta require switching between the polymerase and exonuclease domains. *Mol Cell Biol* 25, 461-471.

Kadyk, L.C., and Hartwell, L.H. (1992). Sister Chromatids Are Preferred Over Homologs as Substrates for Recombinational Repair in *Saccharomyces cerevisiae*. *Genetics* 132, 387-402.

Kamimura, Y., Masumoto, H., Sugino, A., and Araki, H. (1998). Sld2, Which Interacts with Dpb11 in *Saccharomyces cerevisiae*, Is Required for Chromosomal DNA Replication. *Mol Cell Biol* 18, 6102-6109.

Kamimura, Y., Tak, Y.-S., Sugino, A., and Araki, H. (2001). Sld3, which interacts with Cdc45 (Sld4), functions for chromosomal DNA replication in *Saccharomyces cerevisiae*. *EMBO J* 20, 2097-2107.

Kang, L.E., and Symington, L.S. (2000). Aberrant double-strand break repair in rad51 mutants of *Saccharomyces cerevisiae*. *Mol Cell Biol* 20, 9162-9172.

Kaye, J.A., Melo, J.A., Cheung, S.K., Vaze, M.B., Haber, J.E., and Toczyski, D.P. (2004). DNA breaks promote genomic instability by impeding proper chromosome segregation. *Curr Biol* 14, 2096-2106.

Klein, H.L. (1997). RDH54, a RAD54 Homologue in *Saccharomyces cerevisiae*, Is Required for Mitotic Diploid-Specific Recombination and Repair and for Meiosis. *Genetics* 147, 1533-1543.

Kogoma, T. (1976). Two types of temperature sensitivity in DNA replication of an *Escherichia coli* dnaB mutant. *J Mol Biol* 103, 191-197.

Kogoma, T. (1997). Stable DNA replication: interplay between DNA replication, homologous recombination, and transcription. *Microbiol Mol Biol Rev* 61, 212-238.

- Kogoma, T., and Lark, K.G. (1975). Characterization of the replication of *Escherichia coli* DNA in the absence of protein synthesis: stable DNA replication. *J Mol Biol* 94, 243-256.
- Kolodner, R.D. (1995). Mismatch repair: mechanisms and relationship to cancer susceptibility. *Trends Biochem Sci* 20, 397-401.
- Kolodner, R.D., Putnam, C.D., and Myung, K. (2002). Maintenance of Genome Stability in *Saccharomyces cerevisiae*. *Science* 297, 552-557.
- Koy JF, P.P., Wall L, Pramanik A, Martinez M, Moore CW. (1995). Genetic changes and bioassays in bleomycin- and phleomycin-treated cells, and their relationship to chromosomal breaks. *Mutat Res* 336, 19-27.
- Kreuzer, K., Saunders, M., Weislo, L., and Kreuzer, H. (1995). Recombination-dependent DNA replication stimulated by double-strand breaks in bacteriophage T4. *J Bacteriol* 177, 6844-6853.
- Kreuzer, K.N. (2000). Recombination-dependent DNA replication in phage T4. *Trends Biochem Sci* 25, 165-173.
- Krogh, B.O., and Symington, L.S. (2004). Recombination proteins in yeast. *Annu Rev Genet* 38, 233-271.
- Kumar, D., Viberg, J., Nilsson, A.K., and Chabes, A. (2010). Highly mutagenic and severely imbalanced dNTP pools can escape detection by the S-phase checkpoint. *Nucl Acids Res* 38, 3975-3983.
- Kunkel, T.A., and Bebenek, K. (2000). DNA REPLICATION FIDELITY. *Annual Review of Biochemistry* 69, 497.
- Kuzminov, A. (1995). Collapse and repair of replication forks in *Escherichia coli*. *Mol Microbiol* 16, 373-384.
- Kuzminov, A. (1999). Recombinational repair of DNA damage in *Escherichia coli* and bacteriophage lambda. *Microbiol Mol Biol Rev* 63, 751-813, table of contents.
- Lahaye A, S.H., Thines-Sempoux D, Foury F. (1991). PIF1: a DNA helicase in yeast mitochondria. *EMBO J* 10, 11.
- Lang, G.I., and Murray, A.W. (2008). Estimating the per-base-pair mutation rate in the yeast *Saccharomyces cerevisiae*. *Genetics* 178, 67-82.

- Lark, C.A., Riazi, J., and Lark, K.G. (1978). *dnaT*, dominant conditional-lethal mutation affecting DNA replication in *Escherichia coli*. *J Bacteriol* **136**, 1008-1017.
- Larrea, A.A., Lujan, S.A., McElhinny, S.A.N., Mieczkowski, P.A., Resnick, M.A., Gordenin, D.A., and Kunkel, T.A. (2010). Genome-wide model for the normal eukaryotic DNA replication fork. *Proceedings of the National Academy of Sciences* **107**, 17674-17679.
- Lawrence, C., O'Brien, T, Bond J (1984). UV-induced reversion of *his4* frameshift mutations in *rad6*, *rev1*, and *rev3* mutants of yeast. *Mol Gen Genet* **195**, 48-490.
- Lazzaro, F., Sapountzi, V., Granata, M., Pelliccioli, A., Vaze, M., Haber, J.E., Plevani, P., Lydall, D., and Muzi-Falconi, M. (2008). Histone methyltransferase Dot1 and Rad9 inhibit single-stranded DNA accumulation at DSBs and uncapped telomeres. *EMBO J* **27**, 1502-1512.
- Le, S., Moore, J.K., Haber, J.E., and Greider, C.W. (1999). RAD50 and RAD51 define two pathways that collaborate to maintain telomeres in the absence of telomerase. *Genetics* **152**, 143-152.
- Lee GS, S.E., Ritzel RG, Von Borstel RC (1988). The base-alteration spectrum of spontaneous and ultraviolet radiation-induced forward mutations in the *URA3* locus of *Saccharomyces cerevisiae*. *Mol Gen Genet* **214**, 396-404.
- Lee, K., and Lee, S.E. (2007). *Saccharomyces cerevisiae* Sae2- and Tel1-Dependent Single-Strand DNA Formation at DNA Break Promotes Microhomology-Mediated End Joining. *Genetics* **176**, 2003-2014.
- Lee, K., Zhang, Y., and Lee, S. (2008). *Saccharomyces cerevisiae* ATM orthologue suppresses break-induced chromosomal translocations. *Nature* **454**, 543-547.
- Lee, S.E., Moore, J.K., Holmes, A., Umez, K., Kolodner, R.D., and Haber, J.E. (1998). *Saccharomyces* Ku70, *mre11/rad50* and RPA proteins regulate adaptation to G2/M arrest after DNA damage. *Cell* **94**, 399-409.
- Li, X., Stith, C.M., Burgers, P.M., and Heyer, W.-D. (2009). PCNA Is Required for Initiation of Recombination-Associated DNA Synthesis by DNA Polymerase δ . *Molecular Cell* **36**, 704-713.
- Lippert, B. (1992). From cisplatin to artificial nucleases - the role of metal ion-nucleic acid interactions in biology. *Biometals* **5**, 195.

Lisby, M., Barlow, J.H., Burgess, R.C., and Rothstein, R. (2004). Choreography of the DNA Damage Response: Spatiotemporal Relationships among Checkpoint and Repair Proteins. *Cell* 118, 699-713.

Lisby, M., Rothstein, R., and Mortensen, U.H. (2001). Rad52 forms DNA repair and recombination centers during S phase. *Proceedings of the National Academy of Sciences of the United States of America* 98, 8276-8282.

Lobachev, K., Vitriol, E., Stemple, J., Resnick, M.A., and Bloom, K. (2004). Chromosome Fragmentation after Induction of a Double-Strand Break Is an Active Process Prevented by the RMX Repair Complex. *Current Biology* 14, 2107-2112.

Luder, A., and Mosig, G. (1982). Two alternative mechanisms for initiation of DNA replication forks in bacteriophage T4: priming by RNA polymerase and by recombination. *Proceedings of the National Academy of Sciences of the United States of America* 79, 1101-1105.

Lundblad, V., and Blackburn, E.H. (1993). An alternative pathway for yeast telomere maintenance rescues est1- senescence. *Cell* 73, 347-360.

Lundin, C., North, M., Erixon, K., Walters, K., Jenssen, D., Goldman, A.S.H., and Helleday, T. Methyl methanesulfonate (MMS) produces heat-labile DNA damage but no detectable in vivo DNA double-strand breaks. *Nucleic Acids Research* 33, 3799-3811.

Lydall, D., and Weinert, T. (1995). Yeast Checkpoint Genes in DNA Damage Processing: Implications for Repair and Arrest. *Science* 270, 1488-1491.

Lydeard, J.R., Jain, S., Yamaguchi, M., and Haber, J.E. (2007). Break-induced replication and telomerase-independent telomere maintenance require Pol32. *Nature* 448, 820-823.

Lydeard JR, L.-M.Z., Sheu YJ, Stillman B, Burgers PM, Haber JE. (2010). Break-induced replication requires all essential DNA replication factors except those specific for pre-RC assembly. *Genes Dev* 24, 1133-1144.

Ma, J.L., Kim, E.M., Haber, J.E., and Lee, S.E. (2003). Yeast Mre11 and Rad1 proteins define a Ku-independent mechanism to repair double-strand breaks lacking overlapping end sequences. *Mol Cell Biol* 23, 8820-8828.

Magni, G.E. (1963). The Origin of Spontaneous Mutations during Meiosis. *Proc Natl Acad Sci U S A* 50, 975-980.

Majka, J., Binz, S.K., Wold, M.S., and Burgers, P.M.J. (2006). Replication Protein A Directs Loading of the DNA Damage Checkpoint Clamp to 5'-DNA Junctions. *Journal of Biological Chemistry* 281, 27855-27861.

Makovets, S., and Blackburn, E.H. (2009). DNA damage signalling prevents deleterious telomere addition at DNA breaks. *Nat Cell Biol* 11, 1383-1386.

Malkova, A., Ivanov, E.L., and Haber, J.E. (1996a). Double-strand break repair in the absence of RAD51 in yeast: a possible role for break-induced DNA replication. *Proc Natl Acad Sci U S A* 93, 7131-7136.

Malkova, A., Naylor, M.L., Yamaguchi, M., Ira, G., and Haber, J.E. (2005). RAD51-dependent break-induced replication differs in kinetics and checkpoint responses from RAD51-mediated gene conversion. *Mol Cell Biol* 25, 933-944.

Malkova, A., Ross, L., Dawson, D., Hoekstra, M.F., and Haber, J.E. (1996b). Meiotic recombination initiated by a double-strand break in rad50 delta yeast cells otherwise unable to initiate meiotic recombination. *Genetics* 143, 741-754.

Malkova, A., Signon, L., Schaefer, C.B., Naylor, M.L., Theis, J.F., Newlon, C.S., and Haber, J.E. (2001). RAD51-independent break-induced replication to repair a broken chromosome depends on a distant enhancer site. *Genes Dev* 15, 1055-1060.

Mangahas, J.L., Alexander, M.K., Sandell, L.L., and Zakian, V.A. (2001). Repair of Chromosome Ends after Telomere Loss in *Saccharomyces*. *Mol Biol Cell* 12, 4078-4089.

Mann, H.B., and Whitney, D.R. (1947). On a test of whether one of 2 random variables is stochastically larger than the other. *Annals of Mathematical Statistics* 18, 50-60.

Marians, K.J. (2000). PriA-directed replication fork restart in *Escherichia coli*. *Trends Biochem Sci* 25, 185-189.

Markowitz, S., Wang, J., Myeroff, L., Parsons, R., Sun, L., Lutterbaugh, J., Fan, R.S., Zborowska, E., Kinzler, K.W., Vogelstein, B., *et al.* (1995). Inactivation of the type II TGF-beta receptor in colon cancer cells with microsatellite instability. *Science* 268, 1336-1338.

McCulloch, S.D., and Kunkel, T.A. (2008). The fidelity of DNA synthesis by eukaryotic replicative and translesion synthesis polymerases. *Cell Res* 18, 148-161.

- McEachern, M.J., and Haber, J.E. (2006). Break-induced replication and recombinational telomere elongation in yeast. *Annu Rev Biochem* 75, 111-135.
- McGill, C.B., Holbeck, S.L., and Strathern, J.N. (1998). The chromosome bias of misincorporations during double-strand break repair is not altered in mismatch repair-defective strains of *Saccharomyces cerevisiae*. *Genetics* 148, 1525-1533.
- McHugh, P.J., Sones, W.R., and Hartley, J.A. (2000). Repair of Intermediate Structures Produced at DNA Interstrand Cross-Links in *Saccharomyces cerevisiae*. *Mol Cell Biol* 20, 3425-3433.
- Melo, J.A., Cohen, J., and Toczyski, D.P. (2001). Two checkpoint complexes are independently recruited to sites of DNA damage in vivo. *Genes & Development* 15, 2809-2821.
- Meyer, D.H., and Bailis, A.M. (2007). Telomere dysfunction drives increased mutation by error-prone polymerases Rev1 and zeta in *Saccharomyces cerevisiae*. *Genetics* 175, 1533-1537.
- Michel, B., Flores, M.J., Viguera, E., Grompone, G., Seigneur, M., and Bidnenko, V. (2001). Rescue of arrested replication forks by homologous recombination. *Proc Natl Acad Sci U S A* 98, 8181-8188.
- Mimitou, E.P., and Symington, L.S. (2008). Sae2, Exo1 and Sgs1 collaborate in DNA double-strand break processing. *Nature* 455, 770-774.
- Mimitou, E.P., and Symington, L.S. (2009). DNA end resection: Many nucleases make light work. *DNA Repair* 8, 983-995.
- Moore, C.W. (1989). Cleavage of Cellular and Extracellular *Saccharomyces cerevisiae* DNA by Bleomycin and Phleomycin. *Cancer Research* 49, 6935-6940.
- Morrison, A.J., Highland, J., Krogan, N.J., Arbel-Eden, A., Greenblatt, J.F., Haber, J.E., and Shen, X. (2004). INO80 and [gamma]-H2AX Interaction Links ATP-Dependent Chromatin Remodeling to DNA Damage Repair. *Cell* 119, 767-775.
- Morrow, D.M., Connelly, C., and Hieter, P. (1997). "Break copy" duplication: a model for chromosome fragment formation in *Saccharomyces cerevisiae*. *Genetics* 147, 371-382.
- Mortensen, U.H., Bendixen, C., Sunjevaric, I., and Rothstein, R. (1996). DNA strand annealing is promoted by the yeast Rad52 protein. *Proceedings of the National Academy of Sciences of the United States of America* 93, 10729-10734.

Mosig, G. (1998). RECOMBINATION AND RECOMBINATION-DEPENDENT DNA REPLICATION IN BACTERIOPHAGE T4. *Annual Review of Genetics* 32, 379-413.

Motamedi, M.R., Szigety, S.K., and Rosenberg, S.M. (1999). Double-strand-break repair recombination in *Escherichia coli*: physical evidence for a DNA replication mechanism in vivo. *Genes Dev* 13, 2889-2903.

Mueller, J.E., Clyman, J., Huang, Y.J., Parker, M.M., and Belfort, M. (1996). Intron mobility in phage T4 occurs in the context of recombination-dependent DNA replication by way of multiple pathways. *Genes & Development* 10, 351-364.

Murakami-Sekimata, A., Huang, D., Piening, B.D., Bangur, C., and Paulovich, A.G. (2010). The *Saccharomyces cerevisiae* RAD9, RAD17 and RAD24 genes are required for suppression of mutagenic post-replicative repair during chronic DNA damage. *DNA Repair* 9, 824-834.

Myung, K., Chen, C., and Kolodner, R.D. (2001a). Multiple pathways cooperate in the suppression of genome instability in *Saccharomyces cerevisiae*. *Nature* 411, 1073-1076.

Myung, K., Datta, A., and Kolodner, R.D. (2001b). Suppression of spontaneous chromosomal rearrangements by S phase checkpoint functions in *Saccharomyces cerevisiae*. *Cell* 104, 397-408.

Nakada, D., Matsumoto, K., and Sugimoto, K. (2003). ATM-related Tel1 associates with double-strand breaks through an Xrs2-dependent mechanism. *Genes & Development* 17, 1957-1962.

Natarajan, A.T., Obe, G., van Zeeland, A.A., Palitti, F., Meijers, M., and Verdegaal-Immerzeel, E.A.M. (1980). Molecular mechanisms involved in the production of chromosomal aberrations II. Utilization of *Neurospora* endonuclease for the study of aberration production by X-rays in G1 and G2 stages of the cell cycle. *Mutation Research/Fundamental and Molecular Mechanisms of Mutagenesis* 69, 293-305.

New, J.H., Sugiyama, T., Zaitseva, E., and Kowalczykowski, S.C. (1998). Rad52 protein stimulates DNA strand exchange by Rad51 and replication protein A. *Nature* 391, 407-410.

Nick McElhinny, S.A., Gordenin, D.A., Stith, C.M., Burgers, P.M., and Kunkel, T.A. (2008). Division of labor at the eukaryotic replication fork. *Mol Cell* 30, 137-144.

Nick McElhinny, S.A., Pavlov, Y.I., and Kunkel, T.A. (2006). Evidence for extrinsic exonucleolytic proofreading. *Cell Cycle* 5, 958-962.

Nickoloff, J.A., Chen, E.Y., and Heffron, F. (1986). A 24-base-pair DNA sequence from the MAT locus stimulates intergenic recombination in yeast. *Proceedings of the National Academy of Sciences of the United States of America* 83, 7831-7835.

Northam, M.R., Robinson, H.A., Kochenova, O.V., and Shcherbakova, P.V. (2010). Participation of DNA polymerase {zeta} in replication of undamaged DNA in *Saccharomyces cerevisiae*. *Genetics* 184, 27-42.

Orr-Weaver, T.L., and Szostak, J.W. (1983). Yeast recombination: the association between double-strand gap repair and crossing-over. *Proceedings of the National Academy of Sciences of the United States of America* 80, 4417-4421.

Orr-Weaver, T.L., Szostak, J.W., and Rothstein, R.J. (1981). Yeast transformation: a model system for the study of recombination. *Proceedings of the National Academy of Sciences of the United States of America* 78, 6354-6358.

Paciotti, V., Clerici, M., Lucchini, G., and Longhese, M.P. (2000). The checkpoint protein Ddc2, functionally related to *S. pombe* Rad26, interacts with Mec1 and is regulated by Mec1-dependent phosphorylation in budding yeast. *Genes & Development* 14, 2046-2059.

Paques, F., and Haber, J.E. (1999). Multiple pathways of recombination induced by double-strand breaks in *Saccharomyces cerevisiae*. *Microbiol Mol Biol Rev* 63, 349-404.

Paques, F., Leung, W.Y., and Haber, J.E. (1998). Expansions and contractions in a tandem repeat induced by double-strand break repair. *Mol Cell Biol* 18, 2045-2054.

Paques, F., Richard, G.F., and Haber, J.E. (2001). Expansions and contractions in 36-bp minisatellites by gene conversion in yeast. *Genetics* 158, 155-166.

Parsons, R., Myeroff, L.L., Liu, B., Willson, J.K., Markowitz, S.D., Kinzler, K.W., and Vogelstein, B. (1995). Microsatellite instability and mutations of the transforming growth factor beta type II receptor gene in colorectal cancer. *Cancer Res* 55, 5548-5550.

Paulovich, A.G., and Hartwell, L.H. (1995). A checkpoint regulates the rate of progression through S phase in *S. cerevisiae* in Response to DNA damage. *Cell* 82, 841-847.

Paulovich, A.G., Margulies, R.U., Garvik, B.M., and Hartwell, L.H. (1997). RAD9, RAD17, and RAD24 Are Required for S Phase Regulation in *Saccharomyces cerevisiae* in Response to DNA Damage. *Genetics* 145, 45-62.

Pavlov, Y.I., Frahm, C., Nick McElhinny, S.A., Niimi, A., Suzuki, M., and Kunkel, T.A. (2006a). Evidence that errors made by DNA polymerase alpha are corrected by DNA polymerase delta. *Curr Biol* 16, 202-207.

Pavlov, Y.I., Shcherbakova, P.V., and Rogozin, I.B. (2006b). Roles of DNA polymerases in replication, repair, and recombination in eukaryotes. *Int Rev Cytol* 255, 41-132.

Petukhova, G., Stratton, S., and Sung, P. (1998). Catalysis of homologous DNA pairing by yeast Rad51 and Rad54 proteins. *Nature* 393, 91-94.

Pike, J.E., Burgers, P.M.J., Campbell, J.L., and Bambara, R.A. (2009). Pif1 Helicase Lengthens Some Okazaki Fragment Flaps Necessitating Dna2 Nuclease/Helicase Action in the Two-nuclease Processing Pathway. *Journal of Biological Chemistry* 284, 25170-25180.

Putnam, C.D., Jaehnig, E.J., and Kolodner, R.D. (2009). Perspectives on the DNA damage and replication checkpoint responses in *Saccharomyces cerevisiae*. *DNA Repair (Amst)* 8, 974-982.

Rattray, A.J., Shafer, B.K., McGill, C.B., and Strathern, J.N. (2002). The roles of REV3 and RAD57 in double-strand-break-repair-induced mutagenesis of *Saccharomyces cerevisiae*. *Genetics* 162, 1063-1077.

Rossi, M.L., Pike, J.E., Wang, W., Burgers, P.M.J., Campbell, J.L., and Bambara, R.A. (2008). Pif1 Helicase Directs Eukaryotic Okazaki Fragments toward the Two-nuclease Cleavage Pathway for Primer Removal. *Journal of Biological Chemistry* 283, 27483-27493.

Rudolph, K.L., Millard, M., Bosenberg, M.W., and DePinho, R.A. (2001). Telomere dysfunction and evolution of intestinal carcinoma in mice and humans. *Nat Genet* 28, 155-159.

Sabatier, L., Ricoul, M., Pottier, G., and Murnane, J.P. (2005). The loss of a single telomere can result in instability of multiple chromosomes in a human tumor cell line. *Mol Cancer Res* 3, 139-150.

Santocanale, C., and Diffley, J.F.X. (1998). A Mec1- and Rad53-dependent checkpoint controls late-firing origins of DNA replication. *Nature* 395, 615-618.

Sawyer, S.L., Cheng, I.H., Chai, W., and Tye, B.K. (2004). Mcm10 and Cdc45 Cooperate in Origin Activation in *Saccharomyces cerevisiae*. *Journal of Molecular Biology* 340, 195-202.

Schulz, V.P., and Zakian, V.A. (1994). The *saccharomyces* PIF1 DNA helicase inhibits telomere elongation and de novo telomere formation. *Cell* 76, 145-155.

Shinohara, A., and Ogawa, T. (1998). Stimulation by Rad52 of yeast Rad51-mediated recombination. *Nature* 391, 404-407.

Shinohara, M., Shita-Yamaguchi, E., Buerstedde, J.M., Shinagawa, H., Ogawa, H., and Shinohara, A. (1997). Characterization of the Roles of the *Saccharomyces cerevisiae* RAD54 Gene and a Homologue of RAD54, RDH54/TID1, in Mitosis and Meiosis. *Genetics* 147, 1545-1556.

Slater, M.L. (1973). Effect of Reversible Inhibition of Deoxyribonucleic Acid Synthesis on the Yeast Cell Cycle. *J Bacteriol* 113, 263-270.

Sleigh, M.J. (1976). The mechanism of DNA breakage by phleomycin in vitro. *Nucleic Acids Research* 3, 891-902.

Smith, C.E., Lam, A.F., and Symington, L.S. (2009). Aberrant double-strand break repair resulting in half crossovers in mutants defective for Rad51 or the DNA polymerase delta complex. *Mol Cell Biol* 29, 1432-1441.

Smith, C.E., Llorente, B., and Symington, L.S. (2007). Template switching during break-induced replication. *Nature* 447, 102-105.

Solinger, J.A., and Heyer, W.-D. (2001). Rad54 protein stimulates the postsynaptic phase of Rad51 protein-mediated DNA strand exchange. *Proceedings of the National Academy of Sciences of the United States of America* 98, 8447-8453.

Sonoda, E., Hochegger, H., Saberi, A., Taniguchi, Y., and Takeda, S. (2006). Differential usage of non-homologous end-joining and homologous recombination in double strand break repair. *DNA Repair (Amst)* 5, 1021-1029.

Souza, R.F., Appel, R., Yin, J., Wang, S., Smolinski, K.N., Abraham, J.M., Zou, T.T., Shi, Y.Q., Lei, J., Cottrell, J., *et al.* (1996). Microsatellite instability in the insulin-like growth factor II receptor gene in gastrointestinal tumours. *Nat Genet* 14, 255-257.

Sprung, C.N., Reynolds, G.E., Jasin, M., and Murnane, J.P. (1999). Chromosome healing in mouse embryonic stem cells. *Proc Natl Acad Sci U S A* **96**, 6781-6786.

Stavnezer, J., Guikema, J.E.J., and Schrader, C.E. (2008). Mechanism and Regulation of Class Switch Recombination. *Annual Review of Immunology* **26**, 261-292.

Storici, F., Lewis, L.K., and Resnick, M.A. (2001). In vivo site-directed mutagenesis using oligonucleotides. *Nat Biotechnol* **19**, 773-776.

Storici, F., and Resnick, M.A. (2006). The delitto perfetto approach to in vivo site-directed mutagenesis and chromosome rearrangements with synthetic oligonucleotides in yeast. *Methods Enzymol* **409**, 329-345.

Strathern, J.N., Klar, A.J.S., Hicks, J.B., Abraham, J.A., Ivy, J.M., Nasmyth, K.A., and McGill, C. (1982). Homothallic switching of yeast mating type cassettes is initiated by a double-stranded cut in the MAT locus. *Cell* **31**, 183-192.

Strathern, J.N., Shafer, B.K., and McGill, C.B. (1995). DNA synthesis errors associated with double-strand-break repair. *Genetics* **140**, 965-972.

Sugawara, N., Paques, F., Colaiacovo, M., and Haber, J.E. (1997). Role of *Saccharomyces cerevisiae* Msh2 and Msh3 repair proteins in double-strand break-induced recombination. *Proc Natl Acad Sci U S A* **94**, 9214-9219.

Sugiyama, T., New, J.H., and Kowalczykowski, S.C. (1998). DNA annealing by Rad52 Protein is stimulated by specific interaction with the complex of replication protein A and single-stranded DNA. *Proceedings of the National Academy of Sciences of the United States of America* **95**, 6049-6054.

Sun, Z., Hsiao, J., Fay, D.S., and Stern, D.F. (1998). Rad53 FHA Domain Associated with Phosphorylated Rad9 in the DNA Damage Checkpoint. *Science* **281**, 272-274.

Sung, P. (1994). Catalysis of ATP-dependent homologous DNA pairing and strand exchange by yeast RAD51 protein. *Science* **265**, 1241-1243.

Sung, P. (1997). Yeast Rad55 and Rad57 proteins form a heterodimer that functions with replication protein A to promote DNA strand exchange by Rad51 recombinase. *Genes & Development* **11**, 1111-1121.

Szostak, J.W., Orr-Weaver, T.L., Rothstein, R.J., and Stahl, F.W. (1983). The double-strand-break repair model for recombination. *Cell* **33**, 25-35.

- Teng, S.C., Chang, J., McCowan, B., and Zakian, V.A. (2000). Telomerase-independent lengthening of yeast telomeres occurs by an abrupt Rad50p-dependent, Rif-inhibited recombinational process. *Mol Cell* 6, 947-952.
- Teng, S.C., and Zakian, V.A. (1999). Telomere-telomere recombination is an efficient bypass pathway for telomere maintenance in *Saccharomyces cerevisiae*. *Mol Cell Biol* 19, 8083-8093.
- Thelen, M.P., Venclovas, C., and Fidelis, K. (1999). A Sliding Clamp Model for the Rad1 Family of Cell Cycle Checkpoint Proteins. *Cell* 96, 769-770.
- Tran, H.T., Degtyareva, N.P., Koloteva, N.N., Sugino, A., Masumoto, H., Gordenin, D.A., and Resnick, M.A. (1995). Replication slippage between distant short repeats in *Saccharomyces cerevisiae* depends on the direction of replication and the RAD50 and RAD52 genes. *Mol Cell Biol* 15, 5607-5617.
- Tran, H.T., Gordenin, D.A., and Resnick, M.A. (1999). The 3'→5' exonucleases of DNA polymerases delta and epsilon and the 5'→3' exonuclease Exo1 have major roles in postreplication mutation avoidance in *Saccharomyces cerevisiae*. *Mol Cell Biol* 19, 2000-2007.
- Tran, H.T., Keen, J.D., Krickler, M., Resnick, M.A., and Gordenin, D.A. (1997). Hypermutability of homonucleotide runs in mismatch repair and DNA polymerase proofreading yeast mutants. *Mol Cell Biol* 17, 2859-2865.
- Trujillo, K.M., Roh, D.H., Chen, L., Van Komen, S., Tomkinson, A., and Sung, P. (2003). Yeast Xrs2 Binds DNA and Helps Target Rad50 and Mre11 to DNA Ends. *Journal of Biological Chemistry* 278, 48957-48964.
- van Attikum, H., Fritsch, O., Hohn, B., and Gasser, S.M. (2004). Recruitment of the INO80 Complex by H2A Phosphorylation Links ATP-Dependent Chromatin Remodeling with DNA Double-Strand Break Repair. *Cell* 119, 777-788.
- Van Komen, S., Petukhova, G., Sigurdsson, S., Stratton, S., and Sung, P. (2000). Superhelicity-driven homologous DNA pairing by yeast recombination factors Rad51 and Rad54. *Mol Cell* 6, 563-572.
- VanHulle, K., Lemoine, F.J., Narayanan, V., Downing, B., Hull, K., McCullough, C., Bellinger, M., Lobachev, K., Petes, T.D., and Malkova, A. (2007). Inverted DNA repeats channel repair of distant double-strand breaks into chromatid fusions and chromosomal rearrangements. *Mol Cell Biol*.
- Voelkel-Meiman, K., and Roeder, G.S. (1990). Gene conversion tracts stimulated by HOT1-promoted transcription are long and continuous. *Genetics* 126, 851-867.

- Wach, A., Brachat, A., Pohlmann, R., and Philippsen, P. (1994). New heterologous modules for classical or PCR-based gene disruptions in *Saccharomyces cerevisiae*. *Yeast* 10, 1793-1808.
- Wang, J., Gonzalez, K.D., Scaringe, W.A., Tsai, K., Liu, N., Gu, D., Li, W., Hill, K.A., and Sommer, S.S. (2007). Evidence for mutation showers. *Proc Natl Acad Sci U S A* 104, 8403-8408.
- Wang, X., Ira, G., Tercero, J.A., Holmes, A.M., Diffley, J.F., and Haber, J.E. (2004). Role of DNA replication proteins in double-strand break-induced recombination in *Saccharomyces cerevisiae*. *Mol Cell Biol* 24, 6891-6899.
- Weinert, T., and Hartwell, L. (1988). The RAD9 gene controls the cell cycle response to DNA damage in *Saccharomyces cerevisiae*. *Science* 241, 317-322.
- Weinert, T.A., and Hartwell, L.H. (1993). Cell Cycle Arrest of *cdc* Mutants and Specificity of the RAD9 Checkpoint. *Genetics* 134, 63-80.
- Williams, R.S., and Tainer, J.A. (2007). Learning Our ABCs: Rad50 Directs MRN Repair Functions via Adenylate Kinase Activity from the Conserved ATP Binding Cassette. *Molecular Cell* 25, 789-791.
- Wolner, B., van Komen, S., Sung, P., and Peterson, C.L. (2003). Recruitment of the Recombinational Repair Machinery to a DNA Double-Strand Break in Yeast. *Molecular Cell* 12, 221-232.
- Wu, X., Wu, C., and Haber, J.E. (1997). Rules of Donor Preference in *Saccharomyces* Mating-Type Gene Switching Revealed by a Competition Assay Involving Two Types of Recombination. *Genetics* 147, 399-407.
- Xiao, W., Chow, B.L., and Rathgeber, L. (1996). The repair of DNA methylation damage in *Saccharomyces cerevisiae*. *Current Genetics* 30, 461-468.
- Yamamoto, A., Guacci, V., and Koshland, D. (1996). Pds1p is required for faithful execution of anaphase in the yeast, *Saccharomyces cerevisiae*. *The Journal of Cell Biology* 133, 85-97.
- Yang, Y., Sterling, J., Storici, F., Resnick, M.A., and Gordenin, D.A. (2008). Hypermutability of damaged single-strand DNA formed at double-strand breaks and uncapped telomeres in yeast *Saccharomyces cerevisiae*. *PLoS Genet* 4, e1000264.
- Zhou, J., Monson, E.K., Teng, S.C., Schulz, V.P., and Zakian, V.A. (2000). Pif1p helicase, a catalytic inhibitor of telomerase in yeast. *Science* 289, 771-774.

Zhou JQ, Q.H., Schulz VP, Mateyak MK, Monson EK, Zakian VA. (2002). Schizosaccharomyces pombe pfh1+ encodes an essential 5' to 3' DNA helicase that is a member of the PIF1 subfamily of DNA helicases. *mol biol cell* 13, 12.

Zhu, Z., Chung, W.H., Shim, E.Y., Lee, S.E., and Ira, G. (2008). Sgs1 helicase and two nucleases Dna2 and Exo1 resect DNA double-strand break ends. *Cell* 134, 981-994.

Zou, L., and Elledge, S.J. (2003). Sensing DNA Damage Through ATRIP Recognition of RPA-ssDNA Complexes. *Science* 300, 1542-1548.

Zou, L., Liu, D., and Elledge, S.J. (2003). Replication protein A-mediated recruitment and activation of Rad17 complexes. *Proceedings of the National Academy of Sciences of the United States of America* 100, 13827-13832.

VITA

VITA

Angela Kay Deem

Education

- May 2011 PhD in Biology, Purdue University (at the Indiana University Purdue University – Indianapolis campus)
Title: *Genome-destabilizing and Mutagenic Effects of Break-induced Replication in Saccharomyces cerevisiae*
- 2001 M.A. with double major in Biology and Natural Resources and Environmental Management, Ball State University, Muncie, IN
- 1998 B.A. in Environmental Biology, Taylor University, Upland, IN

Professional Experience - Academic

- 2008-2011 **Research Assistant** in yeast genetics and microbiology laboratory; Indiana University Purdue University – Indianapolis Department of Biology; Indianapolis, IN
- 2006-2008 **Teaching Assistant**; Indiana University Purdue University, Indianapolis Department of Biology; Indianapolis, IN
- 2005-2006 **Research Assistant** in plant biochemistry laboratory; Indiana University Purdue University – Indianapolis Department of Biology, Indianapolis, IN
- 1998-2000 **Teaching Assistant**; Ball State University Department of Natural Resources and Environmental Management; Muncie, IN

Professional Experience - Industry

- 2002-2005 **Scientific Communications Associate (Regulatory)**; Eli Lilly and Company; Indianapolis, IN
- 2000-2002 **Contract Scientific Communications Associate (Regulatory)** for Eli Lilly and Company; Kelly Scientific Resources; Indianapolis, IN

Honors and Awards

2009-2010	Co-PI, IUPUI Multidisciplinary Undergraduate Research Institute Grant
2008-2009	Purdue Research Fellowship
2007-2008	Indiana University Purdue University Excellence in Teaching Fellowship
2005-2006	Indiana University Purdue University Indianapolis New PhD Fellowship
2003	Eli Lilly and Company Individual Leadership Award for Scientific Writing

University Service

2006-2007	School of Science Graduate Student Council Representative
2007-2008	School of Science Graduate Student Council President
2008-2010	School of Science Graduate Student Council Representative

Platform Talks

Presentations given by the candidate

Deem A, Barker K, VanHulle K, Vayl A, Blackgrove T, Xu D, and Malkova A. Break-induced replication: a source of genetic instability. "11th Annual Midwest DNA Repair Symposium." Ann Arbor, MI, May 16-17 2009.

Presentations given by others

Malkova A, Downing B, VanHulle K., and **Deem A**. Single-strand annealing between inverted repeats initiated by double-strand breaks. FASEB Summer Research Conference "DNA palindromes: roles, consequences and implications of structurally ambivalent DNA", Saxtons River, VT, July 6–11, 2008.

Poster Presentations

Presentations given by the candidate

Deem A, Coffey B, Blackgrove T, Vayl A, and Malkova A. Break-induced replication is highly mutagenic. FASEB Summer Research Conference "Genetic recombination and genome rearrangements", Snowmass Village, CO, Aug 1 - 5, 2009.

Deem A, Barker K, VanHulle K, Vayl A, Blackgrove T, Xu D, and Malkova A. Break-induced replication: a source of genetic instability. "11th Annual Midwest DNA Repair Symposium." Ann Arbor, MI, May 16-17 2009.

Deem A, VanHulle K., Downing B., Hull K., Brennan C, Morgan R., and Malkova A. Deleterious pathways channeling repair of double-strand breaks into chromosomal rearrangements. FASEB Summer Research Conference "Genetic recombination and genome rearrangements", Snowmass Village, CO, July 29-Aug 2, 2007.

Poster Presentations (Continued)

Deem, A, VanHulle K., Lemoine F. J., Narayanan V., Downing B., Hull K., McCullough C., Bellinger M., Lobachev K., Petes T. D., and Malkova A. Inverted DNA repeats channel repair of distant double-strand breaks into chromatid fusions and chromosomal rearrangements. SALK Institute Research Conference on DNA replication and genomic integrity, San Diego, CA, July 26-29, 2006.

The candidate's data have also been presented by the PI and other lab members at the following conferences: 1st Annual IUPUI Research Day. Indianapolis, IN, April 24, 2009; FASEB Summer Research Conference "DNA palindromes: roles, consequences and implications of structurally ambivalent DNA", Saxtons River, VT, July 6-11, 2008; National Conference on Undergraduate Research, La Crosse, WI, April 16-18, 2009; IUPUI Summer Research Programs Poster Session, Indianapolis, IN, July 23, 2008; Committee on Institutional Cooperation (CIC) Summer Research Opportunities, Lansing MI, July 25-27, 2008.

Publications

Deem A, Keszthelyi A, Blackgrove T, Vayl A, Coffey B, Mathur R, Chabis A, and Malkova A. Break-induced replication is highly inaccurate. PLoS Bio. (9) e1000594.

Downing B, Morgan R, VanHulle K, **Deem A**, and Malkova A 2008. Large inverted repeats in the vicinity of a single double-strand break strongly affect repair in yeast diploids lacking Rad51. Mutat Res. 645(1-2):9-18.

Deem A, Barker K, VanHulle K, Downing B, Vayl A, and Malkova A. 2008. Defective break-induced replication leads to half-crossovers in *Saccharomyces cerevisiae*. Genetics 179: 1845-1860.

Crowell DN, Huizinga DH, **Deem AK**, Trobaugh C, Denton R, Sen SE. 2007. *Arabidopsis thaliana* plants possess a specific farnesylcysteine lyase that is involved in detoxification and recycling of farnesylcysteine. Plant J. 50(5):839-47.

Deem AK, Bultema RL, Crowell DN. 2006. Prenylcysteine methylesterase in *Arabidopsis thaliana*. Gene 380(2):159-166.

Skills and Methods

Yeast genetics: Construction and maintenance of yeast mutants; genetic and physical analyses of chromosome repair; delitto perfetto (Storici *et al.*, *PNAS* 2003)

Plant genetics: Creation and maintenance of mutant lines, identification of phenotypic anomalies in mutant lines

Biochemistry: Western and Southern analyses; in vitro transcription and translation; chromatography; DNA and RNA extractions from yeast, bacteria, and plants; protein expression and purification

Statistical analysis: Chi-square distributions; parametric and non-parametric statistics; matched-pairs analysis; iterative method

Writing: Participated in writing successful grant applications to the NIH and Purdue University; manuscript writing; experience as a professional science writer in the pharmaceutical industry